Better understanding human impacts on river thermal regimes under climate change

Yifan Cheng

A dissertation

submitted in partial fulfillment of the

requirements for the degree of

Doctor of Philosophy

University of Washington

2020

Reading Committee:

Bart Nijssen, Chair

John R. Yearsley

Nathalie Voisin

Program Authorized to Offer Degree:

Civil and Environmental Engineering

University of Washington

Abstract

Better understanding human impacts on river thermal regimes under climate change

Yifan Cheng

Chair of the Supervisory Committee:
Professor WOT Bart Nijssen
Civil and Environmental Engineering

Human activities, especially dam construction, greatly modify the response of river thermal regimes to climate change. Dams impound large water bodies, decrease surface to volume ratios, and increase water residence times. All of these changes affect the interaction between surface meteorology and river systems. During warm seasons, surface energy fluxes can only warm a reservoir's top layer (epilimnion) while the bottom layer (hypolimnion) remains cold. As a result, the cold hypolimnetic releases greatly depress downstream river temperatures. Additionally, reservoir releases during cold seasons can increase downstream river temperatures. Thus far, most large-scale stream temperature studies have ignored seasonal thermal stratification and therefore underestimated the regulation impacts on downstream fluvial thermal regimes. In the papers that constitute this dissertation, I synthesized a physically-based model framework to simulate regulated river flow and temperature, explicitly considering the impacts of reservoir thermal stratification. This model framework laid the basis of this dissertation and was applied in all subsequent analyses. In Chapter 2, I applied this model framework in the southeastern United States and investigated the impacts of reservoir regulation and climate change on mean summer river temperature and cooling potentials, a metric designed to evaluate

the compound impact of river flow and temperatures. Under climate change, summer river temperatures in the regulated rivers will remain colder compared to those in the unregulated rivers but under climate change the effect does not carry as far downstream. The impact of reservoir regulation on cooling potentials remains strong for rivers heavily influenced by thermal stratification, but under climate change higher river temperatures will decrease cooling potentials for all river segments.

In Chapter 3, I examined extreme fluvial thermal events, i.e., high river temperatures, so as to facilitate risk management for regional aquatic ecosystem and power sectors. We introduced a standard characterization with three attributes, i.e., duration-intensity-severity, to quantify the climate change impacts on thermal extremes in a regulated river system. Thermal extremes will be greatly exacerbated by climate change. In the baseline (unregulated) scenarios, duration, intensity, and severity are projected to increase to 85.6 day/year (+77.4 day/year), 5.2 °C (+4.4°C), and 193.4 °C·day/year (+187.9 °C·day/year), respectively, by the 2080s under RCP8.5, with values in parentheses indicating the changes relative to the historical, unregulated values. Even though reservoir mitigation impacts are projected to be stronger, only 12.2%, 19.7%, and 26.0% of duration, intensity, and severity by the 2080s under RCP8.5 can be mitigated by reservoir regulations.

In Chapter 4, I projected potential fish distribution due to climate change in the highly regulated Tennessee River. By coupling the model framework for regulated river systems described in Chapter 2 with a species distribution model, I simulated fish presence probability for historic and future periods considering the effects of dams on flow, thermal regime, and reach connectivity. The number of stream segments that are environmentally suitable for an exotic and lucrative rainbow trout, a coldwater species, will greatly shrink under climate change. Only 4.4% of historically suitable streams will remain, mostly located at reservoir tailwaters. For endemic coolwater species, projected higher river temperature may facilitate their expansion, but it will be constrained due to the physical blockage of dams.

TABLE OF CONTENTS

LIST OF FIGURES

LIST OF TABLES

ACKNOWLEDGEMENTS

First of all, I would like to thank my advisor, Bart Nijssen, for his support, mentorship, and patience to go through every detail in my work. For my first paper, I watched him editing my very raw draft line by line from scratch while he explained to me why we should make this change. This and many other things influenced me and motivated me to be a researcher. I would like to thank the rest of my committee members, John Yearsley, Nathalie Voisin, Paulina Jaramillo, Faisal Hossain, Erkan Istanbulluoglu, my graduate school representatives, Julian Olden, and Daniel Schindler. I want to thank John for being so kind, engaging, and supportive to address my confusions, cheer for my small progress, and generously share his expertise. I want to thank Nathalie for providing all the professional and career advices. I want to thank Paulina (PI of NSF-RIPS project) and everyone in this project for an exciting and interdisciplinary experience.

This dissertation is partly funded by NOAA grant NA14OAR4310250, NSF grant EFRI-1440852 and EFRI-1441131 to the University of Washington. I would like to thank the Department of Civil and Environmental Engineering at University of Washington for partly fund my AGU 2019.

I want to thank my family for their consistent support and always having my back, especially my parents, Hongying Gu and Jian Cheng. I want to thank all my dear friends who helped me through this memorable experience, especially Yiyuan Wang for his help in my work and life.

I want to thank the current and former members of Computational Hydrology Group for all the laughter, encouragements, and helps, and I am truly grateful to have such a supportive working environment throughout my doctoral studies. I want to say special thank you to Joe Hamman, Liz Clark, Yixin Mao, Oriana Chegwidden, Andrew Bennett, Diana Gergel, Hörður Helgason, Jane Harrell, Ryan Niemeyer and Michael Ou for being my labmates and my friends.

DEDICATION

For my family

Chapter 1 INTRODUCTION

1.1. BACKGROUND

Fluvial thermal regimes have been substantially impacted by human activities like damming (Hanna et al., 1999; van Vliet, Yearsley, Franssen, et al., 2012), deforestation (Yearsley et al., 2019), urbanization (Nelson & Palmer, 2007), and thermal effluents from thermoelectric power plants (Madden et al., 2013; Miara et al., 2018). Among these changes, dam-impounded reservoirs have the most profound impact because they change tailwater thermal regimes and this effect can persist for hundreds of kilometers. Examples of this include the Burrendong Dam on the Macquarie River in Australia (Ryan et al., 2014), Glen Canyon Dam on the Colorado River, Colorado, U.S. (Webb et al., 1999), and Hills Creek Dam on the Willamette River, Oregon, U.S. (Angilletta et al., 2008). Manmade reservoirs impound large volumes of water, resulting in increased water storage, smaller surface volume ratio, and increased residence time. All of these effects modify the interaction between surface meteorology and river systems. Additionally, deep reservoirs will be thermally stratified during warm seasons, with the reservoir surface layer (epilimnion) warmed by surface energy fluxes while the bottom layer (hypolimnion) remains cold. Many dams built their penstock intake near the bottom of the reservoir to ensure that penstocks are submerged. These releases of cold water from the hypolimnion cool downstream river temperatures during warm seasons (Chapra, 1997).

Such dam-induced changes of river thermal regime lead to habitat redistribution of freshwater species (Edwards, 1978; Olden & Naiman, 2010; Stanford & Ward, 1979). In the biodiverse southeastern U.S. (SEUS), environmental suitability for endemic species was reduced or compromised by cold hypolimnetic releases from reservoirs (Neves & Angermeier, 1990). However, this cold tailwater provides an ideal habitat for exotic coldwater species such as rainbow trout [*Oncorhynchus mykiss*]. Stocking of rainbow trout at reservoir tailwaters in Tennessee has attracted state-wide anglers, greatly strengthening the local economy as well as enhancing recreational opportunities (Charbonneau & Caudill, 2010). In this study, we focused on rivers instead of reservoirs because the latter have a different biotic system that is often unique to each dam.

River temperatures are projected to increase under climate change (van Vliet et al., 2011). The higher river temperature under climate change will put great pressure on aquatic ecosystems

(Sauter et al., 2001). In the Pacific Northwestern United States, the quality and extent of freshwater habitat of salmon are projected to decrease due to higher river temperature (Mantua, Tohver, Hamlet, et al., 2010). Southern Appalachian streams are also projected to be warmer under climate change and will no longer be suitable for endemic coldwater species (McDonnell et al., 2015). In addition, thermoelectric power plants withdraw cooling water from nearby river systems and those using once-through cooling techniques release heated thermal effluent back into the river systems. Higher river temperature can cause capacity deratings and even power outages because 1) it decreases generators' cooling efficiency, and 2) the thermal effluents are constrained by maximum allowable temperature limits set under the Clean Water Act in the United States (McCall et al., 2016; Raptis & Pfister, 2016). During 2000-2015, 27 out of 36 US power plant curtailments resulted from high river temperatures (McCall et al., 2016). Liu et al. (2017) showed that the average generating capacity in the U.S. would, by the 2060s, decline by 12% if environmental regulations are enforced, with power systems in the eastern U.S. most vulnerable to increases in stream temperature (van Vliet et al., 2016).

It remains a challenge to provide a spatially-consistent evaluation of river temperature and its impacts on aquatic ecosystem in a complicated river-reservoir system. So far, most macroscale river temperature studies ignored thermal stratification and therefore underestimated the regulation impacts on downstream river temperature, especially downstream of large reservoirs. For example, Li et al. (2015) showed a warm bias of over 10°C in simulated summer river temperature downstream of Hoover dam. Yearsley et al. (2019) simulated the impact of stratified reservoirs on downstream temperature and showed a warm bias of as much as 8°C downstream of a reservoir in Connecticut when dam impoundment was not considered. Both studies did not account for seasonal thermal stratification. Strzepek et al. (2015) and Boehlert et al. (2015) did include stratification in their studies but they did not explicitly evaluate the impact of stratification on downstream river temperature.

1.2. OBJECTIVE AND RESEARCH QUESTIONS

The overarching objective of this dissertation is to better understand the compound impacts of climate change and reservoir regulation on thermal regimes in a large multi-reservoir system. The impacts of seasonal thermal stratification are explicitly considered during warm seasons. During cold seasons, well-mixed reservoirs might increase downstream river temperature. This

dissertation aims to provide a consistent evaluation over a region that spans multiple watersheds, where water temperature may affect decision making. Environmental agencies regulate maximum allowable river temperature, constraining a river's ability to provide cooling water for power plants. Therefore, I define a "cooling potential" to quantify the thermal energy that a water body can absorb before exceeding a water temperature threshold. Extreme fluvial thermal events, especially high river temperature or thermal extremes, have negative impacts on aquatic ecosystems and power sectors. A credible representation of thermal extremes under climate change is vital for risk management and mitigation. In addition, as an interdisciplinary exploration, I incorporate what I learned above to investigate the dam impacts on an aquatic ecosystem. To be specific, I explored the change of fish habitat forced by the modified flow and thermal regimes in a regulated river system under climate change.

The research questions I will address in this dissertation are the following:

1. How do reservoir regulation and the resulting thermal stratification modify the responses of stream temperatures and cooling potential to climate change?
2. How does reservoir regulation affect thermal extremes, i.e., high river temperature events, in regulated river systems currently and under climate change?
3. How will fish distribution change under climate change in a heavily regulated river system?

I address each of these questions in Chapters 2, 3, and 4, respectively. To address Question 1, I introduce a synthesized model framework to simulate regulated river flow and temperatures in Chapter 2, which is the basis for all the subsequent analyses. This model framework consists of three physically-based models: (1) a macroscale hydrologic model (Variable Infiltration Capacity model or VIC; Hamman et al., 2018; Liang et al., 1994), (2) a river routing model (Model for Scale Adaptive River Transport or MOSART; H. Li et al., 2013) coupled with a water management model (WM; Voisin et al., 2013), and (3) a stream temperature model (River Basin Model or RBM; Yearsley, 2009, 2012) coupled with a two-layer reservoir thermal stratification module (2L; Niemeyer et al., 2018). While the development of 2L is not part of this dissertation, I actively contributed to the development during the early stages of my doctoral studies and co-authored the paper describing the module (Niemeyer et al., 2018). To address Question 2 (Chapter 3), I adapt a standard characterization of extreme drought events with attributes that can support risk management, i.e., duration-intensity-severity, to evaluate climate

change impacts on thermal extremes in a large, regulated river system. The analyses in Chapter 3 are based on the model configurations developed in Chapter 2. To address Question 3 (Chapter 4), I couple the physically-based model framework developed in Chapter 2 with a well-established species distribution model, Maximum Entropy model (Maxent; Phillips et al., 2006), to simulate the presence probability for selected fish species. I compare the climate-induced changes of fish distribution for an exotic and lucrative fish species, rainbow trout, which currently benefits from cold hypolimnetic releases, and three endemic coolwater fish species, which are negatively impacted by dam constructions. Chapters 2 and 3 coves the entire SEUS with 271 major reservoirs in the system, while Chapter 4 focuses on the Tennessee River Basin, a subregion of the SEUS.

Chapter 2 RESERVOIRS MODIFY RIVER THERMAL REGIME SENSITIVITY TO CLIMATE CHANGE: A CASE STUDY IN THE SOUTHEASTERN UNITED STATES

This chapter has been accepted for publication in its current form in the *Water Resources Research*. © American Geophysical Union. Used with permission. The supplemental material for this chapter is provided in appendix A.

Cheng, Y., N. Voisin, J. Yearsley, and B. Nijssen, 2020: Reservoirs modify river thermal regime sensitivity to climate change: a case study in the southeastern United States. *Water Resources Research*, accepted. doi:10.1029/2019WR025784

ABSTRACT

Seasonal thermal stratification in reservoirs changes the thermal regime of regulated river systems as well as stream temperature responses to climate change. Cold releases from reservoir hypolimnion can depress downstream river temperature during warm seasons. Recent large-scale climate change studies on stream temperature have largely ignored reservoir thermal stratification. In this study, we used established models to develop a framework which considers water demand and reservoir regulation with thermal stratification, and applied this model framework to the southeastern US. About half of all 271 reservoirs in our study area retain strong thermal stratification by the 2080s (2070-2099) under RCP8.5 even as median residence times decrease to 60 days from 69 days in the historic period (1979-2010). Reservoir impacts on downstream temperatures become slightly weaker in the future because of higher air temperature and stronger solar radiation. We defined a "cooling potential" to quantify the thermal energy that a water body can absorb before exceeding a water temperature threshold. In the future, higher river temperatures will reduce the cooling potential for all river segments, but more so for river segments minimally impacted by thermal stratification. Reservoir impacts on cooling potential remain strong for river segments downstream of reservoirs with strong thermal stratification. We conducted a sensitivity analysis to evaluate the robustness of our findings to errors in the hydrological simulations. While river segments subject to reservoir regulation are more sensitive

to errors in hydrology than those without regulation impacts, our overall findings do not materially change due to these errors.

2.1. INTRODUCTION

The objective of the paper is to advance our understanding of the effects of climate change on thermal regimes in heavily regulated rivers and of climate change as a stress multiplier on currently existing water resources infrastructure. We are particularly interested in large spatial domains, as opposed to single reach or small basin studies, to capture the river thermal constraints on regional power networks as well as aquatic ecosystems. Here, we describe a study in the southeastern United States (SEUS), where the power sector is particularly vulnerable to projected changes in stream temperature (Liu et al., 2017; van Vliet et al., 2016). The study region coincides roughly with the service area of the SERC Reliability Corporation, which is responsible for the reliability and security of the electric grid across the southeastern and central regions of the United States. The study region contains a number of highly regulated river systems with more than 300 dams. One third of the region's electricity generation portfolio depends on thermoelectric plants with once-through cooling that require large amounts of water for supporting power operations(Averyt et al., 2013). Once-through cooling systems are legally-mandated to not produce effluent that exceeds certain environmental temperature thresholds. However, historical stream temperatures are already close to environmental thresholds as we will show in Section 2.3.2.

Previous studies have generally shown that projected increases in stream temperature under climate change will put great pressure on potential electricity generation globally (van Vliet et al., 2016; van Vliet, Franssen, et al., 2013; van Vliet, Yearsley, Ludwig, et al., 2012) and over regions of the U.S. (Bartos & Chester, 2015; Boehlert et al., 2015; Liu et al., 2017; Miara et al., 2017; Zhang et al., 2020) by reducing the cooling efficiency of thermoelectric plants. Power plants face capacity derating and resulting power outages if their thermal effluent temperature exceeds specific environmental thresholds (McCall et al., 2016; Raptis & Pfister, 2016). This generation curtailment risk is particularly relevant for power plants using once-through cooling techniques because they release thermal effluent directly into nearby river systems. Liu et al. (2017) showed that the average generating capacity in the U.S. is expected to decline by up to 12% by 2060 if environmental regulations are enforced, with the power system in the eastern

U.S. most vulnerable to increases in stream temperature (van Vliet et al., 2016; van Vliet, Yearsley, Ludwig, et al., 2012).

Reservoir regulation can change a river's thermal response to surface meteorology and its thermal sensitivity to climate change. Manmade reservoirs can modify a river's thermal regime in two ways: 1) reservoirs store a large amount of water with a smaller surface area to volume ratio than a regular river reach and hence modify the thermal response to surface energy fluxes; and 2) deep reservoirs thermally stratify on a seasonal basis and store cold water for later release (Chapra, 1997). Multiple catchment-scale studies have investigated the impacts of simple reservoir systems on downstream river temperatures in a number of locations around the world, e.g., Canada (Maheu et al., 2016), China (Cai et al., 2018), Europe (Arora et al., 2018; Kędra & Wiejaczka, 2018), and the United States (Lowney, 2000). These studies show that seasonal thermal stratification has significant impacts on downstream river temperatures. Stratification results in a density gradient that inhibits mixing between the colder bottom layer (hypolimnion) and the warmer upper layer (epilimnion). Because many reservoir releases (e.g., for hydropower) are made from the bottom layer, summer stream temperatures are often cooler downstream of reservoirs.

While a number of large-scale stream temperature studies (Boehlert et al., 2015; Isaak et al., 2012; Li et al., 2015; Mantua, Tohver, & Hamlet, 2010; Strzepek et al., 2015; Sun et al., 2015; van Vliet, Yearsley, Ludwig, et al., 2012; Zhang et al., 2020) accounted for the effects of reservoir regulation, most of them did not explicitly consider seasonal thermal stratification and therefore underestimate the effects of regulation on stream temperature, particularly downstream of large reservoirs. For example, Li et al. (2015) showed a warm bias of over 10ºC in summer stream temperature downstream of Hoover Dam and Yearsley et al. (2019) showed a warm bias of as much as 8°C downstream of a reservoir in the Connecticut river basin. Those studies that did include the effects of stratification, including recent studies by Boehlert et al. (2015) and Strzepek et al (2015), did not explicitly evaluate reservoir impacts on river temperature further downstream.

Detailed models exist to simulate reservoir temperatures in regulated river systems, e.g., CE-QUAL-W2 (Cole & Wells, 2015), WQRRS (USACE-HEC, 1986) and HEC-5Q (Willey, 1986). These models have been used mainly in single-reservoir studies (Gelda et al., 1998; Hanna et al., 1999), in part because of their extensive data requirements. CE-QUAL-W2 (Hanna

et al., 1999) and WEAP (Rheinheimer et al., 2015) have also been used to study temperature control device applications.

Water resources management requires coordinated decisions at the basin level and consequently needs tools and models that can account for the combined actions and effects of multiple reservoirs. Many regional applications, such as power system planning, require the ability to examine coordinated impacts across an even larger region, consisting of multiple river basins. Boehlert et al. (2015) and Niemeyer et al. (2018) developed simplified modules that represent reservoirs as two-layer systems that account for thermal stratification and incorporated these modules into distributed stream temperature models, that can represent the aggregate effect of tens or even hundreds of reservoirs.

In this study, we include the reservoir module of Niemeyer et al. (2018) in a regional model setup to examine climate change effects on stream temperature across a large region with hundreds of reservoirs. We account explicitly for reservoir regulation, including the effects of seasonal thermal stratification, on system-wide stream temperatures, enabling us to evaluate the individual and joint contributions of climate change and reservoir impacts on river thermal regimes. We focus on thermal regimes during the summer when high air temperature, high water demand, and low streamflow coincide in our study region and when thermal stratification is strongest and has the greatest impact on downstream river temperature.

While a large-domain model setup allows for a system-wide evaluation of the thermal response and thermal sensitivity to climate change, large-domain model applications are typically subject to larger errors than small-domain or single-site applications. These larger errors result from process simplifications, limited information about site characteristics, and model parameters that cannot always be calibrated across all sites in a consistent manner, because of limited observations and computing resources. To address this general shortcoming of large-domain model implementations, we conclude this paper with a sensitivity experiment to assess the robustness of our findings to errors in the hydrological simulations.

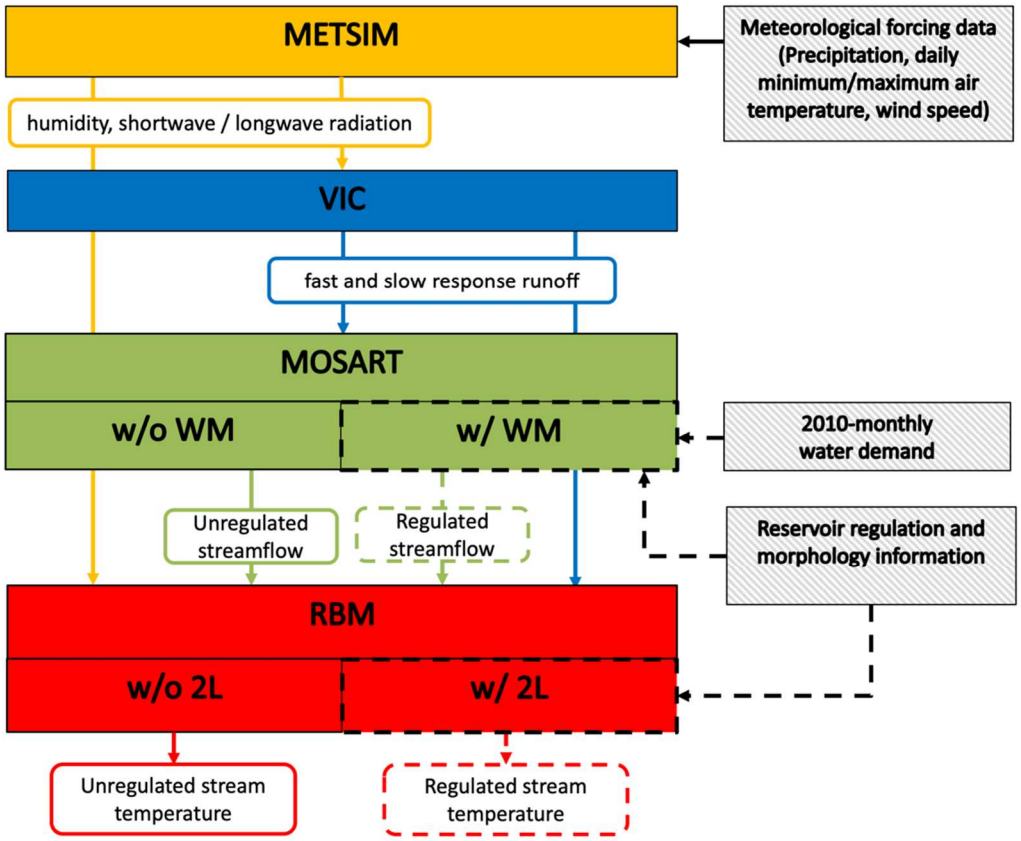

Figure 2.1. Model diagram

2.2. METHODS

Our process-based modeling approach uses a series of established models (Figure 2.1). It consists of a large-scale, spatially-distributed hydrological model (Variable Infiltration Capacity or VIC; Hamman et al., 2018; Liang et al., 1994), a river routing model (Model for Scale Adaptive River Transport or MOSART; Li et al., 2013), coupled to a spatially-distributed water management model (WM; Voisin et al., 2013, 2017), and a stream temperature model (River Basin Model or RBM; Yearsley, 2009, 2012) that includes a two-layer reservoir thermal stratification module (2L; Niemeyer et al., 2018). We can disable the WM and 2L modules to simulate unregulated river conditions (solid frames in Figure 2.1), which we also refer to as the unregulated model setup. Historic meteorological forcings and downscaled climate change projections are pre-processed using MetSim (Bennett et al., 2020) so that they can be used as input to our model chain.

2.2.1. *Study area*

The study region (SEUS; 1.19 million km^2, Figure 2.2) was selected because it coincides roughly with the service area of the SERC Reliability Corporation. We adjusted the area in some places to capture river basin boundaries. The SEUS includes large river basins that cover all or parts of Florida, Georgia, Alabama, Mississippi, Louisiana, Texas, Oklahoma, Arkansas, Missouri, Iowa, Illinois, Kentucky, Tennessee, Virginia, North Carolina, and South Carolina. Over the past century, more than 300 dams and locks were constructed in the area. Some of these are run-of-river dams or navigation locks, which we excluded, because they do not have a significant effect on streamflow or stream temperature. We explicitly simulate 271 major reservoirs based on information in the Global Reservoir and Dam Database (GRanD; Lehner et al., 2011). Most of the dams in the region were built in the headwaters rather than on the mainstem of the major rivers, with the exception of the Tennessee River, which has seven mainstem reservoirs (Table A.1, with 'A' indicating material in the Appendix).

2.2.2. *Meteorological forcings*

Gridded meteorological forcings were used as input to our model chain. We used gridMET (Abatzoglou, 2013) for the historical period (1979 – 2010). For the future climatological period (2070 – 2099, hereafter referred to as the 2080s), we used projections from the Coupled Model Intercomparison Project, Phase 5 (CMIP5; Taylor et al., 2012), downscaled using the Multivariate Constructed Analog (MACA; Abatzoglou & Brown, 2012) method. Since gridMET is the training dataset for MACA, consistency between the historical and future projections is ensured. The gridMET and MACA datasets were regridded from 1/24º to 1/8º latitude-longitude resolution for our application. We used an ensemble of 20 global climate models (GCMs; Table A.2) and one representative concentration pathway (RCP; RCP8.5) for a total of 20 future scenarios. Daily gridMET and MACA data, i.e., daily maximum and minimum air temperature, precipitation and wind speed, were disaggregated to the 3-hourly VIC model time step using MetSim v2.0.0 (Bennett et al., 2020). Other subdaily meteorological forcings, including relative humidity, surface air pressure, and incoming shortwave and longwave radiation were estimated by MetSim using algorithms from the Mountain Micro Climate Simulator (MTCLIM) (Bohn et al., 2013; Thornton & Running, 1999). Wind speed was assumed constant throughout the day.

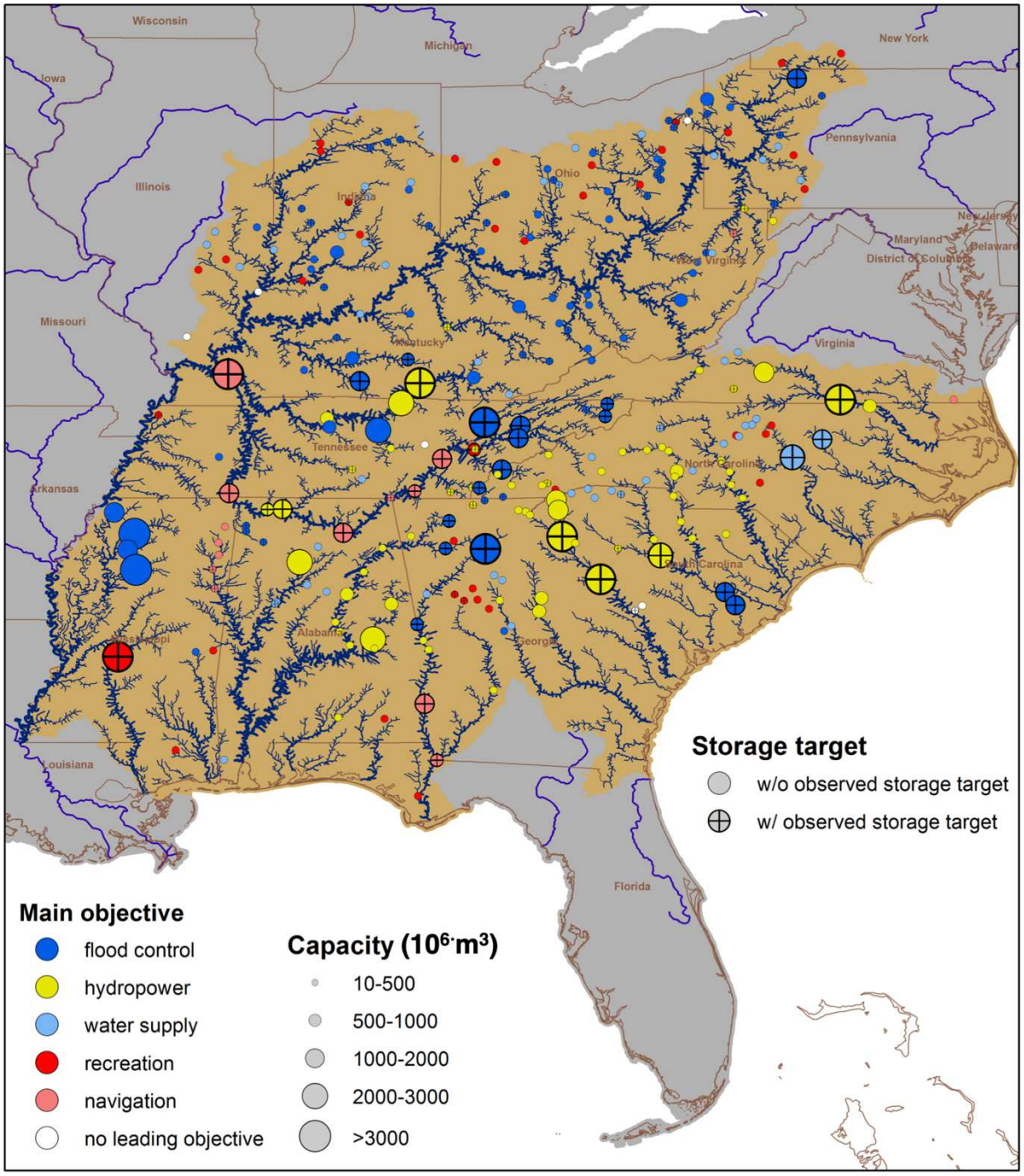

Figure 2.2. Study region. All reservoirs included in this study are represented by the circles.

2.2.3. *Streamflow and stream temperature*

2.2.3.1. Hydrology and runoff

We used VIC version 5 (VIC5) (Hamman et al., 2018) at a 1/8º spatial resolution to simulate the hydrology of the SEUS. Model parameters were taken from Maurer et al. (2002) and modified over part of the domain to reduce a high streamflow bias in the South Atlantic Region. VIC was run at the 3-hourly time step and fast and slow response runoff were output at the daily time step to be consistent with the temporal resolution of the river routing and stream temperature models. We initialized the VIC simulation using a 32-year spin-up run forced by historical meteorological data to allow sufficient time for model states, e.g., deep layer soil moisture, to equilibrate.

2.2.3.2. Streamflow and reservoir regulation

MOSART-WM (Voisin, Li, et al., 2013) is a fully-coupled spatially-distributed river routing and water management model that accounts for reservoir operations and multi-zectoral water demands to simulate regulated streamflow over large regions (Hejazi et al., 2015; Voisin et al., 2017; Voisin, Li, et al., 2013; Zhou et al., 2018). We implemented MOSART (Li et al., 2013) with and without the water management module (WM; Voisin et al., 2017; Voisin, Li, et al., 2013) at a daily time step with a 1/8° spatial resolution. WM estimates daily reservoir releases based on monthly storage targets and accounts for daily constraints such as environmental flow, minimum and maximum storage, and water demands. We substituted WM's original computation of dynamic storage targets at the end of each month (Voisin, Li, et al., 2013) with specified, observed monthly storage targets calculated from storage or reservoir height observations or based on a guide curve (see Text A.1.1 for details, including Figure A.1, Figure A.2, Figure A.3, Figure A.4, and Table A.3, Table A.4, Table A.5, and Table A.6). We collected guide curves or calculated them from observed storages or reservoir elevations for 92 reservoirs in the study area based on information from the Tennessee Valley Authority (TVA), United States Geological Survey (USGS), and U.S. Army Corps of Engineers (USACE) (data source for each reservoir is summarized in Table A.5). Storage targets for reservoirs without observations were estimated based on their primary regulation objective and the relative degree to which they were filled on average (Text A.1.1). In addition to the storage targets, inputs for MOSART-WM included runoff from VIC, reservoir information from the GRanD Database, and 2010 level water demand as used in Voisin et al. (2017) and Zhou et al. (2018). We used fixed water

demand from year 2010 for all years to isolate the effects of climate change from other anthropogenic influences which can significantly impact the hydrologic response (Voisin et al., 2016; Voisin, Liu, et al., 2013).

2.2.3.3. Stream temperature

RBM is a one-dimensional stream temperature model which solves the energy balance equation for surface energy fluxes in the river channel (Yearsley, 2009, 2012). To account for seasonal thermal stratification, we used a module (2L) developed by Niemeyer et al. (2018) that simulates the temperature in two thermally distinct layers: an epilimnion (top layer) and a hypolimnion (bottom layer). This module uses inflow, outflow, and storage data for each reservoir as simulated by MOSART-WM. To calculate surface energy exchange between the water and the overlying atmosphere, RBM and RBM-2L (i.e. without and with reservoir representation) use output from VIC and MetSim. Headwater temperatures, i.e., the most upstream river temperature, which form a boundary condition when solving the energy balance equation for river systems, were estimated using a non-linear relationship with air temperature (Mohseni et al., 1998). Fitted parameters for the Mohseni equations were taken from Niemeyer et al. (2018). We assumed that all reservoir releases were made from the hypolimnion so our result represents a lower bound of possible river temperatures under reservoir regulations. RBM and RBM-2L were initialized separately by setting all model elements to the same water temperature and running the model for a one-year spin-up period.

2.2.4. *Evaluation metrics*

We examine the impacts of climate change on water availability, residence time, regulated stream temperature, and "cooling potential", a metric used to evaluate the compound impacts of water availability and stream temperature. Reservoir residence time was calculated as the mean annual storage divided by the mean annual outflow from that reservoir. In summer, reduced streamflow and increased stream temperature can both constrain the operations of thermoelectric power plants. The cooling potential (E^{cp} [W]) combines the effects of stream temperature and streamflow and represents the additional amount of energy that a body of water can absorb, e.g., from thermoelectric power plants, before exceeding a water temperature threshold. We define the cooling potential as

$$E^{cp} = \begin{cases} \rho C_p (T_{threshold} - T_{summer}) Q_{summer} & if\ T_{summer} < T_{threshold} \\ 0 & if\ T_{summer} \geq T_{threshold} \end{cases} \quad (2.1)$$

where ρ is water density [kg/m^3], C_p is the heat capacity for water [4186 J/kg·°C], $T_{threshold}$ is a stream temperature threshold [°C], T_{summer} is the mean summer stream temperature [°C], and Q_{summer} is the mean summer streamflow [m^3/s]. For $T_{threshold}$ we used one single value for the entire region for a spatially consistent analysis. We set $T_{threshold}$ to 31°C, which is the median of the maximum stream temperature standards of all states in our study region as imposed by the United States Environmental Protection Agency (EPA). In other words, the cooling potential represents a river system's ability to absorb waste thermal energy from thermoelectric power plants if environmental regulations are enforced. We examine climate change impacts on the cooling potential not only at the sites of existing thermoelectric power plants, but for the entire regulated river system.

One of our goals is to quantify the effect of reservoir regulation on the thermal sensitivity of the system to climate change. To this end, we define a rate of change (ΔR) as

$$\Delta R = \left(\frac{\left| \Delta E^{cp}{}_{(reg,2080s-nat,2080s)} \right|}{\left| \Delta E^{cp}{}_{(reg,hist-nat,hist)} \right|} - 1 \right) \times 100\% \quad (2.2)$$

where $\Delta E^{cp}{}_{(reg,t-nat,t)}$ is the change in cooling potential due to regulation during period t. The metric ΔR ranges from -100% to positive infinity. Positive values indicate that future climate will enhance the ability of regulation to maintain the cooling potential, while negative values for ΔR indicate that future climate will reduce the ability of regulation to maintain the cooling potential. In other words, negative ΔR means that rivers are less able to absorb waste heat before exceeding the threshold temperature, potentially affecting cooling for thermal power plants and hence power generation under climate change.

2.2.5. *Sensitivity Analysis*

Large-domain model simulations are typically subject to larger errors than small-domain or single-site applications and these errors are often not easy to reduce. In our model chain, errors in regulated streamflow mainly result from biased runoff from the hydrological model and fixed monthly storage targets. To determine the robustness of our findings to errors in the hydrological simulations, we performed a sensitivity analysis.

As part of our climate change experiment we already created 20 individual hydrological simulations, each corresponding to the downscaled meteorological forcings of a single GCM, and each resulting in a different, but internally consistent streamflow. In the sensitivity analysis, we used these 20 different hydrological simulations as alternative streamflow scenarios, which

we then combined with the meteorological forcings from a single GCM as input to the stream temperature model. The subsequent spread in river temperatures resulted directly from the spread in hydrologic conditions. We repeated this process for three different climate change scenarios selected from our 20 GCM simulations (high - HadGEM2-CC365, medium - CSIRO-Mk3-6-0, low - inmcm4; based on mean projected air temperatures) resulting in 60 (3×20) stream temperature simulations. The three temperature scenarios account for potential differences in sensitivity to hydrological error for different changes in air temperature. We ran this experiment using both regulated and unregulated model setups, resulting in a total of 120 (2×60) stream temperature simulations.

We designed a metric (ϕ) which relates the spread in stream temperature or cooling potential to the spread in hydrologic conditions. Large ϕ values indicate that changes in hydrological conditions result in a large spread in simulated stream temperature or cooling potential. For stream temperature we calculated this metric as the ratio of the standard deviation (σ) of the projected increase in mean summer river temperature (ΔT), in unit of °C, to the coefficient of variation (CV) of mean annual streamflow (Q). The resulting ϕ-values for stream temperature are in unit of °C. We categorized river segments based on river size and whether they are subjected to reservoir regulation. River size is based on the historical mean annual regulated streamflow (Q) with each segment receiving a classification (l) of small ($Q \in$[0,50] m^3/s; l=1), medium ($Q \in$[50,100] m^3/s; l=2), or large ($Q \geq$100 m3/s; l=3). All river segments located downstream of reservoirs are subjected to reservoir regulations (m=true) while the rest are not (m=false). We calculated the metric for each group as follows

$$\phi_{i,l,m,r} = \frac{\sigma_{\widetilde{\Delta T}_{i,[\![j]\!],[\![k]\!]_{l,m},r}}}{CV_{\tilde{Q}_{i,[\![j]\!],[\![k]\!]_{l,m},r}}} \tag{2.3}$$

$$\widetilde{\Delta T}_{i,j,k,r} = \Delta T_{i,j,k,r} - \overline{[\Delta T_{i,k,r}]_J} \tag{2.4}$$

$$\tilde{Q}_{i,j,k,r} = \frac{Q_{i,j,k,r}}{\overline{[Q_{i,k,r}]_J}} \tag{2.5}$$

where i denotes the climate change scenarios (i=high, medium, low), j denotes the streamflow scenario based on each GCM (j=1, 2, …, 20), the double brackets $[\![j]\!]$ indicate that we calculate the statistic across all values of j, k denotes the grid cells in our model domain, $[\![k]\!]_{l,m}$ denotes all grid cells within river size l and subjected to regulation scenario m, and r denotes the regulated

and unregulated model setups, i.e., WM and 2L are enabled (*r*=reg) and disabled (*r*=unreg), respectively . In equation (2.4) we removed $\overline{[\Delta T_{\iota,k,r}]_J}$, i.e., the mean value across 20 GCMs, from the temperature change, $\Delta T_{i,j,k,r}$ so that the hydrology-induced spread ($\widetilde{\Delta T}$) can be aggregated across all grid cells within each group. Similarly, we divided the $Q_{i,j,k,r}$ values by $\overline{[Q_{\iota,k,r}]_J}$, i.e., the mean across 20 GCMs (equation (2.5)). $\phi_{i,l,m,r}$ quantifies the temperature spread caused by hydrologic errors, with larger $\phi_{i,l,m,r}$ values indicating that temperatures are more sensitive to errors in hydrology.

We related the calculated sensitivities to the errors in our hydrological simulations during the historic period. That is, we used $\phi_{i,l,m,r}$ and the hydrologic errors from model evaluation to estimate the resulting error in the stream temperature simulations as follows

$$\hat{\sigma}_{\widetilde{\Delta T}_{i,l,m,r}} = \phi_{i,l,m,r} \times \widehat{CV}_{\tilde{Q}_{[\![\hat{k}]\!]_{l,m}}} \tag{2.6}$$

$$\tilde{Q}_{\hat{k}} = \frac{Q_{sim,\hat{k}}}{Q_{obs,\hat{k}}} \tag{2.7}$$

where $\hat{\sigma}_{\widetilde{\Delta T}}$ denotes errors in the stream temperature change resulting from errors in our hydrological simulations, $\hat{k}$ denotes corresponding grid cells with USGS observations ($\hat{k}$=1,2,…,111; $[\![\widehat{k}]\!]$=[1,2,…,111]), $Q_{sim,\hat{k}}$ and $Q_{obs,\hat{k}}$ denote simulated and observed mean annual streamflow for site $\hat{k}$, and the accent hat indicates estimates based on comparison with observations. Unlike the sensitivity analysis above with 20 hydrologic scenarios, we only have one historical scenario, so we calculated a representative value of hydrological errors for each group using all corresponding USGS sites. We divided the $Q_{sim,\hat{k}}$ values by $Q_{obs,\hat{k}}$ (equation (2.7)) to aggregate multiple USGS sites within the same group.

We repeated the same analysis for cooling potentials (E^{cp}). Instead of $\widetilde{\Delta T}_{i,j,k,r}$ (equation (2.4)), we used the projected relative changes of cooling potentials as follows:

$$\Delta r{E^{cp}}_{i,j,k,r} = \frac{[{E^{cp}}_{i,j,k,r}]_{2080s} - [{E^{cp}}_{k}]_{hist}}{[{E^{cp}}_{k}]_{hist}} \tag{2.8}$$

$$\widetilde{\Delta r{E^{cp}}}_{i,j,k,r} = \Delta r{E^{cp}}_{i,j,k,r} - \overline{[\Delta r{E^{cp}}_{\iota,k,r}]_j} \tag{2.9}$$

where subscript "hist" denotes historical periods with other subscripts as above, and ΔrE^{cp} represents the projected relative changes in cooling potential. Furthermore, we removed the mean of ΔrE^{cp} across 20 GCMs, similar to what we did for the mean summer temperature.

2.3. RESULTS

2.3.1. *Model evaluation*

2.3.1.1. Streamflow

To evaluate the simulated streamflow and stream temperature in a regulated river system, we used USGS observations at 111 sites with both streamflow and stream temperature data (USGS, 2019; summarized in Table A.7. Site selection was subject to two criteria: (1) each site had to have at least one-year of observations that overlapped with our historical simulation period and (2) the contributing area of the site had to be larger than the size of a single model grid cell (approx. 150 km^2). Sixty-three of the 111 sites were located downstream of reservoirs and therefore subject to reservoir regulation. The remaining 48 sites were only minimally affected by regulation and were used to evaluate whether poor performance at regulated sites was the result of poor performance of the hydrology model or the water management model. We used the relative bias at the annual time step and the Nash-Sutcliffe (NS) coefficient at the monthly time step to evaluate overall water availability and streamflow seasonality, respectively (Figure A.5).

Across the 111 sites with observations, the median relative bias in mean annual simulated streamflow was 0.05, which includes the effects of regulation for sites downstream of reservoirs. Sixty-three sites, representing a mixture of regulated and unregulated sites, had a relative bias with an absolute value less than 0.2. Seven had a relative bias with an absolute value greater than 0.5. The NS coefficient for the monthly flows shows lower values for sites with a larger relative bias. In addition, the simulated flows generally show higher NS coefficients for sites that are not subject to regulation. The median NS coefficient for the 48 unregulated sites was 0.70 compared to 0.55 for the 63 regulated sites. Three unregulated sites and 17 regulated sites had an NS coefficient less than 0. The South Atlantic region generally had the worst performance as measured by the NS coefficient, in part because multiple sites (n=6) downstream of Buford reservoir on the Chattahoochee river showed relatively poor performance. The impacts of hydrologic errors on stream temperature simulations are further investigated through the sensitivity analysis in Section 4.3.

2.3.1.2. Reservoir storage

For the 92 reservoirs with guide curves (Section 2.3.2), we compared simulated storage to the specified guide curves. Because we specify the guide curves in MOSART-WM, the model storage is expected to closely follow these curves, unless streamflow is too low to fill the

reservoir or daily release-constraints force a deviation from the specified guide curve. We calculated the normalized root mean square error (nRMSE) of multi-year mean monthly storage (12 mean monthly values based on the 32-year daily time series) and the relative bias of mean annual storage to evaluate seasonality and bias, respectively, in the thermal mass of the reservoirs. Simulated storage showed only a small relative bias and a small nRMSE for the 92 sites with guide curves, with median values of -0.01 and 0.06 respectively, indicating that the water balance model captures the volume and seasonality of the storage in the study region.

2.3.1.3. Stream temperature

In the SEUS, low flow occurs during the summer when it coincides with high air temperatures, resulting in high stream temperatures. Summer is also the time when reservoir stratification is most pronounced. We therefore focus our evaluation on the mean summer river temperature (Figure A.5), with summer defined as the three-month period from June to August.

Simulated mean summer stream temperatures generally show a cold bias with a median value of -0.7 ºC across the 111 sites with stream temperature observations. The mean bias was less than $\pm$2 ºC at 87 of these sites. The bias was generally smaller at the unregulated sites (median bias -0.3 ºC, n=48) than at the regulated sites (median bias -0.9 ºC, n=63). For the 63 regulated sites, 45 had a bias less than 2 ºC. Nine regulated sites had a cold bias larger than 4 °C.

The Supporting Information contains site-specific information of model performance, including time series plots of observed and simulated streamflow (Figure A.6) and stream temperature (Figure A.7) for sites downstream of the five largest reservoirs with downstream temperature observations and a discussion of the source of hydrological errors (Text A.1.2).

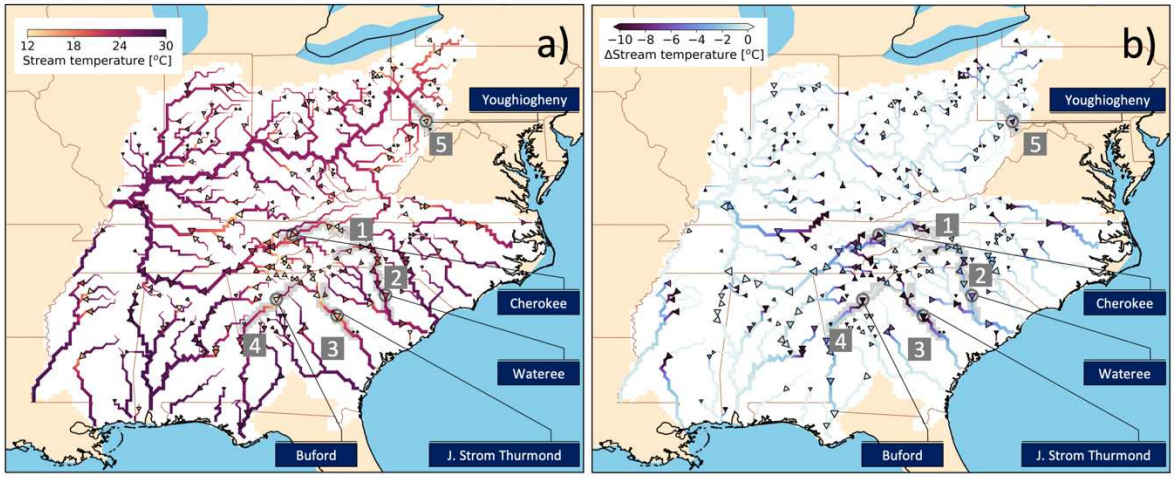

Figure 2.3. (a) Historical mean summer river temperature for the regulated scenario; (b) difference in historical mean summer temperature between the regulated and unregulated model setups. Triangles denote reservoir locations and point downstream; gray-shaded river channels were selected to show the temperature profile along the river, i.e., 1-Tennessee River, 2-Catawba River, 3-Savannah River, 4-Chattahoochee River, 5-Youghiogheny River (see Figure 2.7). Selected reservoirs discussed in the manuscript are circled with the dam names as shown.

2.3.2. *Historical analysis: Reservoir impacts typically maintain or reduce mean summer stream temperature*

Figure 2.3a and Figure 2.3b show, respectively, the simulated mean summer temperature for the historic period for the regulated river system and the impact of regulation on stream temperature. Seasonal thermal stratification results in lower stream temperatures immediately downstream of large reservoirs and gradually attenuates further downstream. Smaller reservoirs, which do not stratify, have little to no impact on downstream river temperature.

Larger reservoirs with longer residence times tend to have stronger thermal stratification and impact downstream temperature more strongly. For example, summer outflow from Buford Reservoir (residence time of 402 days) on the Chattahoochee River is 15.2 °C cooler in the regulated than in the unregulated scenario. Youghiogheny Reservoir on the Youghiogheny River has a shorter residence time (208 days) and a smaller cooling effect of 7.4 °C. Reservoirs with even shorter residence times often have little to no impact on mean summer stream temperature as shown by a number of reservoirs on the Catawba River.

Reservoirs with larger outflows depress stream temperature for a longer distance downstream of the dam because their greater thermal mass makes them (1) less sensitive to surface energy fluxes and (2) less affected by mixing of tributary flows. For example, Deep Creek Reservoir on the Youghiogheny River (upstream of Youghiogheny Reservoir) has a small mean summer outflow of 3 m^3/s and a tailwater temperature that is 12 ºC colder in the regulated case. This temperature difference reduces to only 3 ºC over a distance of less than 18 km. In contrast, J. Strom Thurmond Reservoir on the Savannah River has a much larger mean summer outflow of 111 m^3/s and the temperature difference due to regulation decreases from 11 °C to 4 °C over about 100 km. So, while residence time affects seasonal thermal stratification and therefore the tailwater temperature, the outflow volume affects how far downstream this temperature depression persists.

2.3.3. *Climate change impacts on regulated river temperature*

In general, stream temperature in the southeast is projected to increase, mainly resulting from increased air temperature (Figure 2.4a). Stream temperature increases are larger in the northern part of the study domain and smaller in the southern coastal region. The spatial pattern of stream temperature increase is strongly correlated with the spatial pattern of air temperature increase (Figure A.9). Even though reservoir residence time decreases by the 2080s, reservoir regulation still results in colder stream temperatures downstream of reservoirs with seasonal thermal stratification than would occur in the absence of these reservoirs (Figure 2.4b). However, the cooling effect of reservoirs on downstream river segments slightly decreases by the 2080s. Figure 2.4c shows the change in the median temperature effect of reservoirs between the 2080s and the historic period. Red colors indicate less cooling due to regulation in the future than in the past. Blue indicates greater cooling. By the 2080s, reservoir impacts on downstream river temperatures attenuate faster in the downstream direction, i.e., tailwater temperatures return to unregulated temperatures in a shorter distance. Even if a reservoir releases cool water from the hypolimnion, this cooling effect on tailwater temperature will dissipate faster under climate change as a result of greater surface energy fluxes. In other words, under climate change summer stream temperatures in regulated rivers increase faster than in unregulated rivers and are more sensitive to climate change.

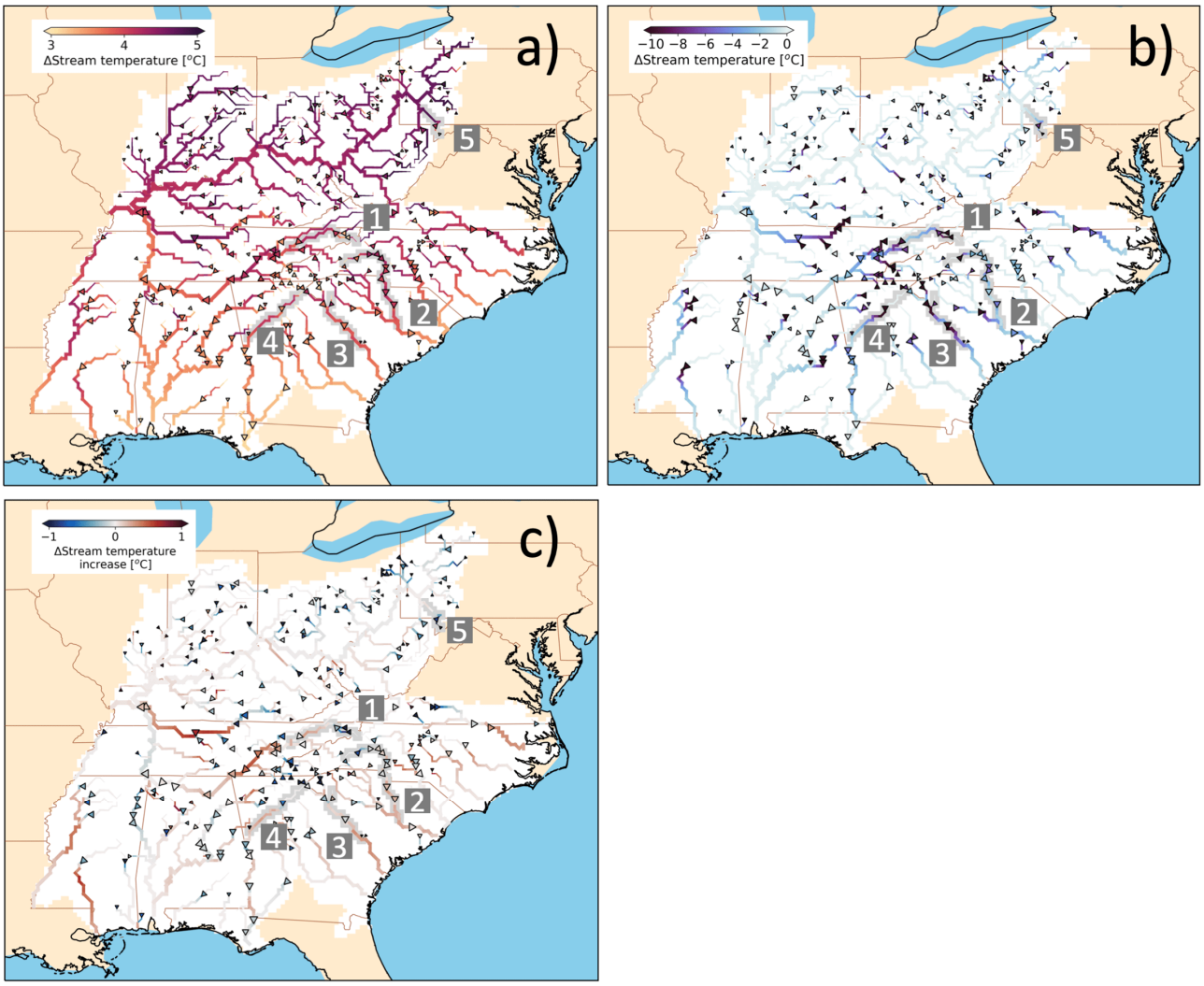

Figure 2.4. Projected mean summer river temperature (a) increases in regulated river system ($\Delta T_{reg,2080s-reg,hist}$), (b) differences between regulated and unregulated model setups in 2080s ($\Delta T_{reg,2080s-nat,2080s}$), and (c) projected changes in the median reservoir impacts on temperatures between the 2080s under RCP8.5 and historical period, i.e., $\Delta(\Delta T_{reg,2080s-nat,2080s} - \Delta T_{reg,hist-nat,hist})$. We highlight the same five rivers as in Figure 2.3: 1-Tennessee River, 2-Catawba River, 3-Savannah River, 4-Chattahoochee River, 5-Youghiogheny River.

2.3.4. *Climate change modulates reservoir impacts through water availability and residence time*

We evaluated the projected changes in reservoir outflow and residence time by the 2080s, to separate the contributions of changes in water availability from changes in thermal dynamics on the overall changes in stream temperature. Because we maintained the same storage targets in the future as during the historical period, the median projected changes for reservoir storage are within 5% for all reservoirs.

Residence times are projected to decrease for almost all reservoirs. Because we imposed the same storage targets in the future, projected increases in reservoir outflow lead to shorter residence times (Figure A.10). Projected increases in reservoir outflows are generally greater in the north and coastal regions than in the central and southwestern parts of the study domain. The 20 GCM projections show strong agreement in the sign of the change signal. For most reservoirs more than 16 out of 20 models agree that outflows will increase, and residence times will decrease (Figure A.11). This increase in outflow mostly results from increased precipitation in the region. Although evapotranspiration also increases, it does not compensate for the increase in precipitation.

2.3.5. *Cooling potential will decrease under climate change*

Cooling potential (equation (2.1)) is influenced by both streamflow and stream temperature. During the historical period, cooling potential is greater in the regulated scenario for river segments downstream of reservoirs with strong thermal stratification, e.g., the Savannah River and the upper reaches of the Tennessee River (green in Figure 2.5d). Downstream of reservoirs with little to no thermal stratification, the cooling potential tends to be lower in the regulated scenario because reservoir operations and water withdrawals lead to lower summer streamflow than in the unregulated scenario, e.g., mainstem Ohio River (blue in Figure 2.5d).

Stream temperature is projected to increase in all GCM projections, contributing to a reduction in cooling potential. At the same time, streamflow is projected to increase in most GCMs, increasing cooling potential by increasing the thermal mass. The combined effects result in a net decrease in projected cooling potential during the summer by the 2080s for most GCM projections under RCP 8.5 (blue in Figure 2.5c). Therefore, the change in cooling potential is dominated by projected increases in stream temperature.

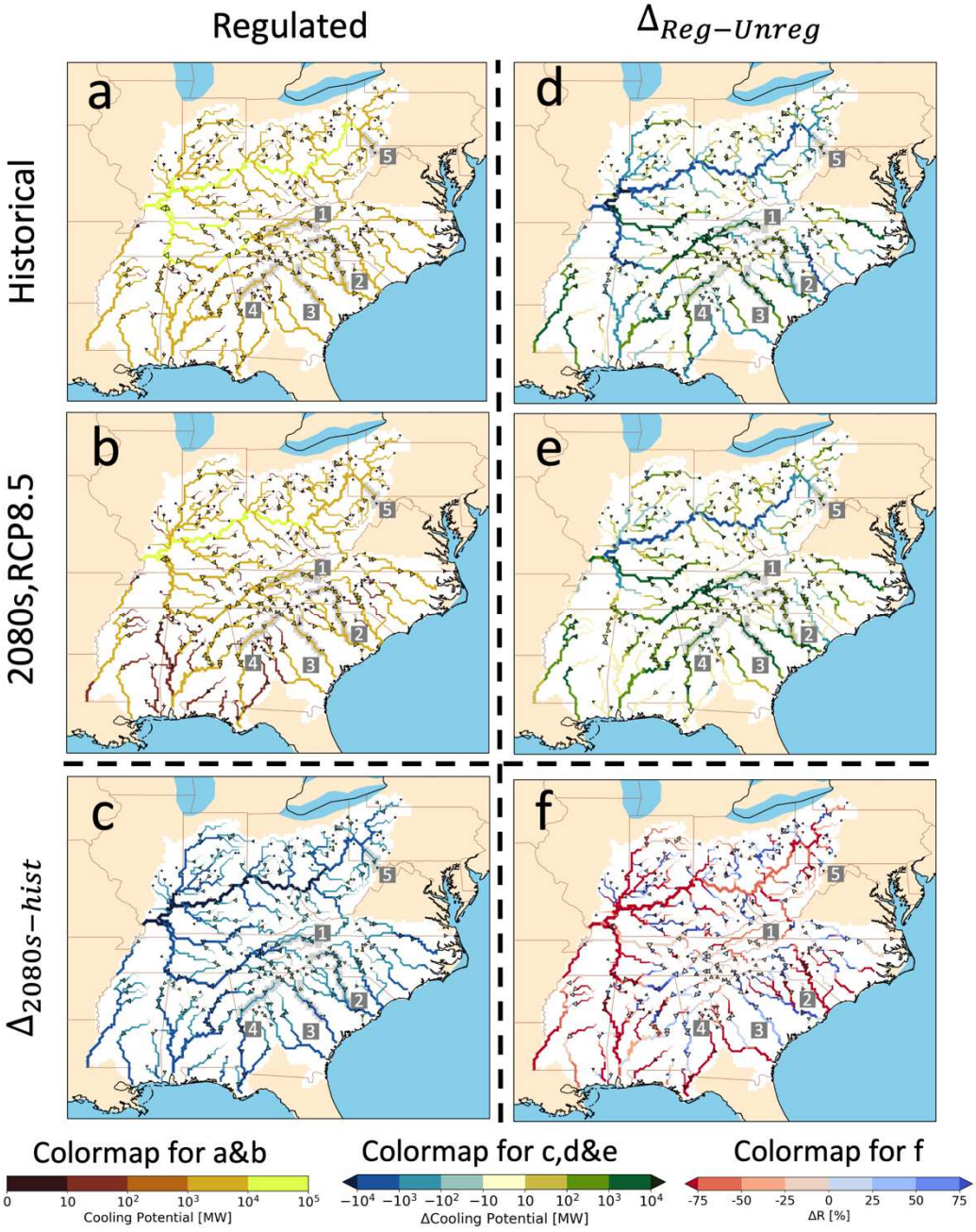

Figure 2.5. Spatial maps of regulated cooling potential for (a) historical period and (b) 2080s under RCP8.5; climate change impacts on regulated cooling potential under RCP8.5 (c, $\Delta E_{cp(reg,2080s-reg,hist)}$); difference of cooling potential between regulated and unregulated model setups for (d) historical period and (e) 2080s under RCP8.5 and (f) the change in the effect of regulation on cooling between the future and historic periods (Eqn. (2.2)).

Larger rivers tend to show a greater loss in cooling potential than smaller rivers because of their greater thermal mass, e.g., the Ohio River, the largest river in our study region. Over most of its length, the Ohio River will lose over 10 GW (10^4 MW) of cooling potential by the 2080s under RCP8.5. Regulation impacts on cooling potential for the historical period and the 2080s under RCP8.5 are shown in Figure 5d and 5e, respectively. Rivers with reservoirs that experience strong thermal stratification (Figure 2.3b and Figure 2.4b) have more cooling potential under the regulated scenario in both the historical and future periods. Rivers with reservoirs that do not stratify, have less cooling potential in the regulated scenario (Figure 2.5d and Figure 2.5e). For these rivers, regulation reduces cooling potential because of water withdrawals and lower summer streamflow.

Figure 2.5f summarizes whether the impact of regulation on cooling potential will increase or decrease in the future. If ΔR value is close to 0%, regulation impacts on cooling potential will persist under climate change. If ΔR approaches -100%, regulation impacts will mostly disappear. For river segments downstream of reservoirs with strong seasonal thermal stratification, the regulation impact on cooling potential remains strong in the future, with ΔR mostly larger than -25% (Figure 2.5f). For river segments minimally impacted by upstream thermal stratification, regulation impacts on cooling potential decrease dramatically by the 2080s under RCP8.5 ($\Delta R <$ -75%; Figure 2.5f). For these river segments, the effect of regulation on cooling potential largely disappears by the 2080s.

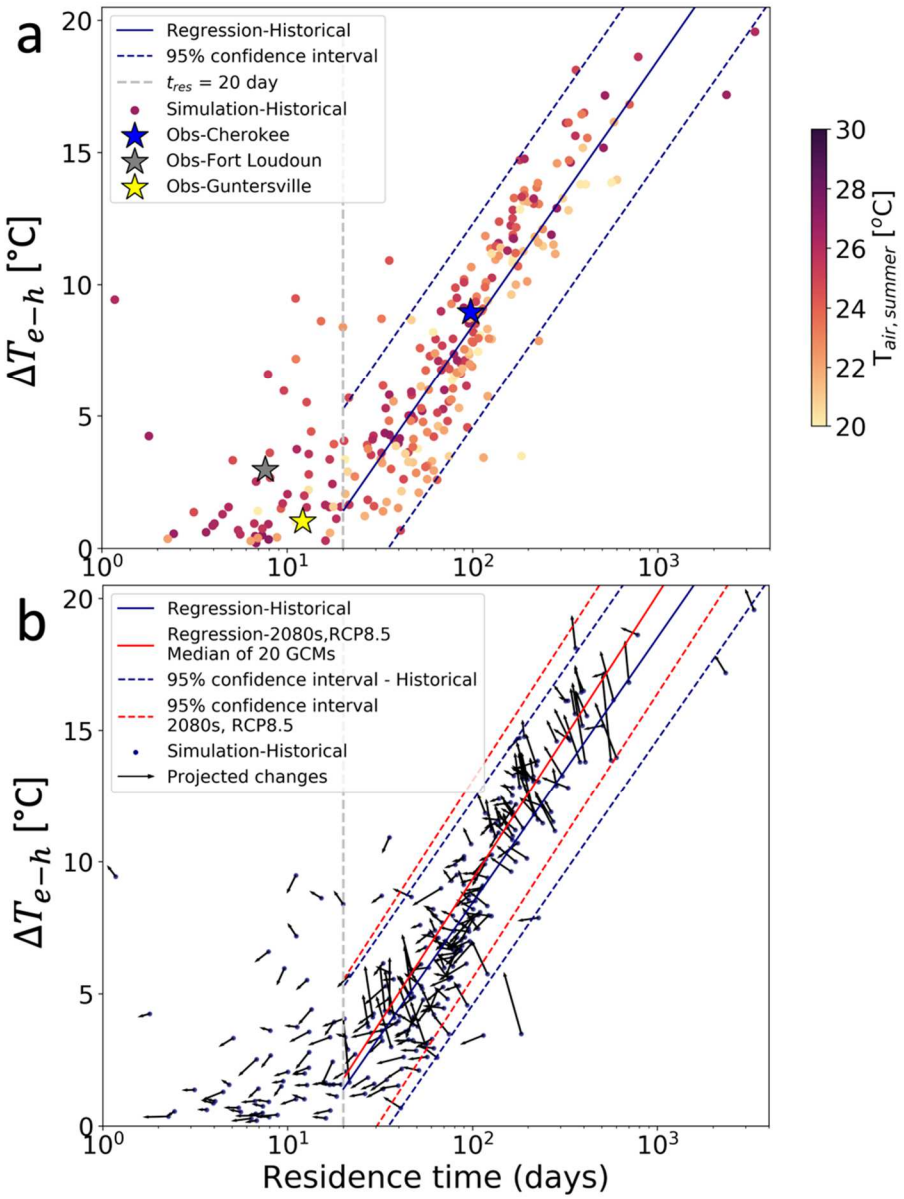

Figure 2.6. (a) Simulated reservoir thermal stratification versus residence time during the historical period. Each dot represents the simulated result for one reservoir during the historical period. The dot color represents the mean air temperature at each reservoir location. Stars represent the observations, with blue, grey and yellow stars representing Cherokee, Fort Loudoun and Guntersville Reservoirs, respectively. (b) Climate change impacts on the relationship between thermal stratification and residence time. Each dot is the same as in (a) with an arrow pointing to the median simulated result (20 GCMs) by the 2080s under RCP8.5 for the same reservoir.

2.4. DISCUSSION

2.4.1. *Reservoir residence time and thermal stratification*

We used the mean summer temperature difference between the epilimnion and the hypolimnion (ΔT_{e-h}) as a measure of thermal stratification, with larger values indicating stronger stratification. To quantify the impacts of reservoir residence time on thermal stratification, we compared simulated residence times and corresponding ΔT_{e-h} values for all 271 (Figure 2.6a). Thermal stratification is weak when the reservoir residence time is shorter than 20 days. For reservoirs with a simulated residence time greater than 20 days, we fitted a log-linear regression model for ΔT_{e-h} as a function of residence time. Confidence intervals (95%) for the predicted ΔT_{e-h} values were calculated based on Devore (2011) and are shown as dashed lines in Figure 2.6. For the three reservoirs for which we have observations of reservoir storage, outflow and reservoir temperatures with depth, we calculated the mean residence time and ΔT_{e-h}values (stars in Figure 2.6a). Of these three, only Cherokee Reservoir had a residence time longer than 20 days. Fort Loundon and Guntersville reservoirs have short residence times of 8 and 12 days, respectively, and their thermal stratification is weak.

By the 2080s under RCP8.5, thermal stratification will be stronger in about half the reservoirs. This finding is somewhat counterintuitive. Because we assume that the future guide curves will remain the same as for the historic period, increased streamflow results in reduced reservoir residence time by the 2080s (arrows generally point left in Figure 2.6b) and should therefore lead to weaker stratification (Figure 2.6a). Median residence time of all 271 reservoirs is projected to decrease from 69 days (historic) to 60 days (2080s). This decrease in residence time should be accompanied by a median decrease in thermal stratification of 0.7ºC (Figure 2.6a). While some smaller reservoirs with shorter residence times show the expected decrease in thermal stratification, median thermal stratification for all reservoirs is almost identical in the historic and future scenarios and about half of the reservoirs (135 out of 271) are more stratified by the 2080s, especially larger reservoirs with longer residence times (black arrows to the right in Figure 2.6b).

This counterintuitive result occurs because thermal stratification is also influenced by surface energy exchange during the summer season. In general, thermal stratification increases with increasing air temperature for reservoirs with similar residence times (Figure 2.6a). As air temperature increases along with stronger solar radiation, the epilimnion temperature increases

faster than the hypolimnion temperature because the latter is warmed only by advective and diffusive energy exchange with the epilimnion. As a result, seasonal thermal stratification in our study region is stronger as air temperature increases, resulting in a change in slope in the relationship between residence time and thermal stratification under climate change (contrasting red and blue lines in Figure 2.6b).

2.4.2. *Stream temperature and cooling potentials downstream of reservoirs*

Cold hypolimnetic releases equilibrate with the environment as a result of surface heat fluxes. Reservoir impacts on river thermal regimes dissipate completely when stream temperatures reach the unregulated river temperature. The distance it takes from the reservoir outlet to reach the unregulated river temperature is influenced by both streamflow and surface energy fluxes.
We used the model simulations performed in support of the sensitivity analysis (Section 2.2.5) to evaluate the relative contribution of streamflow and surface meteorology to the tailwater thermal regimes. In reality, it is not feasible to directly calculate the distance to reach the unregulated river temperature, because reservoir outflow might not reach this temperature before it flows into a downstream reservoir or merges with another stream. Instead, we evaluated the impacts of surface meteorology by comparing downstream temperatures at a fixed distance downstream of a reservoir for the cold, medium and hot scenarios (Section 2.2.5).

Surface meteorology has a strong impact on tailwater thermal regimes. For example, median outflow temperature increases 6.8°C, 7.4°C and 9.0°C under cold, medium, and hot scenarios, respectively, 50 km downstream of Youghiogheny Reservoir (Figure 2.7). Even though the thermal stratification is stronger in the hot scenario, the temperature of the released water also increases more rapidly downstream of the reservoir. Regulated stream temperature is relatively insensitive to changes in streamflow, in part because we use the same guide curves for all scenarios. In spite of the large spread in simulated streamflow, the spread in outflow temperature from Youghiogheny Reservoir across the twenty different hydrological inputs reduces from 3°C to about 0.2°C within 50 kilometers (Figure 2.7).

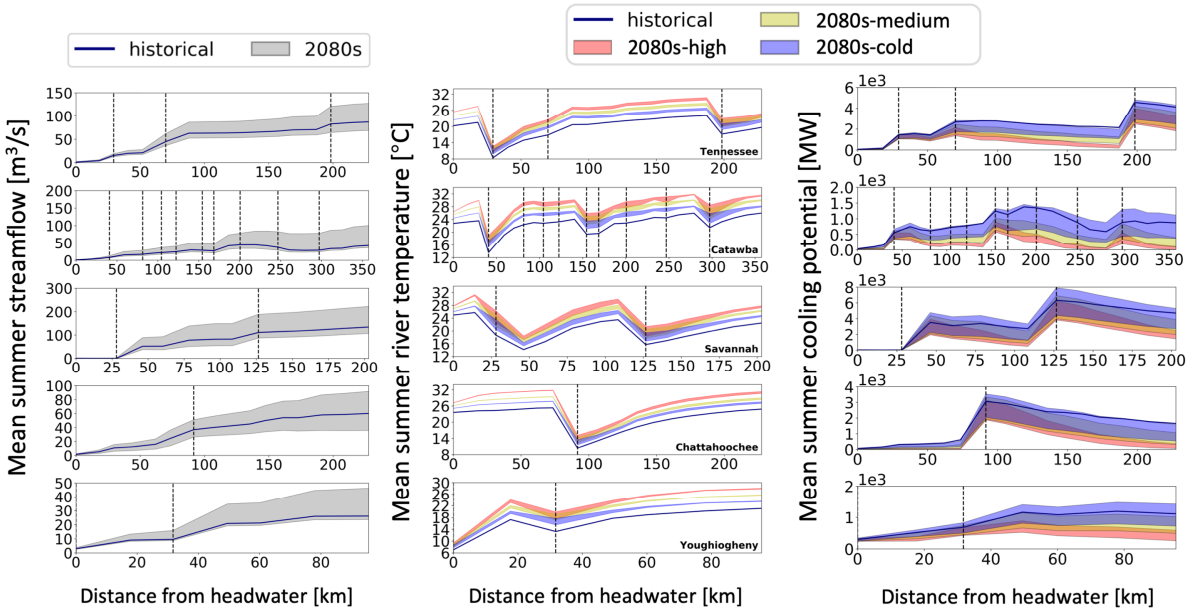

Figure 2.7. Sensitivity experiment: mean summer streamflow (left), stream temperature (middle), and cooling potential (right) profiles for the historical period and the 2080s under RCP8.5 along five selected river channels, i.e., Tennessee River, Catawba River, Savannah River, Chattahoochee River, and Youghiogheny River (from top to bottom). In the left panel, the grey shaded area denotes ranges of projected mean summer streamflow. In the middle and right panels, the shaded areas denote the ranges in projected mean summer river temperature and cooling potential, respectively. The vertical dashed lines denote dam locations.

Immediately downstream of reservoirs, cooling potential is impacted by changes in stream temperature as well as changes in streamflow. Compared to unregulated rivers, cold outflow from stratified reservoirs increases the cooling potential (Eq. 1), and the amount of flow (Q) is also different than in unregulated rivers. Once the stream temperature approaches the unregulated river temperature, regulation impacts cooling potential only by altering streamflow.

2.4.3. *Sensitivity to errors in hydrology*

In this section, we limit our analysis to river segments subject to regulation (*m*=true) and compare their behavior in the regulated and unregulated model setups (*r*=reg, unreg). Analysis (not shown) revealed that the sensitivity of river segments not subject to regulation (*m*=false) is similar to the sensitivity of river segments subject to regulation in the unregulated model setup (*m*=true, *r*=unreg).

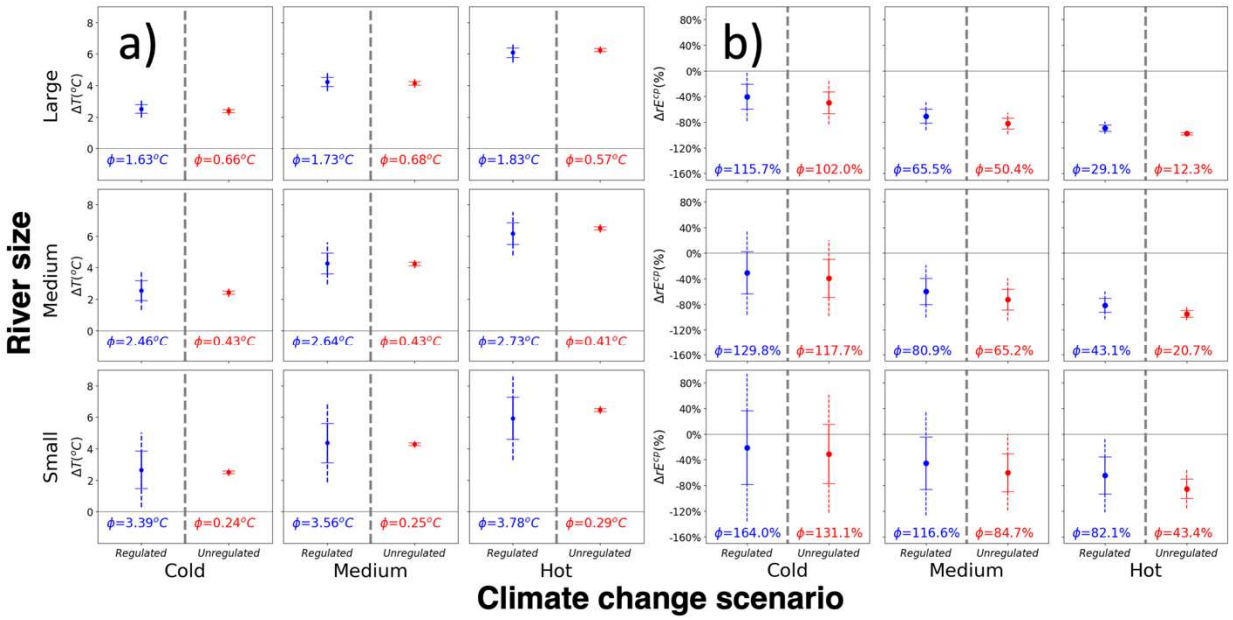

Figure 2.8. Projected changes in (a) mean summer river temperature and (b) mean summer cooling potential by river size and climate changes scenarios. Estimates are provided for river segments subject to regulation (m=true) for both the regulated (r=reg; blue) and unregulated (r=unreg; red) model setups. The solid and dashed bands around the mean denote one and two times the error in the estimates (σˆ in Eqn. (2.6)) as a result of hydrological errors.

Figure 2.8a shows the projected increases in mean summer stream temperature (ΔT) as well as our estimate of the error ($\hat{\sigma}_{\widetilde{\Delta T}}$). This error only reflects the effects of errors in the hydrological simulations. Each panel shows $\Delta T \pm \hat{\sigma}_{\widetilde{\Delta T}}$ (solid line) and $\Delta T \pm 2\hat{\sigma}_{\widetilde{\Delta T}}$ (dashed line) for the regulated and unregulated scenario. Projected increases in mean summer temperature range from +2°C to +6°C while the hydrology-induced errors ranges from 0.09°C to 1.33°C. The hydrology-induced error in stream temperature is greatest immediately downstream of reservoirs (Figure 2.7) and gradually decreases as the river flows downstream.

River segments in the regulated model setup (*m*=true, *r*=reg) are more sensitive to errors in hydrology ($\hat{\sigma}_{\widetilde{\Delta T}}$ ranges from 0.27°C to 1.33°C) than the same segments in the unregulated model setup (*m*=true, *r*=unreg; $\hat{\sigma}_{\widetilde{\Delta T}}$ ranges from 0.09°C to 0.11°C). This is especially true for small river segments which have greater ϕ values than larger rivers (*m*=true, *r*=reg). While ϕ

values differ across river size and whether we represent the effects of regulation (*r*=reg, unreg), they are similar across all three climate change scenarios.

Figure 2.8b shows the same information as Figure 2.8a, but for the change in cooling potential rather than change in mean summer temperatures. Errors in the hydrological simulations have the largest effect on the relative change in cooling potential for small rivers ($\bar{Q}$<50m^3/s) under the cold scenario. In that case, mean projected relative changes in cooling potential ($\overline{\Delta r E^{cp}}$) are -21.0% and -31.0% while the hydrology-induced errors ($\hat{\sigma}_{\widehat{\Delta r E^{cp}}}$) are 46.0% and 57.6% for regulated and unregulated model setups, respectively (Figure 2.8b). In all other cases, the $\overline{\Delta r E^{cp}}$ values are larger than the $\hat{\sigma}_{\widehat{\Delta r E^{cp}}}$ (upper bound of solid line is below zero in Figure 2.8b), implying that the sign of the change is not sensitive to the errors in hydrology in our simulations. Uncertainties in the relative change in cooling potentials decrease with increasing river size and increases with projected air temperature. Reservoir regulation does not have a strong impact on the sensitivity of the relative change in cooling potentials to hydrologic errors, with similar $\phi_{\widehat{\Delta r E^{cp}}}$ values for regulated and unregulated river segments (Figure 2.8b).

Overall, we conclude that the errors in our hydrological simulations affect our quantitative estimates of changes in stream temperature and cooling potential in the following way. Errors in our change estimates are greater in the regulated model setup (*r*=reg) than the unregulated setup (*r*=unreg) and are largest for the smaller river segments. However, in general, the errors do not affect the sign of the change signals nor the relative ranking of the change signals across river sizes, regulation status or climate scenario. The effect of hydrological simulations on changes in mean summer stream temperature for river segments not affected by regulation (*m*=false) is small.

2.5. CONCLUSION

River temperatures play an important role in aquatic ecosystems and affect the efficiency of once-through thermoelectric power plants. In this study, we applied a physically-based model chain to simulate hydrology and stream temperature for a large part of the southeastern United States. Seasonal thermal stratification was explicitly represented. We used an ensemble of future climate forcings to quantify the impacts of climate change on the summer stream temperatures and cooling potential of southeastern rivers for the 2080s. The model chain was applied with and without water management to quantify changes in the effect of regulation on cooling potential as

a result of climate change. We evaluated reservoir flow, storage, and stream temperature, along with their interactions and the overall response to climate change, which has not been done before. The novel cooling potential approach provides a new opportunity to support multi-sectoral long-term planning. We conducted a sensitivity analysis to quantify the robustness of our findings to errors in the hydrological simulations. Our approach has the advantage that it provides a consistent evaluation over a region that spans multiple watersheds, where water management decisions may affect stream temperatures. This region may be defined by institutional governance for natural conservation, electricity operations, and other activities. The approach is applicable to other, individual watersheds, although we would recommend using operational water management models for the basin of interest to simulate the hydrology.

We would like to highlight a few areas for further research and improvement. Reservoir operations are more complex than the generic operating rules or rule curves used in this study. More complex rules that use foresight and optimization across the system could be considered, especially if these rules are allowed to change with time. An explicit link with power system models could further our understanding of the response to local stresses as well as feedbacks onto electricity operations and downstream river systems. For example, Miara et al.(2018) demonstrated the dynamic link with power system operations but lacked the representation of reservoir operations and their impact on stream temperature. Finally, to isolate the effects of changes in meteorological forcings in a changing climate, we kept land use and urbanization constant in our model simulations, even though they may impact both hydrology and stream temperature. Explicit representation of these changes may enhance our understanding of the co-evolution of complex interconnected systems.

Major findings are as follows:

- Reservoir regulations, and the resulting seasonal thermal stratification, influence downstream river temperatures. Reservoirs with longer residence times are more stratified and store cold water from earlier seasons in their hypolimnion. They therefore have stronger impacts on downstream river temperatures. Among reservoirs with similar residence times, thermal stratification tends to be stronger in warmer locations where reservoirs are subject to stronger surface energy fluxes.
- Reservoir regulation changes how river temperature responds to climate change, especially through changing thermal stratification. Summer stream temperatures in

regulated rivers are lower than those in unregulated rivers, but they are more sensitive to climate change. By the 2080s under RCP8.5, compounded impacts of higher air temperature and shorter residence times result in stronger thermal stratification for over half of all reservoirs in the SEUS, especially for reservoirs with longer residence times. Thermal stratification impacts on downstream river temperatures mostly persist but are slightly weakened, because of higher air temperature and stronger surface energy inputs.

- Cooling potential is the energy required to warm rivers to a threshold temperature and represents a river system's ability to absorb waste thermal energy from thermoelectric power plants if environmental regulations are enforced, indicating the compound impacts of both streamflow and stream temperature. For rivers experiencing strong thermal stratification impacts, regulation increases cooling potential immediately downstream of reservoirs because the cooling impact on downstream river temperature dominates the signal. For rivers minimally impacted by thermal stratification, regulation decreases cooling potential because of lower summer streamflow under reservoir regulation.
- Cooling potential is projected to decrease for all river segments under climate change. The Ohio River will lose over 10 GW cooling potential for most of its length by the 2080s under RCP8.5. Regulation changes how cooling potential responds to climate change. Regulation impacts on cooling potential remain strong when rivers are strongly influenced by thermal stratification ($\Delta R > -25\%$, Figure 2.6f) because cooling impacts on downstream river temperatures mostly persist under climate change. For rivers minimally impacted by thermal stratification, the magnitude of regulation impacts on cooling potential decreases dramatically ($\Delta R < -75\%$, Figure 2.6f) because river temperatures are higher by the 2080s under RCP8.5.
- Sensitivity analyses show that our findings about climate change effects on mean summer river temperature and cooling potentials are relatively insensitive to errors in the hydrological simulation. Mean summer temperatures in smaller rivers tend to be more sensitive to errors in hydrology than those in larger rivers. Mean summer temperatures in regulated river segments are much more sensitive to

hydrological errors than those in unregulated river segments. However, regulation has little impact on the sensitivity of changes in cooling potential to hydrological errors.

ACKNOWLEDGEMENT

This project was funded in part by NOAA grant NA14OAR4310250 and NSF grant EFRI-1440852 to the University of Washington. We also wish to thank the Tennessee Valley Authority for providing data, and Xiao Zhang at Pacific Northwest National Laboratory for help with routing and water management model setup. We acknowledge the World Climate Research Programme's Working Group on Coupled Modelling, which is responsible for CMIP, and we thank the climate modeling groups (listed in Table S2 in the Supporting Information) for producing and making available their model output. For CMIP the U.S. Department of Energy's Program for Climate Model Diagnosis and Intercomparison provides coordinating support and led development of software infrastructure in partnership with the Global Organization for Earth System Science Portals. The source codes for the models used in this study are publicly available as follows: MetSim v2.0.0 — https://github.com/UW-Hydro/MetSim; VIC v.5 — https://github.com/UW-Hydro/VIC; MOSART-WM — https://github.com/IMMM-SFA/wm; RBM-2L — https://github.com/UW-Hydro/RBM/tree/RBM_res_develop.

Chapter 3 THERMAL EXTREMES IN REGULATED RIVER SYSTEMS UNDER CLIMATE CHANGE: AN APPLICATION TO THE SOUTHEASTERN U.S. RIVERS

This chapter has been accepted for publication in its current form in the *Environmental Research Letters*. © IOPscience. Used with permission. The supplemental material for this chapter is provided in appendix B.

Cheng, Y., N. Voisin, J. Yearsley, and B. Nijssen, 2020: Thermal extremes in regulated river systems under climate change: an application to southeastern U.S. rivers. Environmental Research Letters, accepted. doi:10.1088/1748-9326/ab8f5f

ABSTRACT

High river temperatures, or "thermal extremes", can cause fish mortality and thermoelectric powerplant derating. Under climate change, projected higher air temperature and stronger surface energy fluxes will lead to increased water temperatures, exacerbating thermal extremes. However, cold hypolimnetic releases from thermally stratified reservoirs can depress tailwater temperatures and therefore alleviate thermal extremes. Thermal extremes are more harmful when they coincide with low flows, which we refer to as "hydrologic hot-dry events". To assess multi-sectoral impacts of climate change over large regions, we evaluate thermal events according to three impact attributes: duration (D), intensity (I), and severity (S). We apply an established model framework to simulate streamflow and stream temperature over the southeastern US regulated river system. We quantify climate change impacts (by the 2080s under RCP8.5) by comparing historical and future periods and quantify regulation impacts by comparing unregulated and regulated model setups. We find that climate change will exacerbate thermal extremes (all three metrics) in both unregulated and regulated model setups, albeit less in the regulated setup. Thermal mitigation from reservoir regulation will be stronger under climate change, decreasing the three metrics compared to the unregulated case. Even so, thermal extremes in the regulated setup will still be more severe under climate change, and only 12.2%, 19.7%, and 26.0% of D, I, and S can be mitigated by reservoirs. Despite stronger reservoir stratification, the number of regulated river segments that experience simultaneous high

temperature and low flow events (hydrologic hot-dry events) will increase by 21.4% by the 2080s under RCP8.5. These events will have a median annual duration of 10.3 days/year, over 10 times the historical value.

3.1. INTRODUCTION

High river temperatures have negative impacts on aquatic ecosystems and power sectors (Ketabchy et al., 2018; Koch & Vögele, 2009; Sauter et al., 2001). Excessive heat reduces dissolved oxygen and increases metabolism of cool- and cold-water fish, causing them to burn essential energy at a faster rate (Breau et al., 2007; Coutant, 1990) and results in death when river temperature exceeds their physiological limits (Eaton et al., 1995). Furthermore, high river temperatures can disrupt the operations of thermoelectric power plants by 1) lowering power plant operating efficiency and maximum generation capacity and 2) causing power curtailment or even shutdown to avoid violating environmental regulations (Liu et al., 2017). McCall et al. (2016) assessed that 27 of 36 US power plant curtailments during 2000 – 2015 resulted from high river temperatures. Studies have shown that the projected climate change trend of increasing global river temperatures will impose greater thermal stress (Eaton & Scheller, 1996; van Vliet et al., 2011; van Vliet, Vögele, et al., 2013). In this study we focus on extreme high river temperature events in regulated river systems, referred to as “thermal extremes”.

Cold hypolimnetic outflow from reservoirs, i.e. releases from deeper reservoir layers, can alleviate thermal extremes in regulated river systems. During warm seasons, deep reservoirs with long residence times are thermally stratified and cold hypolimnetic releases depress downstream river temperature (Chapra, 1997). As a result, peak river temperature and the annual temperature range decrease at tailwater locations, suppressing the occurrence of thermal extremes (Cheng et al., 2020). As almost all global major river systems are highly regulated, quantifying the mitigation impacts due to reservoir regulation is valuable for regional risk management.

The detrimental impacts of thermal extremes will be exacerbated when they coincide with low flows. Besides intense thermal stress, concurrent low flow can expose the shallow river system to strong insolation, elevate solute concentrations, and constrain fish mobility, preventing them from seeking more favorable shelters (Bradford & Heinonen, 2008; Matthews & Zimmerman, 1990). Under these circumstances, thermoelectric power plants may also be unable

to generate at full capacity due to a lack of sufficient cooling water (Rutberg, 2012; van Vliet, Yearsley, Ludwig, et al., 2012).

We focus on the southeastern United States (SEUS), which is a global hotspot of freshwater biodiversity. Two-thirds of US fish species exist here, and these fish are vulnerable to changes in river thermal regimes (Elkins et al., 2016). Historical river temperatures in the region already approach the limit set by environmental regulations (Cheng et al., 2020; Liu et al., 2017; Madden et al., 2013). High air temperatures in the region result in a high electricity demand for air conditioning (Auffhammer et al., 2017). These conditions often coincide with river thermal extremes and low flows, thus limiting the cooling potential for power plants that depend on river water. As a result, the electricity sector in the SEUS may be exposed to higher risks under climate change (Kimmell & Veil, 2009).

The objective of this study is to characterize extreme thermal events with attributes that can support risk management, i.e. duration-intensity-severity, and evaluate climate change impacts on thermal extreme events in a large, regulated river system. This characterization is standard in drought research but has not been applied to fluvial thermal events due to limited capability in simulating river temperatures for complicated river-reservoir systems. A recent innovation of a regional-scale spatially-distributed modeling framework enables us to directly quantify the impact of reservoir regulation on thermal extremes (Cheng et al., 2020). We use this framework to examine the impact of climate change on thermal extremes and on concurrent high stream temperature, low flow events, which we term hydrologic hot-dry events. This work can be used to inform existing multi-sectoral impact assessments as well as adaptation planning at relevant scales, especially for the freshwater fisheries and power sectors.

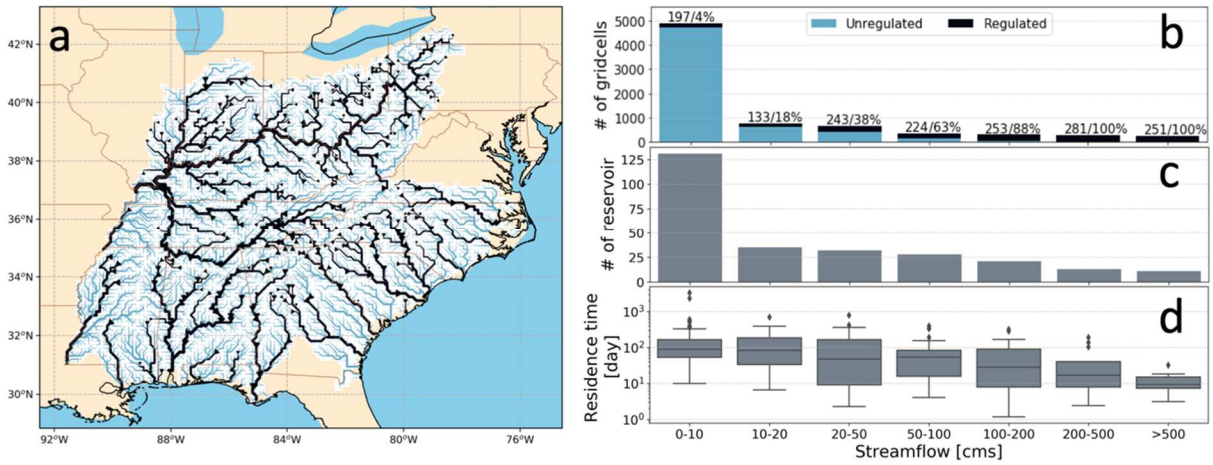

Figure 3.1. (a) Spatial map of the study's regulated river system. Panel (b) displays the number of grid cells at different river sizes, with the bars divided according to grid cells influenced by regulation (black) and unregulated grid cells (light blue). Numbers on top of each column denote number of regulated grid cells (left) and its percentage of total grid cells under each river size. The color scheme of panel (b) is also used to label streams in the domain map. Panels (c) and (d) show the number of reservoirs and distribution of residence time at different river sizes.

3.2. METHODS

3.2.1. *Study domain and reservoir information*

Our study domain (Figure 3.1a) consists of the SEUS and contains 271 major reservoirs. In our model setup (see Section 3.2.2) 21% of river segments are located downstream of these 271 reservoirs and therefore are subject to regulation. This includes all river segments in large rivers, those with average annual flow ($\overline{Q_a}$) greater than 200 m^3/s (Figure 3.1b). About half the reservoirs are located in small streams, for which $\overline{Q_a}$ is less than 10 m^3/s. The remaining 79% of river segments are located upstream of one of these reservoirs.

Reservoir outflow and residence times determine the extent to which reservoirs impact tailwater temperatures. Reservoirs with larger outflow influence temperature farther downstream because 1) their outflows are less affected by mixing of flows from smaller tributaries and 2) larger rivers respond less rapidly to surface energy fluxes because they generally have a smaller surface area to volume ratio. Reservoirs with longer residence times have stronger seasonal thermal stratification and therefore have stronger cooling impacts on downstream river

temperatures. Reservoir residence time generally decreases with increasing river sizes (Figure 3.1c). In the following analysis only grid cells influenced by reservoir regulation (black segments in Figure 3.1a) will be analyzed.

3.2.2. *Model setup*

In this study, we used the physically-based modeling framework as applied in Cheng et al. (2020) to simulate streamflow and stream temperature for the entire river network of the SEUS, considering reservoir regulation and thermal stratification. This model framework includes a spatially distributed hydrological model (Variable Infiltration Capacity model or VIC, Hamman et al., 2018; Liang et al., 1994), a large-scale river routing model (Model for Scale Adaptive River Transport or MOSART, Li et al., 2013) that is dynamically coupled with a water management model (WM, Voisin, Li, et al., 2013), and a distributed river temperature model (River Basin Model or RBM, Yearsley, 2009, 2012). RBM includes a two-layer thermal stratification module (2L, Niemeyer et al., 2018).

This model framework was run at a daily time step with a latitude-longitude resolution of 1/8 degree (~12km). For the historical period (1980-2009), we used gridded meteorological forcing data, gridMET (Abatzoglou, 2013), as input into the model chain. The future period spans from 2070-2099 and is referred to as the 2080s. For the 2080s, we used an ensemble of meteorological forcing data from 20 global climate models (GCMs; Table B.1) based on a high carbon emission scenario (RCP8.5) from the Coupled Model Intercomparison Project, Phase 5 (CMIP5; Taylor et al., 2012), downscaled using the Multivariate Constructed Analog (MACA; Abatzoglou & Brown, 2012) method. We selected RCP8.5 because it is the highest carbon emission scenario and represents the greatest warming among RCPs. To quantify the impacts of reservoir regulation, we conducted an experiment in which we simulated streamflow and stream temperature for both regulated and unregulated model setups. The baseline (unregulated) setup is one in which there are no impoundments in the river system. In the regulated setup, we explicitly considered reservoir regulation, thermal stratification, and water withdrawal. To isolate the impacts of climate change in a regulated system, reservoir regulations remain the same for both historical and future periods. Because release information for individual reservoirs is generally lacking, we assume that all reservoirs release water from the hypolimnion, as in Cheng et al. (2020). Consequently, our results provide a lower bound estimate of reservoir release temperatures and thus an upper bound estimate of the extent to which reservoir regulation can

alleviate thermal extremes. For more details concerning the model configuration, evaluation and errors, we refer to Cheng et al. (2020). A summary of model performance for the historic period is provided in the Supporting Information (Text B.1.1).

3.2.3. *Three metrics to evaluate thermal extremes*

We define thermal extreme events as periods when river temperatures exceed a threshold temperature (T_{thres}). We used three metrics to characterize thermal extreme events: duration, intensity and severity, each explained below. These three metrics, when combined, provide a comprehensive characterization to support multi-sectoral impact assessments and adaptation strategies.

Duration, D (day/period), measures the length of thermal extreme events within a defined period (e.g., per month). Extreme event durations are compared to the maximum lengths of bearable stressful periods for fish or power plants. While limited durations may be acceptable, durations that are too long can result in fish mortality and power plant shutdowns. For a defined period of time (from t_{start} to t_{end} in Figure 3.2a), duration is the total time during which the river temperature exceeds T_{thres} as in

$$D = \sum_{i=1}^{n} (t_{te}^{i} - t_{ts}^{i}) \tag{3.1}$$

where t_{ts} and t_{te} represent the starting and ending time, respectively, of intervals during which the river temperature exceeds T_{thres} and n represents the number of periods.

Intensity, I (°C), is the maximum excursion of the stream temperature above T_{thres} during a specific interval,

$$I = \begin{cases} T_{max} - T_{thres} & \text{if } T_{max} > T_{thres} \\ 0 & \text{if } T_{max} \leq T_{thres} \end{cases} \tag{3.2}$$

where T_{max} is the maximum river temperature within the defined time period. Intensity is zero if the river temperature never exceeds T_{thres}. When intensity reaches a certain value, it may lead to immediate fish mortality or complete shutdown of power plants if environmental regulations are enforced.

Severity, S (°C·day/period), quantifies the cumulative impacts of thermal extremes and is widely used in fish models (Chezik et al., 2014; Trudgill et al., 2005) and power curtailment models (McDermott & Nilsen, 2014). Severity is the time integrated value of the river temperature above T_{thres} within a defined period (red highlighted area in Figure 3.2a).

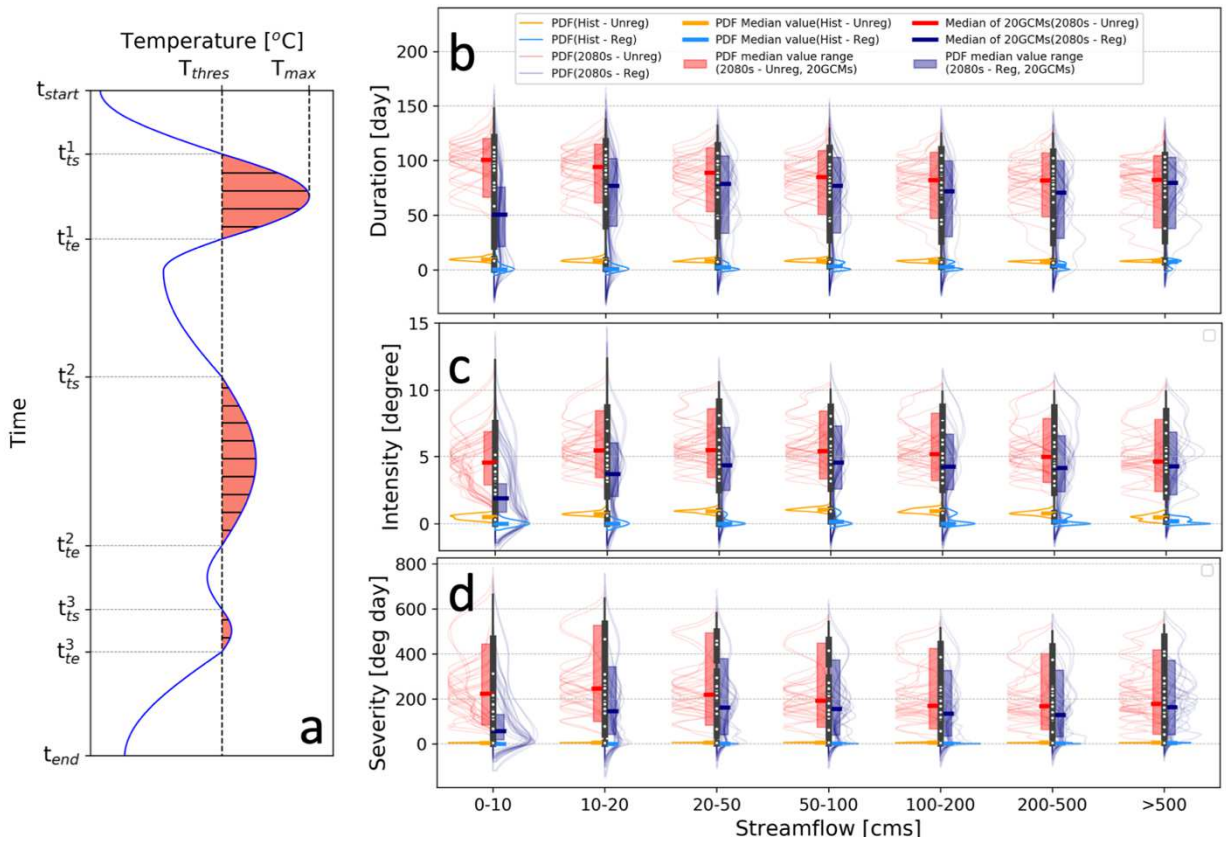

Figure 3.2. (a) Diagram to explain attributes of temperature timeseries used by this paper, i.e., duration, intensity and severity. Panels (b), (c), and (d) respectively show the distribution of mean annual duration, intensity, and severity of thermal extreme events for different river sizes separated according to the horizontal axis at the bottom of the figure. Left (orange and red) and right (blue and navy) sides of the vertical distributions denote unregulated and regulated model setups, respectively. Orange and blue are for the historical period; red and navy are for the 2080s under RCP8.5. Thin lines display smoothed probability density functions (PDFs) of each different GCM; shaded areas represent ranges of median values of PDFs for 20 GCMs by the 2080s under RCP8.5; thick horizontal lines represent PDF median values for the historical period and median of PDF median values among all 20 GCMs for the future period.

Defining a single T_{thres} for the entire region is infeasible as a result of the diversity of fish species and the different power plant regulations in an area as large as our study region. We use the simulations for the historical period to define a spatially-varying T_{thres}, with a separate value for each model grid cell. We selected the maximum weekly average stream temperature with a recurrence interval of 2 years or 7T2 as our threshold temperature. Each 7T2 value was calculated from the 30-year time series of simulated unregulated temperatures for the historical period. While the maximum weekly average temperature is a widely used metric in defining an upper temperature tolerance for freshwater fishery (Eaton et al., 1995; Welsh et al., 2001) the addition of a return period (as in the 7T2) makes the method more robust to individual outliers. The 7T2 is analogous to the widely used 7Q2 metric mentioned in the next section. We calculate each of the three metrics for both regulated and unregulated model setups to quantify the regulation impacts on thermal extremes, and for both historical and future periods to quantify the overall impacts of climate change.

We conducted a sensitivity analysis to evaluate the robustness of our findings to our selection of thresholds values. We selected the maximum weekly average stream temperature with recurrence intervals of two, five, ten and twenty years, or 7T2, 7T5, 7T10, and 7T20, respectively, and repeated our analysis (see Section 4).

3.2.4. *Concurrence of thermal extremes and low flows*

Low flow events, also known as hydrologic drought, are defined as periods when streamflow falls below a threshold (Q_{thres}). We use the 7Q2 value, which is the minimum weekly average streamflow with a recurrence interval of 2 years. The 7Q2 value has been widely used as a low flow metric for maintenance of aquatic ecosystems and water quality (Ontario Ministry of Natural Resources and Watershed Science Centre, 2001; Pyrce, 2004). The 7Q2 values were based on simulations under the regulated setup to account for water withdrawals. Concurrence of thermal extremes (TE) and low flows (LF) is defined as a period when the river temperature exceeds T_{thres} while streamflow falls below Q_{thres}. We refer to these periods as hydrologic hot-dry events ($TE \cap LF$).

To summarize the spatial and temporal heterogeneity of hydrologic hot-dry events, we grouped all regulated grid cells into different river size categories and organized the time series by month for each category. We calculated the conditional probability of hydrologic hot-dry events given that thermal extreme events had already happened, i.e., $P_{R,M}(TE \cap LF|TE)$, and the

conditional probability of hydrologic hot-dry events given that low flow events had already happened, i.e., $P_{R,M}(TE \cap LF|LF)$,

$$P_{R,M}(TE \cap LF|TE) = \frac{P_{R,M}(TE \cap LF)}{P_{R,M}(TE)} \quad (3.3)$$

$$P_{R,M}(TE \cap LF|LF) = \frac{P_{R,M}(TE \cap LF)}{P_{R,M}(LF)} \quad (3.4)$$

where $P_{R,M}(TE \cap LF)$, $P_{R,M}(TE)$ and $P_{R,M}(LF)$ denote the probability of hydrologic hot-dry events, thermal extremes and low flows, respectively, occurring at river size *R* and month *M*. Note that $P_{R,M}(TE \cap LF|LF)$ can be simplified to $P_{R,M}(TE|LF)$ and $P_{R,M}(TE \cap LF|TE)$ can be simplified to $P_{R,M}(LF|TE)$. When $P_{R,M}(LF|TE)$ exceeds $P_{R,M}(TE|LF)$, a hydrologic hot-dry event is more likely to occur in case of a thermal extreme event rather than a low flow event.

3.3. RESULTS

3.3.1. *Regulation modulates thermal extremes*

Within the historical period reservoirs alleviated thermal extreme events. Figure 3.2(b), (c), and (d) show the distributions of duration, intensity, and severity as probability density functions (PDFs) for all regulated river segments in each river size category from Figure 3.1. We used the unregulated model setup (left side in each violin plot) as a baseline and compared it with the regulated setup (right side) to evaluate reservoir impacts on thermal extremes, with horizontal lines denoting median values. Historical regulation impacts on thermal extremes are quantified by the distance between the orange and blue horizontal lines in Figure 3.2, i.e., the median values in the regulated model setup minus those in the unregulated setup ($\boldsymbol{\Delta M_{hist}}$, where M is the metric of interest; Table 3.1); the more negative $\boldsymbol{\Delta M_{hist}}$, the greater the mitigation by reservoir regulation of thermal extreme events. For all three metrics, lower blue lines indicate that reservoirs can depress downstream thermal extremes by releasing cold hypolimnetic water. Under reservoir regulation, median values of mean annual duration, intensity, and severity are 3.0 days/year (-5.1 days/year), 0 °C (-0.8 °C), and 1.6 °C·day/year (-3.9 °C·day/year) for all regulated river segments. Values in parentheses indicate the regulation-induced offset in the historical period.

Reservoir regulation has stronger impacts on smaller rivers. We grouped all segments into two size categories (smaller and larger rivers) based on a threshold of $\overline{Q_a}$ of 100 m^3/s. For larger

rivers reservoir regulation leads to a change in median duration, intensity, and severity of -3.3 days/year, -0.6 °C, and -2.6°C·day/year in the historical period, respectively. For smaller rivers these metrics are -7.3 days/year, -0.9 °C, and -5.0°C·day/year, respectively, indicating that reservoir regulation can strongly mitigate thermal extremes in smaller rivers during the historical period. Smaller rivers experience stronger regulation impacts for two main reasons, namely, a greater number of reservoirs in smaller rivers (Figure 3.1c), and longer residence times of reservoirs in smaller rivers (Figure 3.1d). Reservoirs with longer residence times tend to be more stratified with colder hypolimnetic releases than those with shorter residence times, resulting in a stronger mitigating impact on downstream thermal extremes.

3.3.2. *Regulation impacts are reinforced under climate change*

Climate change will exacerbate thermal extreme events. Figure 3.2 shows the effects of climate change for an unregulated system (red traces). Without regulation, duration, intensity, and severity increase to 85.6 days/year (+77.4 days/year), 5.2 °C (+4.4°C), and 193.4 °C·day/year (+187.9 °C·day/year), respectively by the 2080s under RCP8.5, with values in parentheses indicating the changes relative to the historical, unregulated values. These values are determined by calculating the median across all river segments for each GCM and then taking the median across all 20 GCMs. Severity, as an integral of time and temperature, increases faster than both duration and intensity under climate change.

In general, climate change will also exacerbate thermal extremes in the regulated river system. Median duration, intensity, and severity in the regulated model setup are projected to increase to 75.2 days/year (+72.1 days/year), 4.2 °C (+4.2 °C), and 143.1 °C·day/year (+141.5 °C·day/year), respectively, which are only slightly lower than climate-induced increases in the unregulated setup. Furthermore, for all regulated river segments, reservoir regulation can only mitigate 12.2% (-10.4 days/year), 19.7% (-1.0 °C), and 26.0% (-50.3 °C·day/year) of duration, intensity, and severity, respectively, by the 2080s under RCP8.5, with values in parentheses indicating the regulation-induced offset under climate change.

Table 3.1. Summary of baseline and regulation impacts on duration, intensity, and severity for each river size category. We also group the river segments by smaller and larger sizes, i.e., $\overline{\boldsymbol{Q_a}}$ below and exceeding 100m^3/s. $\boldsymbol{M}$ denotes median values of selected metrics for all regulated river segments in each river size category, subscripts $\boldsymbol{hist}$ and $\boldsymbol{2080s}$ denote historical period and 2080s under RCP8.5 respectively, subscripts $\boldsymbol{unreg}$ and $\boldsymbol{reg}$ denote unregulated and regulated model setups. $\boldsymbol{M_{2080s,X}}$ denotes median of PDF median values among all 20 GCMs for the future period, i.e., red and navy horizontal lines for unregulated and regulated model setups in Figure 3.2.

Variable	River size (mean annual flow, $\overline{Q_a}$, m^3/s)	Baseline		Regulated model setup		Regulation impact				
						Historical		2080s		Projected changes
		$M_{hist,unreg}$	$M_{2080s,unreg}$	$M_{hist,reg}$	$M_{2080s,reg}$	ΔM_{hist} ($= M_{hist,reg} - M_{hist,unreg}$)	$\frac{\Delta M_{hist}}{M_{hist,unreg}}$	ΔM_{2080s} ($= M_{2080s,reg} - M_{2080s,unreg}$)	$\frac{\Delta M_{2080s}}{M_{2080s,unreg}}$	$\Delta M_{2080s} - \Delta M_{hist}$
Duration (day/year)	0-10	9.53	100.80	0.25	50.47	-9.28	-97.4%	-50.33	-49.9%	-41.05
	10-20	8.72	94.12	0.88	76.97	-7.84	-90.0%	-17.15	-18.2%	-9.31
	20-50	8.38	89.07	2.28	78.78	-6.10	-72.8%	-10.29	-11.5%	-4.19
	50-100	8.39	84.91	3.31	76.76	-5.08	-60.5%	-8.15	-9.6%	-3.07
	100-200	8.00	82.13	2.75	72.03	-5.25	-65.6%	-10.10	-12.3%	-4.85
	200-500	7.56	81.75	3.88	70.75	-3.69	-48.7%	-11.00	-13.5%	-7.32
	>500	8.03	82.53	7.25	79.62	-0.78	-9.7%	-2.91	-3.5%	-2.13
	Smaller river ($\boldsymbol{Q_a \leq 100}$)	8.78	91.23	1.50	75.95	-7.28	-82.9%	-15.28	-16.8%	-8.00
	Larger river ($\boldsymbol{Q_a > 100}$)	7.81	81.65	4.50	74.32	-3.31	-42.4%	-7.33	-9.0%	-4.02
	All regulated grid cells	8.16	85.57	3.03	75.15	-5.13	-62.9%	-10.42	-12.2%	-5.29
Intensity (°C)	0-10	0.52	4.56	0.00	1.92	-0.52	-100.0%	-2.65	-58.0%	-2.12
	10-20	0.74	5.45	0.00	3.70	-0.74	-100.0%	-1.75	-32.1%	-1.01

	20-50	0.94	5.50	0.00	4.37	-0.94	-100.0%	-1.13	-20.6%	-0.19
	50-100	1.06	5.40	0.17	4.56	-0.89	-84.3%	-0.84	-15.6%	0.05
	100-200	0.96	5.19	0.00	4.26	-0.96	-99.6%	-0.93	-17.9%	0.03
	200-500	0.68	4.99	0.19	4.17	-0.49	-71.7%	-0.82	-16.4%	-0.33
	>500	0.48	4.63	0.21	4.28	-0.27	-57.2%	-0.35	-7.6%	-0.08
	Smaller river ($\boldsymbol{Q_a \leq 100}$)	0.88	5.38	0.00	3.93	-0.88	-100.0%	-1.45	-27.0%	-0.57
	Larger river ($\boldsymbol{Q_a > 100}$)	0.78	4.99	0.18	4.21	-0.60	-76.8%	-0.78	-15.6%	-0.18
	All regulated grid cells	0.82	5.19	0.00	4.17	-0.82	-100.0%	-1.02	-19.7%	-0.20
Severity (°C·day/year)	0-10	4.85	224.08	0.08	57.20	-4.77	-98.4%	-166.88	-74.5%	-162.11
	10-20	5.36	245.72	0.28	145.45	-5.08	-94.8%	-100.27	-40.8%	-95.19
	20-50	5.77	219.55	1.02	162.28	-4.75	-82.4%	-57.27	-26.1%	-52.52
	50-100	6.16	191.54	1.78	156.56	-4.38	-71.1%	-34.98	-18.3%	-30.60
	100-200	5.77	169.30	1.44	134.82	-4.33	-75.0%	-34.48	-20.4%	-30.16
	200-500	5.28	168.42	2.51	128.68	-2.77	-52.5%	-39.74	-23.6%	-36.97
	>500	5.15	178.12	4.48	162.90	-0.67	-13.1%	-15.22	-8.5%	-14.54
	Smaller river ($\boldsymbol{Q_a \leq 100}$)	5.66	211.94	0.66	137.87	-5.01	-88.4%	-74.07	-34.9%	-69.07
	Larger river ($\boldsymbol{Q_a > 100}$)	5.35	170.23	2.74	145.91	-2.61	-48.7%	-24.32	-14.3%	-21.71
	All regulated grid cells	5.53	193.44	1.62	143.13	-3.91	-70.8%	-50.31	-26.0%	-46.40

While climate change will exacerbate thermal extreme events in both the regulated and unregulated model setups, the differences between them will be larger under future conditions. The distance between the red and navy horizontal lines in Figure 3.2 ($\boldsymbol{\Delta M_{2080s}}$ in Table 3.1) quantifies the regulation impacts in the future. We quantify the change in regulation impacts between the 2080s and the historical period ($\boldsymbol{\Delta M_{2080s-hist}}$) as

$$\boldsymbol{\Delta M_{2080s-hist} = \Delta M_{2080s} - \Delta M_{hist}} \quad (3.5)$$

Positive values of $\boldsymbol{\Delta M_{2080s-hist}}$ indicate that reservoir regulation will have a weaker impact on stream temperature in the future than in the past. Negative values indicate that regulation will have a stronger impact in the future than in the past. For all regulated river segments, $\boldsymbol{\Delta M_{2080s-hist}}$ for duration, intensity, and severity is -5.3 days/year, -0.2°C, and -46.4 °C·day/year, which indicates that by the 2080s, reservoir regulation buffers thermal extremes to a greater extent than in the historical period. For all river size categories and all three metrics, $\boldsymbol{\Delta M_{2080s-hist}}$ is generally negative, indicating that reservoir regulation will have stronger mitigating impacts for all river sizes under climate change.

Under climate change, mitigation of thermal extremes as a result of reservoir regulation is stronger for smaller rivers. For smaller river segments, the values of $\boldsymbol{\Delta M_{2080s-hist}}$ for duration, intensity, and severity are -8.0 days, -0.6 °C, and -69.0 °C·day, respectively. For larger river segments, these values are -4.0 days, -0.2 °C, and -21.7°C·day, respectively. For all three metrics $\boldsymbol{\Delta M_{2080s-hist}}$ generally becomes more negative as river size decreases, indicating that under climate change, stream temperatures in smaller rivers will be more strongly affected by reservoir regulation. As a result, in regulated systems, climate change has somewhat less of an impact on thermal extremes in smaller rivers, especially in river segments with $\overline{Q_a}$ below 10 m^3/s.

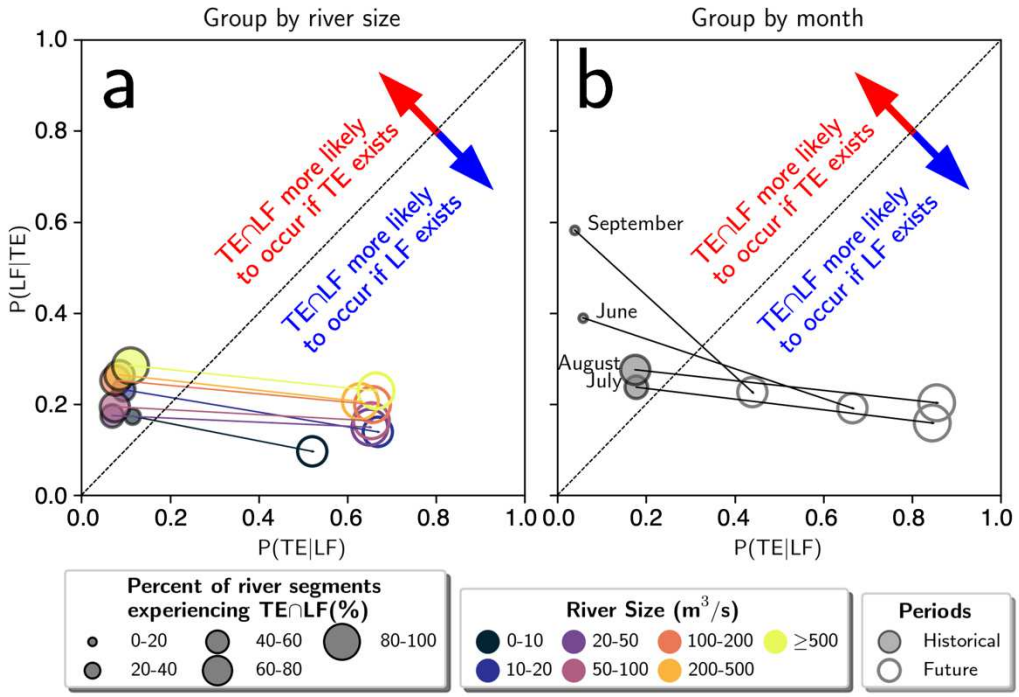

Figure 3.3. Conditional probability of hydrologic hot-dry events given that low flow events already happened, i.e., P(TE|LF), versus conditional probability of hydrologic hot-dry events given that thermal extremes already happened, i.e., P(LF|TE). Panels a) and b) represent categorizations by river sizes and months, respectively. Dot color denotes river sizes, and dot size denotes percentage of river segments experiencing hydrologic hot-dry events. Solid dots with black outline and open circles denote historical and future periods, respectively.

3.3.3. *Prolonged hydrologic hot-dry events will occur at more river segments under climate change*

More river segments will experience hydrologic hot-dry events under climate change (hollow circles are larger than solid circles in Figure 3.3). In the following, median values are calculated only for stream segments that experience hot-dry events. In the historical period, 65.7% of regulated river segments experienced hydrologic hot-dry events with a median annual duration of 0.8 days/year, while 34.3% never experience a hot-dry event. Under climate change hydrologic hot-dry events will occur in 87.1% of regulated river segments, with a median annual duration of 10.3 days/year, over ten times the historical value. The concurrent events increase both because of an increase in thermal extremes as well as an increase in the number of low flow events. Even though the regional mean annual precipitation is projected to increase slightly by 41.4 mm/year

(3.4%), the median annual duration of low flow events will be prolonged from 15.9 days/year to 21.8 days/year. Because thermal extremes do not increase as much in smaller regulated rivers under climate change, fewer smaller regulated river segments will experience concurrent extreme events, especially for river segments with $\overline{Q_a}$ below 10 m^3/s (smaller hollow circle sizes for smaller rivers in Figure 3.3(a)).

Under climate change the concurrent events will be more likely to occur if there exist low flow events rather than thermal extremes. In the historical period the duration of low flow events is almost three times the duration of thermal extremes, leading to a higher $P(LF)$ and therefore a lower $P(TE|LF)$. The hydrologic hot-dry events are thus more likely to occur when thermal extremes occur historically (solid circles located in the upper left corner in Figure 3.3). However, the large increase of thermal extremes under climate change greatly elevates the possibility of its coincidence with low flow events, especially in warmer seasons. By the 2080s under RCP8.5, median monthly durations of thermal extremes for July and August are 27.1 days/month and 26.6 days/month respectively, which almost guarantees that low flow events will also be hydrologic hot-dry events ($P(TE|LF) > 0.8$; Figure 3.3b).

3.4. DISCUSSION

The sensitivity analysis shows that the choice of threshold temperature does not have a large impact on our results. In general, reservoir regulation can alleviate historical thermal extremes to a certain extent. The values of all three metrics increase sharply under climate change for both the unregulated and regulated model setups, but they increase slightly less for the regulated case. In addition, for all three metrics, $\boldsymbol{\Delta M_{2080s-hist}}$ generally becomes more negative as river size decreases, a consistent finding under all thresholds (see Supporting Information Figure B.1). As a result, our conclusion that regulation impacts are more enhanced for regulated rivers with smaller flows is relatively insensitive to the choice of the threshold value.

Besides the choice of threshold, assumptions in river temperature simulations can also influence the results. In this study, we assumed that all reservoirs released water from the hypolimnion. This assumption was our default because of limited access to reservoir regulation data across different operating agencies. As a result, the regulation impacts shown in this study are the upper limit of mitigation that can be provided by existing reservoir infrastructures. Although reservoir releases are optimized for downstream temperature control at a few select

reservoirs at present (e.g. Detroit Dam in Oregon; Rounds & Buccola, 2015), this is currently not a common practice.

3.5. CONCLUSION

Leveraging a newly established model framework, we investigated the impacts of climate change and reservoir regulations on thermal extreme characteristics as defined by three metrics: duration, intensity, and severity. Concurrent thermal extremes and low flow events, i.e., hydrologic hot-dry events, can increase damages to local aquatic ecosystems due to low fish mobility and can further reduce the flexibility and ability of the electricity sector to meet electricity demand due to disruption of thermoelectric plant operations. We also determined the conditional probability of hydrologic hot-dry events given the occurrence of either a thermal extreme or low flow event. Our analysis focused on river segments in the study area that are subject to regulation during the historical period. Major findings are as follows:

- Climate change greatly exacerbates thermal extremes. In the unregulated simulations, duration, intensity, and severity are projected to increase to 85.6 days/year (+77.4 days/year), 5.2 °C (+4.4°C), and 193.4 °C·day/year (+187.9 °C·day/year), respectively, by the 2080s under RCP8.5, with values in parentheses indicating the changes relative to the historical, unregulated values.
- Thermal extremes will increase in the regulated system under climate change. The climate-induced increases are only slightly lower in the regulated model setup than those in the unregulated model setup. Furthermore, by the 2080s under RCP8.5, only 12.2%, 19.7%, and 26.0% of duration, intensity, and severity, respectively, can be mitigated by reservoir regulation, assuming all releases come from the hypolimnion.
- Regulation can alleviate thermal extremes and this ability will be enhanced under climate change. Reservoir regulation buffers thermal extremes to a greater extent under climate change, by reducing duration, intensity, and severity by -10.4 days/year, -1.0°C, and -50.3 °C·day/year, which are 2.0, 1.2, and 12.9 times greater than the historical offset due to reservoir regulation. In addition, the mitigating effects of reservoir regulation on thermal extremes are greater on smaller rivers

because of a greater number of reservoirs and because of longer reservoir residence times.

- More regulated river segments will experience prolonged hydrologic hot-dry events under climate change, with a median annual duration of 10.3 days, over ten times the historical value. In addition, under climate change, the occurrence of thermal extreme events increases more than the occurrence of low flow events. As a result, the occurrence of concurrent hot-dry events becomes more conditionally dependent on the occurrence of a low flow event (since thermal extreme events will become more common).

Dams and reservoirs have a wide range of impacts on fish populations and environmental process, from restricting movement, to changing habitat, to changes in sediment transport (Dang et al., 2010). This study clarifies and quantifies the extent to which management of reservoir infrastructure can be used to modify tailwater thermal regimes in a large river system. While this opportunity for modification is limited, it can offer important local opportunities for managing thermal conditions.

ACKNOWLEDGEMENT

This project was funded in part by the National Science Foundation (NSF) as part of the Resilient Interdependent Infrastructure Processes and Systems (RIPS) program through grants EFRI-1440852 and EFRI-1441131 to the University of Washington. We also wish to thank Xiao Zhang at Pacific Northwest National Laboratory for initial contributions to this work. We acknowledge the World Climate Research Programme's Working Group on Coupled Modelling, which is responsible for CMIP, and we thank the climate modeling groups (listed in Table S1 in the Supporting Information) for producing and making available their model output. For CMIP the U.S. Department of Energy's Program for Climate Model Diagnosis and Intercomparison provides coordinating support and led development of software infrastructure in partnership with the Global Organization for Earth System Science Portals. The data that support the findings of this study are openly available at the following DOI: https://doi.org/10.5281/zenodo.3753590.

Chapter 4 PROJECTED POTENTIAL FISH DISTRIBUTION UNDER CLIMATE CHANGE IN A HEAVILY REGULATED, FRAGMENTED RIVER SYSTEM

This chapter is being prepared for submission to *Frontiers in Ecology and the Environment* as Cheng, Y., B. Nijssen, and G. Holtgrieve 2020: Projected potential fish distribution under climate change in a heavily regulated, fragmented river system.

ABSTRACT

Both climate change and dam construction greatly impact fish distribution. Capturing dam impacts, especially dam-induced changes in flow and thermal regimes, on environmental suitability remains a challenge at regional-scale studies. To address this challenge, we incorporated a recent advance in hydrologic modeling for regulated river systems with a species distribution model and applied it in the highly regulated Tennessee River system in the southeastern United States. We also accounted for stream network fragmentation resulting from dam blockage. We projected the climate-induced changes of environmental suitability for the exotic coldwater rainbow trout, which is stocked for sport fisheries, and three endemic coolwater darter species with varying thermal tolerance. Only 4.4% of historically suitable streams for rainbow trout will remain by the 2080s (2070-2099), mostly located at cold reservoir tailwaters. Higher river temperature may facilitate the expansion for some endemic species, but the expansion will be constrained by dam blockages.

4.1. INTRODUCTION

Dams impound large water bodies, block fish passages, change river flow and thermal regimes, and therefore cause a redistribution of local freshwater biota (Agostinho et al., 2008; Letcher et al., 2007; Ligon et al., 1995; Olden & Naiman, 2010). As a global hotspot of freshwater biodiversity, the southeastern US (SEUS) lost suitable habitat for endemic fish species as a result of dam construction over the past century (Jenkins et al., 2015; Liermann et al., 2012). For example, during warm seasons, cold hypolimnetic releases from stratified reservoirs expel local species in the SEUS (Neves & Angermeier, 1990). However, the cold outflow also creates new

habitat, for example, for an exotic coldwater species such as rainbow trout (*Oncorhynchus mykiss*). *O mykiss* has been stocked at multiple reservoir tailwaters and attracts anglers in the SEUS (especially in Tennessee), which strengthens the local economy and enhances recreational opportunities (Brooks et al., 2018).

Freshwater fish species are vulnerable to climate change and strong human impacts (Comte & Olden, 2017). For example, under climate change, projected higher river temperature may cause significant loss in cold-water fish habitat, e.g., salmonids in the Pacific Northwest and brook trout in the eastern United States, while facilitating the invasion of nonnative warmwater species, e.g., smallmouth bass (Bassar et al., 2016; Lawrence et al., 2014; Rubenson & Olden, 2020; Ruesch et al., 2012). This climate-induced invasion of nonnative smallmouth bass can present an additional challenge to threatened Pacific salmon.

Reservoir tailwater temperature is projected to increase in the SEUS under climate change, which may restore habitat for endemic species. Even though projected reservoir thermal stratification will remain strong under climate change, the temperature suppression will dissipate over a shorter distance downstream of the reservoir due to higher air temperature and stronger solar radiation (Cheng et al., 2020). As a result, we can hypothesize that the projected higher temperature may lead to a shrinkage of environmentally suitable streams for *O mykiss* at reservoir tailwaters while facilitating the colonization of endemic species (Shea et al., 2015). However, due to dam blockage, endemic species cannot always migrate to newly suitable streams under climate change without human intervention (Kano et al., 2016).

The regional assessment of fish distribution in a regulated fluvial system remains a great challenge for freshwater fish conservation (Olden, 2015). Recent studies have investigated dam-induced isolation on fish redistribution under climate change (Fukushiam et al., 2007; Kano et al., 2016). They mostly used surface meteorological variables as predictors to simulate fish presence probability, and therefore did not consider the impact of reservoir regulation. Rubenson & Olden (2020) projected fish presence probability using the regulated river temperature from the NorWest project, which did not capture the climate-induced changes of reservoir thermal stratification on downstream river temperature. Because dam impacts dissipate as rivers flow downstream, their influence on river flow and thermal regimes may be inconsequential at continental or global scales (Liermann et al., 2012). However, this impact is vital for endemic fish species with limited spatial coverage.

The objective of this study is to examine the potential fish redistribution under climate change for *O mykiss*, an exotic but lucrative species, and multiple endemic species in the Tennessee River Basin, a highly regulated river system. By coupling a recent advance in hydrologic modeling for regulated river systems with a well-established species distribution model, we quantified the projected changes in environmentally suitable streams as a result of modified flow and thermal regimes (Cheng et al., 2020; Phillips et al., 2006). This study focuses on rivers instead of reservoirs because the latter have a very different biotic system. We explicitly account for the impacts of reservoir operation and thermal stratification on downstream river flow and temperature and account for stream network fragmentation resulting from dam blockage.

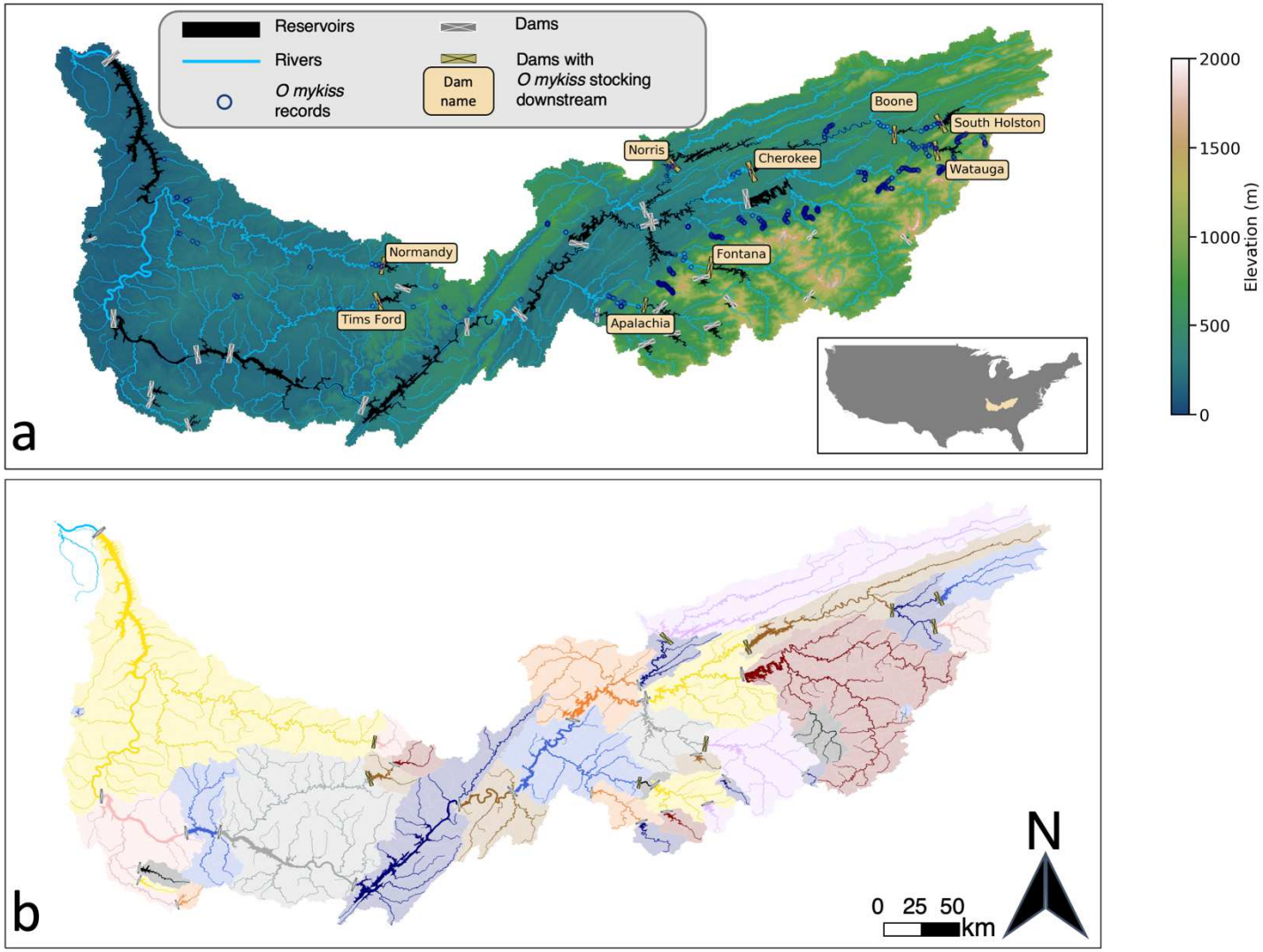

Figure 4.1. a) study domain with reservoir and *O mykiss* stocking locations and b) fragmented river networks

4.2. METHODS

4.2.1. *Study domain*

We chose the Tennessee River Basin (TRB) as our study domain, a U.S. hotspot of freshwater biodiversity (Jenkins et al., 2015). The TRB accommodates many endemic fish species, especially in the southwestern realm of the southern Appalachian Mountains (southeastern corner in Figure 4.1a). In addition, the TRB has a highly regulated river system with 36 major dams constructed over the past century, mostly regulated by the Tennessee Valley Authority (Lehner et al., 2011). Nine dams in the Tennessee River impound extensive reservoirs, covering most of the Tennessee River (reservoirs are masked using black in Figure 4.1a). As a result, most of the mainstem Tennessee River is excluded in this study.

4.2.2. *Model setup*

We leveraged a recently established model framework to simulate river flow and temperatures in the complicated river-reservoir system in Tennessee (Cheng et al., 2020). This model framework comprises three physically-based models: (1) a large-scale spatially-distributed hydrologic model (Variable Infiltration Capacity model or VIC; Liang *et al.* 1994; Hamman *et al.* 2018), (2) a river routing model (Model for Scale Adaptive River Transport or MOSART; Li *et al.* 2013) coupled with a water management model (WM; Voisin *et al.* 2013), and (3) a stream temperature model (River Basin Model or RBM; Yearsley 2012) coupled with a two-layer reservoir thermal stratification module (2L; Niemeyer *et al.* 2018). To better capture the reservoir's impacts on downstream temperature, we used reservoir operation data and other relevant information to determine whether a reservoir releases from the surface layer (epilimnion) or bottom layer (hypolimnion; Table C.1). This is in contrast to Cheng et al. (2020) who assumed that all reservoirs release from the hypolimnion. More details are discussed in C.1.1.

We used the Maximum Entropy model (Maxent), a species distribution model (SDM), to calculate a species' presence probability over a defined region using fish presence data with environmental variables (Phillips et al., 2006). Generally, Maxent predicts environmental suitability for the species as a function of given environmental variables. We set up the SDM following VanCompernolle et al. (2019). We used the same spatial resolution (400-m grid) for the river network and selected the same nine environmental variables as model inputs. Six climate-related variables were based on the model framework mentioned above (mean annual

maximum/minimum monthly river flow and temperatures, i.e., Q_{max}, Q_{min}, T_{max}, T_{min}, and coefficient of variation of monthly flow and temperatures, i.e., Q_{CV}, T_{CV}). The remaining three were non-climatic, i.e., primary surface rock type, land cover, and slope (data sources and processing procedures are detailed in C.1.1). For each fish species, we randomly used half of the fish presence data to train the Maxent model and used the remaining half for validation. A pixel, i.e., a 400-m grid, is categorized as a suitable stream segment when its presence probability exceeds a threshold. We set the threshold equal to the value that excludes the 10 percent of localities with the lowest predicted values (P^{10}). Compared to another common metric, i.e., the lowest presence threshold, this metric is more stable and relatively insensitive to outliers (Radosavljevic & Anderson, 2014). Details of the Maxent setup and evaluation can be found in Text C.1.1.

4.2.3. *Fish data*

We obtained location information for *O mykiss* stocking from the Tennessee Wildlife Resources Agency (TWRA; accessed through TWRA website, https://data2017-09-06t154623620z-twra.opendata.arcgis.com/, 2020-02-08) and location information for local fish species from a list of agencies (Table C.2; accessed through the Fishnet2 Portal, www.fishnet2.org, 2020-02-07). We examined 50 local fish species with the most records in Fishnet2 and selected three species of darters with varying thermal tolerance for further analysis (*Percidae*; black darter, *Etheostoma duryi*; blueside darter, *Etheostoma jessiae*; blackfin darter, *Etheostoma nigripinne*). The selected coolwater species are endemic and unique to the TRB and the trained Maxent model for these species passed the performance criterion used in VanCompernolle *et al.* (2019), see Text C.1.1 for details. We only examined coolwater species because local coldwater species mostly reside in headwaters, which are minimally impacted by reservoirs (McDonnell et al., 2015).

4.2.4. *Meteorological forcing data*

We forced the modeling framework using both historical and future meteorology data. For the historical period (1980-2009), we used gridMET (Abatzoglou 2013), a gridded meteorology dataset. For the future period (2070-2099, 2080s), we used downscaled meteorology data from 20 Global Climate Models (GCM; Table C.3) based on a high emission scenario (RCP 8.5) from the Coupled Model Intercomparison Project, Phase 5 (CMIP5; Taylor *et al.* 2012), downscaled using the Multivariate Constructed Analogue method (MACA; Abatzoglou and Brown 2012).

We assumed that the three non-climatic variables remain the same under climate change. In addition, only pixels for which the probability of presence exceeded the P^{10}-threshold for at least 16 GCMs were classified as suitable by the 2080s.

4.2.5. *Dams fragment river network*

While the modeling techniques capture the dam impacts on fish redistribution via modified river flow and thermal regimes, they do not account for the physical blockage of fish passages. Basically, without human intervention, fish cannot migrate across dams. Therefore, we evaluated the accessibility of fish habitat to address the impacts of dam blockage. We fragmented the river network at dam locations as shown in Figure 4.1b. Fish are only able to migrate within each colored subregion. For each fish species, we defined a subregion accessible based on fish observations from FishNet2. That is, if a fish species exists anywhere within a given subregion, then that entire subregion will be marked as accessible.

4.2.6. *Main environmental drivers for changes in environmental suitability*

As part of our analysis, we determined for each pixel the variable that contributed the most to changes in environmental suitability. The Maxent model provided the relative contribution of each environmental variable to fish presence probability (permutation importance) for the historic period, but does not tell us which variable contributed most to a change in this probability. We introduced the Shapley decomposition to determine the main environmental driver of changes in environmental suitability. The Shapley decomposition originated from cooperative game theory, where it was applied to determine each player's unique contribution to a total surplus generated by a coalition of all players. Recently, this method has also been applied in energy and environmental analysis (Ang et al., 2003; Yu et al., 2014). We adapted the Shapley decomposition to quantify the contribution of each climate-related variable (φ_v) to the projected changes in fish presence probability (ΔP), with subscript *v* representing the six climate-related variables (Ang et al., 2003). We kept the three non-climatic variables constant under climate change so their contribution to ΔP is zero. This technique is able to provide a decomposition without residuals, i.e.,

$$\Delta P = \sum_{v} \varphi_v \tag{4.1}$$

Therefore, the relative contribution (R_v) can be quantified as

$$R_v = \frac{\varphi_v}{\Delta P} \tag{4.2}$$

The corresponding variable with the largest R_v value is defined as the primary driver of changes in environmental suitability under climate change, which is calculated for every pixel. More details can refer to Text C.1.2.

4.3. RESULTS

Streams that are environmentally suitable for rainbow trout will shrink and no new streams will become suitable under climate change. In Figure 4.2, domain colors denote accessibility with red and blue denoting accessible and inaccessible subregions, respectively. Accessibility is based on historic presence of a fish species combined with dam blockage information. Colors of the streams denote the projected change of environmental suitability. Generally, 95.6% of historically suitable streams (including most southern Appalachian streams) will disappear for rainbow trout (red pixels in Figure 4.2d). The remaining suitable streams (blue pixels in Figure 4.2d) are mostly at reservoir tailwaters, e.g., downstream of the South Holston dam, Watauga dam and Fontana dam. Even at these reservoir tailwaters, the number of stream segments that are environmentally suitable for rainbow trout will shrink.

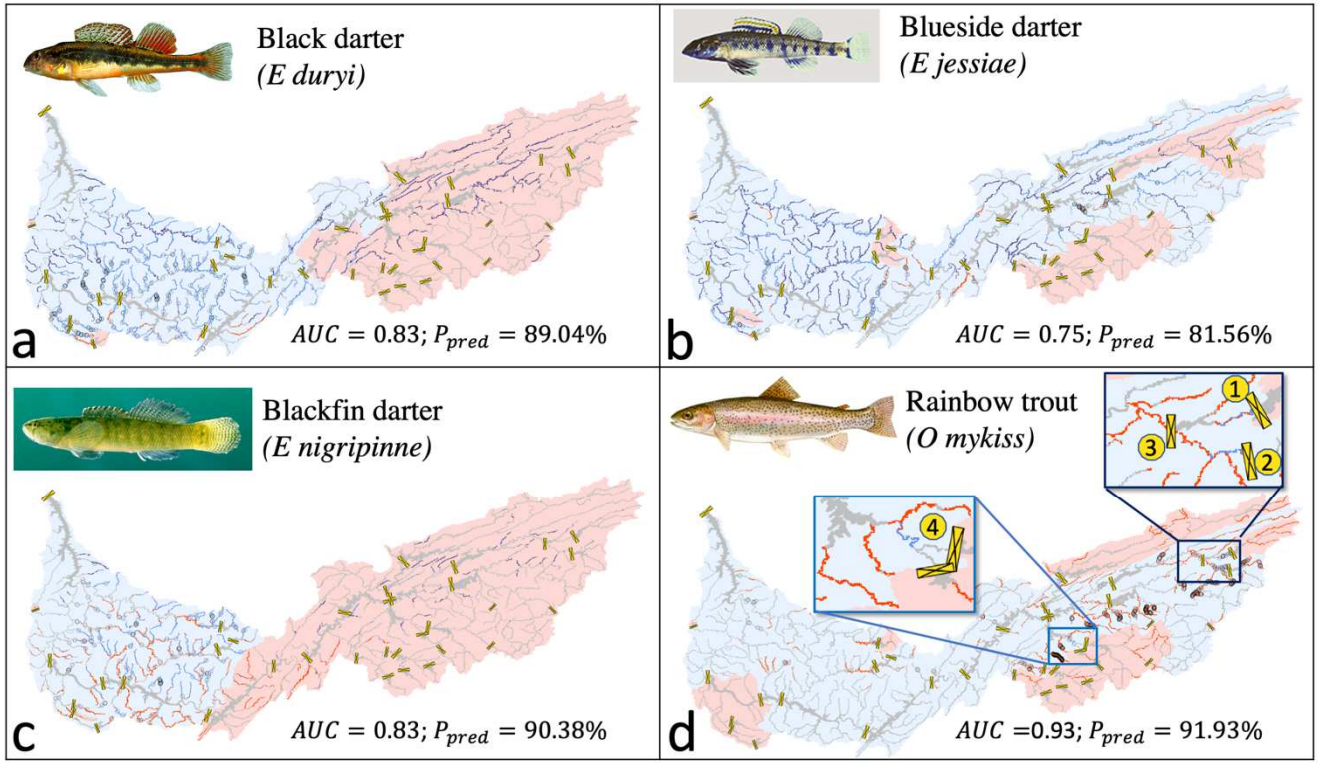

Figure 4.2. For each fish species, its accessibility is represented by the color of the subregions. Projected changes of environmental suitability under climate change are represented by the color of the river network. Black hollow circles denote observed fish locations from FishNet2. Yellow circles with number 1, 2, 3, and 4 inside represent South Holston, Watauga, Boone, and Fontana dams, respectively.

For endemic coolwater species, more stream segments may become environmentally suitable under climate change, but any potential expansion will be reduced by dam blockage. Without accounting for dam blockage, the suitable streams for *E duryi*, *E jessiae*, and *E nigripinne* are projected to change by +67%, +76%, -35%, respectively, by the 2080s. Accounting for dam blockage, accessible suitable streams for the same three species are projected to change by +20%, +62%, -53%, respectively. Two-thirds of the projected new suitable streams for *E duryi* located in upper TRB (dark blue pixels in red domain in Figure 4.2a) are inaccessible because this species historically resides only in the lower TRB and thus will not migrate there without human intervention. *E jessiae* is more extensively distributed in the TRB and dam blockage has a weaker impact on its ability to access newly suitable streams. Only one-fifth of the new environmentally suitable streams are inaccessible (dark blue pixels in red domain in Figure 4.2b). The difference between the impacts of dams on projected distributions for *E duryi* and *E jessiae* shows that fish with limited spatial coverage are more vulnerable to dam blockages under climate change. Among the three endemic species, dam blockage has the largest impact on *E nigripinne* because its historically suitable streams shrink under climate change while most of the projected environmentally suitable streams are inaccessible (Figure 4.2c).

Among the six climate-related variables, changes in environmental suitability under climate change are primarily driven by projected changes in river temperatures, including increases in T_{max}, $T_{min}$and decreases in T_{CV} by the 2080s (Figure C.1). For subregions with a net gain or net loss of environmentally suitable streams, we determined the primary drivers of all corresponding river segments and took their mode as the sub-regional primary driver. In Figure 4.3, for each subregion, domain colors denote the primary environmental driver of changes in environmental suitability; black and red boundaries denote accessible and inaccessible subregions, respectively; and non-hatching or hatching denote gaining or losing in environmentally suitable streams. Among all four fish species, all sub-regional primary drivers were temperature rather than flow-related (Figure 4.3). Primary drivers vary among different species. Projected higher T_{min} contributed most to the expansion of *E duryi* and *E jessiae*; projected higher T_{max} led to shrinkage of environmentally suitable streams for *E nigripinne* in the lower TRB; and projected higher T_{max} or T_{min} led to shrinkage of these streams for *O mykiss* depending on location.

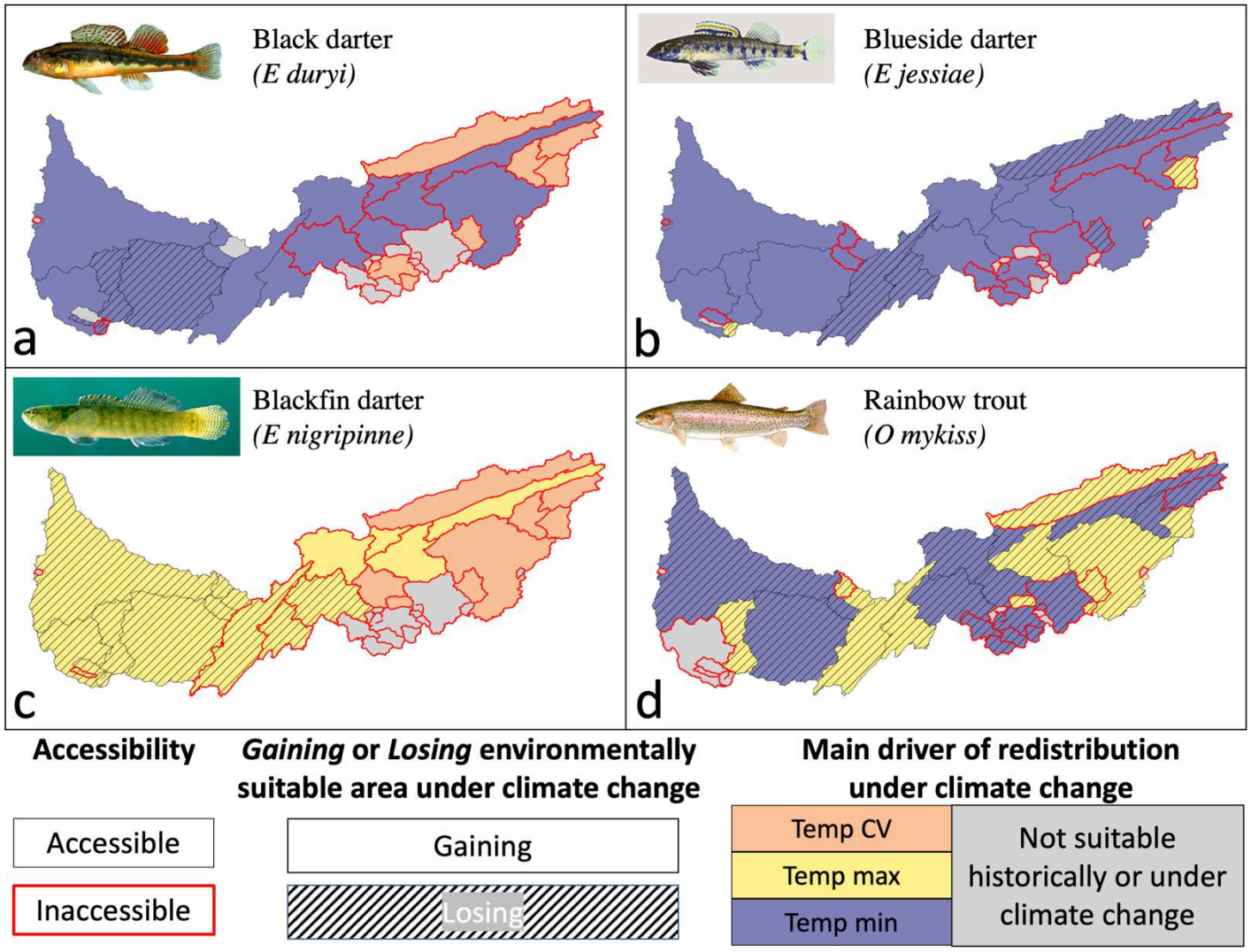

Figure 4.3. Main environmental drivers of changes in environmental suitability under climate change.

4.4. DISCUSSION

The result shows that projected higher river temperatures do not always favor colonization by endemic coolwater species, which is consistent with previous studies (Eaton & Scheller, 1996; Poff et al., 2002). For example, higher T_{max} leads to a shrinking of environmentally suitable areas for *E nigripinne* in the lower TRB (Figure 4.3c). Heat tolerance varies among species, so excessive heat can reduce the environmental suitability for some coolwater species.

Reservoir tailwaters, historically too cold for coolwater species, may become suitable under climate change. For example, tailwaters downstream of multiple reservoirs become suitable for *E jessiae* by the 2080s (dark blue pixels in Figure 4.2b). Under climate change, cold reservoir tailwaters may alleviate the excessive thermal stress for lucrative rainbow trout as well as for endemic coolwater species. However, this alleviation will be more spatially constrained and dissipate faster due to stronger solar radiation under climate change compared to the historical period.

Early studies assigned high priorities for environmental variables with large permutation importance in climate change assessment (VanCompernolle et al., 2019). However, we found variables with high permutation importance did not necessarily have large contributions in climate-induced changes in environmental suitability. For example, T_{CV} has the highest permutation importance for *E duryi* (Table C.4), while the primary driver of changes in environmental suitability is the projected increasing T_{min}. Since the permutation importance is only based on historical environmental variables, it does not account for climate-induced changes. Therefore, we would recommend that future climate impact studies use the Shapley decomposition, which synthesizes both permutation importance as well as climate-induced changes of environmental variables;

Because cold, hypoxic dam releases have imperiled tailwater habitats in the Tennessee River, TVA and local environmental agencies have made great efforts to restore the tailwater ecosystems by boosting oxygen levels and by stocking coldwater species, including the exotic and lucrative rainbow trout as well as endemic coldwater species, e.g., brook trout, and some mussels (Bettinger & Bettoli, 2002; Layzer & Scott, 2006). As our results show that environmentally suitable streams for rainbow trout will shrink at reservoir tailwaters, it is reasonable to infer that the same will happen for other coldwater species.

One main limitation of this work is that our model framework cannot capture the impacts of riparian vegetation on river thermal regimes. Lawrence et al. (2014) and Yearsley et al. (2019) showed that restoration of riparian vegetation can reduce solar radiation and mitigate the climate change impact on river temperatures. Without accounting for this impact, we might overestimate the stream temperatures at the Southern Appalachian streams, which are covered by forest, and underestimate their environmental suitability for rainbow trout under climate change.

4.5. CONCLUSION

This study evaluates dam impacts on fish redistribution under climate change. We have four main findings:

- Climate change will almost wipe out historically suitable habitat for rainbow trout and the reservoir tailwaters will become their last sanctuary. Only 4.4% of historically suitable streams for exotic *O mykiss* will remain by 2080s. Similar changes in environmental suitability downstream of reservoirs can be inferred for other coldwater species.
- Projected higher river temperature will facilitate the expansion of some endemic coolwater species, but much of this new environmentally suitable streams will remain inaccessible as a result of dams. Dam blockage has a greater impact on species with limited historic distribution than on species that are more widely distributed.
- Changes in stream temperature rather than flow regime form the primary driver of changes in environmental suitability for all four fish species evaluated here.
- Variables with the largest permutation importance in species distribution modeling do not necessarily explain the largest amount of change in environmental suitability under climate change. We recommend the use of the Shapley decomposition to determine the dominant change factors.

ACKNOWLEDGEMENT

This project was funded in part by the National Science Foundation (NSF) as part of the Resilient Interdependent Infrastructure Processes and Systems (RIPS) program through grants

EFRI-1440852 to the University of Washington. We acknowledge the World Climate Research Programme's Working Group on Coupled Modelling, which is responsible for CMIP, and we thank the climate modeling groups (listed in Table C.3 in the Supporting Information) for producing and making available their model output. For CMIP the U.S. Department of Energy's Program for Climate Model Diagnosis and Intercomparison provides coordinating support and led development of software infrastructure in partnership with the Global Organization for Earth System Science Portals. We thank Julian Olden, Nathalie Voisin, and John Yearsley for insightful comments.

Chapter 5 CONCLUSIONS AND RECOMMENDATIONS

5.1. CONCLUSIONS

This dissertation furthers understanding of the climate change impacts on fluvial thermal regimes in a regulated river system. In Chapter 2, a model framework was synthesized and evaluated, which laid the basis for all subsequent analysis. The climate change signals in the mean summer temperature and the cooling potentials were evaluated for the SEUS. Instead of conducting an exhaustive model calibration, a sensitivity analysis was designed to evaluate the robustness of our findings to model errors. In Chapter 3, the subject remained river temperature, but I pivoted my focus to the extreme events so as to inform risk management. By adapting a standard characterization of extreme drought events with three attributes, i.e., duration-intensity-severity, I explicitly quantified the regulation impacts on thermal extremes under climate change. In Chapter 4, I explored shifts in fish distribution. The modeling techniques developed in Chapter 2 were coupled with a species distribution model to quantify the presence probability for selected species in a regulated river system. This is the first time, to our knowledge, that dam-induced changes in flow and thermal regimes and the impacts of dams' blockage are both explicitly considered to quantify fish redistribution under climate change.

An important assumption in each study is whether reservoirs release from the epilimnion or hypolimnion. In Chapters 2 and 3, I assumed all reservoirs release from the hypolimnion (cold bottom layer) due to the limited accessibility of reservoir operation data for all 271 reservoirs across the SEUS. Therefore, conclusions in Chapters 2 and 3 are both based on a lower bound of possible river temperatures (i.e. I assume the greatest regulation impacts). However, in Chapter 4, I determined whether reservoirs release from epilimnion or hypolimnion based on reservoir operation data and other relevant information as a result of 1) smaller study area with fewer reservoirs, i.e., Tennessee River Basin with only 36 reservoirs, and 2) comprehensive dam operation data provided by the Tennessee Valley Authority. The conclusions for each chapter are described as follows.

Chapter 2 concludes that reservoir regulation modifies the response of summer river temperatures to climate change, mainly through changing reservoir thermal stratification and surface energy fluxes. In general, summer river temperatures in regulated rivers are projected to be lower than those in unregulated rivers, but more sensitive to climate change. By the 2080s,

under RCP8.5, compound impacts of higher air temperature and shorter residence times result in stronger thermal stratification for about half of all reservoirs in the SEUS, especially for reservoirs with longer residence times. Thermal stratification impacts on reservoir tailwaters will mostly persist but will be slightly weakened because of stronger shortwave radiation and higher air temperatures under climate change. In the future, regulation impacts on tailwater cooling potential mostly remain for river segments strongly impacted by thermal stratification. However, projected higher river temperature will decrease river cooling potential for all river segments. Furthermore, while regulated river segments are more susceptible to hydrologic errors than unregulated rivers, the findings in this study do not materially change as a result of these hydrologic errors.

Chapter 3 quantified the compound impacts of climate change and reservoir regulations on thermal extremes in the SEUS. Under climate change, thermal extremes will be greatly exacerbated but less so in the rivers subject to reservoir regulations. Even though the thermal mitigation from reservoir regulation will become stronger in the future, thermal extremes are projected to be much more severe under climate change. In the baseline (unregulated) scenarios, duration, intensity, and severity are projected to increase to 85.6 day/year (+77.4 day/year), 5.2 °C (+4.4°C), and 193.4 °C·day/year (+187.9 °C·day/year), respectively, by the 2080s under RCP8.5, with values in parentheses indicating the changes relative to the historical, unregulated values. Reservoir regulation can only mitigate 12.2%, 19.7%, and 26.0% of duration, intensity, and severity by the 2080s under RCP8.5.

In Chapter 4, I predicted the fish distribution in a regulated river system under climate change. This study considers, as no study has done before, the compound impact of dam-induced river flow and thermal regime changes and dams' physical blockage on fish distribution. As an exotic coldwater fish species, higher river temperature will result in drastic shrinkage of rainbow trout distribution by the 2080s. Only 4.4% of its historically suitable streams will remain, mostly at reservoir tailwaters. This reduction in stream segments suitable for rainbow trout will negatively impact local sports fishing industry and economy. On the other hand, more streams will be environmentally suitable for some endemic coolwater species by the 2080s, but the expansion is constrained by dam blockages. By the 2080s, the suitable streams of *E duryi*, *E jessiae*, and *E nigripinne* is projected to change by +67%, +76%, -35%, respectively, without the

impact of dam blockage. And the projected changes will be +20%, +62%, -53% respectively when we excluded the inaccessible streams due to dam blockage.

5.2. FUTURE WORK RECOMMENDATIONS

Many areas for improvement and further research remain in a study of this scope, but I would like to highlight a few.

This dissertation adapted a monthly guide curve to operate reservoirs, consistent throughout the historical and future periods. In reality, reservoir operations are highly dynamic and flexible, and updated based on forecast. Therefore, accounting for forecast and optimization information into the reservoir operations component would help improve the regional assessment of regulation impacts. So far, optimization of river temperatures in a complicated multi-reservoir system remains a great challenge in water management community because operation of each single reservoir can be constrained by many competing objectives. Limited accessibility of dam operation data further constrains inclusion of these effects in a modeling framework. The tools used in this dissertation cannot be used to optimize regulation rules for downstream river temperatures, but they can be used to test the impact of different regulation rules on downstream temperature.

High-resolution satellite imagery can facilitate the inspection of human impacts on reservoir tailwater flow and thermal regimes. For example, Bonnema et al. (2020) used satellite imagery to study the impacts of dam constructions on downstream river temperature in the Mekong River Basin. Remote sensing could provide a valuable insight for countries with booming dam constructions but few observations, e.g., the southeastern Asia, Africa and South America. In addition, if the resolution of satellite image is high enough, we may develop an algorithm to better parameterize the operation rules for multiple reservoirs, which can be used to better estimate dam impacts at regional scales.

Coupling with power system models can further our understanding of the dynamics between river thermal regimes and power systems. To be specific, we can explicitly quantify the impacts of thermal effluents to downstream river temperatures as well as the power curtailment due to river temperature constraint on power operations. For example, Miara et al. (2018) dynamically coupled fluvial thermal regimes with power sectors but ignored the impacts of reservoir regulations. As the power plants using once-through cooling techniques are phased out

and retired in the United States, the constraints of river temperature on thermoelectric power sectors become weaker in the future. However, reservoir regulation along with many other human activities greatly affects the water availability and seasonality in the river system. As shown in Chapter 3, prolonged low flow periods can bring additional pressure to the power sectors because the cooling water withdrawal can be constrained by environmental flow regulations, i.e., maintaining a minimum flow for a healthy aquatic ecosystem.

This dissertation assumed static landcover throughout both historical and future periods. However, human activities, e.g., urbanization and deforestation, will greatly change landcovers and thus affect fluvial thermal regimes (Nelson & Palmer, 2007; Yearsley et al., 2019). Therefore, coupling landcover change in future works could provide a more comprehensive evaluation of human activities on river temperature. Our model framework does not currently account for the impacts of reduced solar radiation by riparian vegetation on river temperature, which might overestimate the river temperatures at streams covered by dense forest. Properly accounting for shading by riparian vegetation at regional studies can be ecologically important because shaded reaches might provide sanctuaries for cold water species under climate change.

BIBLIOGRAPHY

Abatzoglou, J. T. (2013). Development of gridded surface meteorological data for ecological applications and modelling. *International Journal of Climatology*, *33*(1), 121–131. https://doi.org/10.1002/joc.3413

Abatzoglou, J. T., & Brown, T. J. (2012). A comparison of statistical downscaling methods suited for wildfire applications. *International Journal of Climatology*, *32*(5), 772–780. https://doi.org/10.1002/joc.2312

Agostinho, A. A., Pelicice, F. M., & Gomes, L. C. (2008). Dams and the fish fauna of the Neotropical region: Impacts and management related to diversity and fisheries. *Brazilian Journal of Biology*, *68*(4 SUPPL.), 1119–1132. https://doi.org/10.1590/S1519-69842008000500019

Ang, B. W., Liu, F. L., & Chew, E. P. (2003). Perfect decomposition techniques in energy and environmental analysis. *Energy Policy*, *31*(14), 1561–1566. https://doi.org/10.1016/S0301-4215(02)00206-9

Angilletta, M. J., Ashley Steel, E., Bartz, K. K., Kingsolver, J. G., Scheuerell, M. D., Beckman, B. R., & Crozier, L. G. (2008). Big dams and salmon evolution: changes in thermal regimes and their potential evolutionary consequences. *Evolutionary Applications*, *1*(2), 286–299. https://doi.org/10.1111/j.1752-4571.2008.00032.x

Arora, R., Toffolon, M., Tockner, K., & Venohr, M. (2018). Thermal discontinuities along a lowland river: The importance of urban areas and lakes. *Journal of Hydrology*, *564*, 811–823. https://doi.org/10.1016/j.jhydrol.2018.05.066

Auffhammer, M., Baylis, P., & Hausman, C. H. (2017). Climate change is projected to have severe impacts on the frequency and intensity of peak electricity demand across the United States. *Proceedings of the National Academy of Sciences of the United States of America*, *114*(8), 1886–1891. https://doi.org/10.1073/pnas.1613193114

Averyt, K., Macknick, J., Rogers, J., Madden, N., Fisher, J., Meldrum, J., & Newmark, R. (2013). Water use for electricity in the United States: An analysis of reported and calculated water use information for 2008. *Environmental Research Letters*, *8*(1). https://doi.org/10.1088/1748-9326/8/1/015001

Bartos, M. D., & Chester, M. V. (2015). Impacts of climate change on electric power supply in the Western United States. *Nature Climate Change*, *5*(8), 748–752.

https://doi.org/10.1038/nclimate2648

Bassar, R. D., Letcher, B. H., Nislow, K. H., & Whiteley, A. R. (2016). Changes in seasonal climate outpace compensatory density-dependence in eastern brook trout. *Global Change Biology*, *22*(2), 577–593. https://doi.org/10.1111/gcb.13135

Bennett, A., Hamman, J., & Nijssen, B. (2020). MetSim: A Python package for estimation and disaggregation of meteorological data. *Journal of Open Source Software*, *5*(47), 2042. https://doi.org/10.21105/joss.02042

Bettinger, J. M., & Bettoli, P. W. (2002). Fate, Dispersal, and Persistence of Recently Stocked and Resident Rainbow Trout in a Tennessee Tailwater. *North American Journal of Fisheries Management*, *22*(2), 425–432. https://doi.org/10.1577/1548-8675(2002)022<0425:fdapor>2.0.co;2

Boehlert, B., Strzepek, K. M., Chapra, S. C., Fant, C., Gebretsadik, Y., Lickley, M., Swanson, R., McCluskey, A., Neumann, J. E., & Martinich, J. (2015). Climate change impacts and greenhouse gas mitigation effects on U.S. water quality. *Journal of Advances in Modeling Earth Systems*, *7*(3), 1326–1338. https://doi.org/10.1002/2014MS000400

Bohn, T. J., Livneh, B., Oyler, J. W., Running, S. W., Nijssen, B., & Lettenmaier, D. P. (2013). Global evaluation of MTCLIM and related algorithms for forcing of ecological and hydrological models. *Agricultural and Forest Meteorology*, *176*, 38–49. https://doi.org/10.1016/j.agrformet.2013.03.003

Bonnema, M., Hossain, F., Nijssen, B., & Holtgrieve, G. (2020). *Environmental Research Letters Hydropower's hidden transformation of rivers in the Mekong*. https://doi.org/10.1088/1748-9326/ab763d

Bradford, M. J., & Heinonen, J. S. (2008). Low Flows, Instream Flow Needs and Fish Ecology in Small Streams. *Canadian Water Resources Journal*, *33*(2), 165–180. https://doi.org/10.4296/cwrj3302165

Breau, C., Cunjak, R. A., & Bremset, G. (2007). Age-specific aggregation of wild juvenile Atlantic salmon Salmo salar at cool water sources during high temperature events. *Journal of Fish Biology*, *71*(4), 1179–1191. https://doi.org/10.1111/j.1095-8649.2007.01591.x

Brooks, S., Phil, K., Fiss, F., & Cummings, M. (2018). *TVA, Fish and Wildlife Service to Continue Popular Trout Stocking Program | U.S. Fish & Wildlife Service*. https://www.fws.gov/southeast/news/2018/10/tva-fish-and-wildlife-service-to-continue-

popular-trout-stocking-program/

Cai, H., Piccolroaz, S., Huang, J., Liu, Z., Liu, F., & Toffolon, M. (2018). Quantifying the impact of the Three Gorges Dam on the thermal dynamics of the Yangtze River. *Environmental Research Letters*, *13*(5). https://doi.org/10.1088/1748-9326/aab9e0

Chapra, S. (1997). *Surface Water-quality modeling*. McGraw-Hill Education. http://www.mhcollege.com

Charbonneau, J., & Caudill, J. (2010). *An Assessment of Economic Contributions from Fisheries and Aquatic Resource Conservation*. https://www.fws.gov/fhc/PDFs/fish_report_Sept2010.pdf

Cheng, Y., Voisin, N., Yearsley, J. R., & Nijssen, B. (2020). Reservoirs modify river thermal regime sensitivity to climate change: a case study in the southeastern United States. *Water Resources Research*. https://doi.org/10.1029/2019WR025784

Chezik, K. A., Lester, N. P., & Venturelli, P. A. (2014). Fish growth and degree-days I: selecting a base temperature for a within-population study. *Canadian Journal of Fisheries and Aquatic Sciences*, *71*(1), 47–55. https://doi.org/10.1139/cjfas-2013-0295

Cole, T. M., & Wells, S. A. (2015). *CE-QUAL-W2: A two-dimensional, laterally averaged, hydrodynamic and water quality model, Version 4.0*.

Comte, L., & Olden, J. D. (2017). Climatic vulnerability of the world's freshwater and marine fishes. *Nature Climate Change*, *7*(10), 718–722. https://doi.org/10.1038/nclimate3382

Coutant, C. C. (1990). Temperature□Oxygen Habitat for Freshwater and Coastal Striped Bass in a Changing Climate. *Transactions of the American Fisheries Society*, *119*(2), 240–253. https://doi.org/10.1577/1548-8659(1990)119<0240:THFFAC>2.3.CO;2

Dang, T. H., Coynel, A., Orange, D., Blanc, G., Etcheber, H., & Le, L. A. (2010). Long-term monitoring (1960-2008) of the river-sediment transport in the Red River Watershed (Vietnam): Temporal variability and dam-reservoir impact. *Science of the Total Environment*, *408*(20), 4654–4664. https://doi.org/10.1016/j.scitotenv.2010.07.007

Eaton, J. G., McCormick, J. H., Goodno, B. E., O'Brien, D. G., Stefany, H. G., Hondzo, M., & Scheller, R. M. (1995). A Field Information-based System for Estimating Fish Temperature Tolerances. *Fisheries*, *20*(4), 10–18. https://doi.org/10.1577/1548-8446(1995)020<0010:afisfe>2.0.co;2

Eaton, J. G., & Scheller, R. M. (1996). Effects of climate warming on fish thermal habitat in

streams of the United States. *Limnology and Oceanography*, *41*(5), 1109–1115. https://doi.org/10.4319/lo.1996.41.5.1109

Edwards, R. J. (1978). The Effect of Hypolimnion Reservoir Releases on Fish Distribution and Species Diversity. *Transactions of the American Fisheries Society*, *107*(1), 71–77. https://doi.org/10.1577/1548-8659(1978)107<71:teohrr>2.0.co;2

Elkins, D. C., Sweat, S. C., Hill, K. S., Kuhajda, B. R., Wenger, S. J., George, A. L., Angermeier, P., Baer, K., Darden, T., Elkins, D. C., Hill, K. S., Kuhajda, B. R., George, A. L., & Wenger, S. J. (2016). *The Southeastern Aquatic Biodiversity Conservation Strategy*.

Fukushiam, M., Kameyama, S., Kaneko, M., Nakao, K., & Ashley Steek, E. (2007). Modelling the effects of dams on freshwater fish distributions in Hokkaido, Japan. *Freshwater Biology*, *52*(8), 1511–1524. https://doi.org/10.1111/j.1365-2427.2007.01783.x

Gelda, R. K., Owens, E. M., & Effler, S. W. (1998). Calibration, verification, and an application of a two-dimensional hydrothermal model [ce-qual-w2(t)] for cannonsville reservoir. *Lake and Reservoir Management*, *14*(2–3), 186–196. https://doi.org/10.1080/07438149809354330

Hamman, J. J., Nijssen, B., Bohn, T. J., Gergel, D. R., & Mao, Y. (2018). The variable infiltration capacity model version 5 (VIC-5): Infrastructure improvements for new applications and reproducibility. *Geoscientific Model Development*, *11*(8), 3481–3496. https://doi.org/10.5194/gmd-11-3481-2018

Hanna, R. B., Saito, L., Bartholow, J. M., & Sandelin, J. (1999). Results of simulated temperature control device operations on in-reservoir and discharge water temperatures using CE-QUAL-W2. *Lake and Reservoir Management*, *15*(2), 87–102. https://doi.org/10.1080/07438149909353954

Hejazi, M. I., Voisin, N., Liu, L., Bramer, L. M., Fortin, D. C., Hathaway, J. E., Huang, M., Kyle, P., Leung, L. R., Li, H.-Y., Liu, Y., Patel, P. L., Pulsipher, T. C., Rice, J. S., Tesfa, T. K., Vernon, C. R., & Zhou, Y. (2015). 21st century United States emissions mitigation could increase water stress more than the climate change it is mitigating. *Proceedings of the National Academy of Sciences of the United States of America*, *112*(34), 1421675112-. https://doi.org/10.1073/pnas.1421675112

Homer, C., Dewitz, J., Jin, S., Xian, G., Costello, C., Danielson, P., Gass, L., Funk, M., Wickham, J., Stehman, S., Auch, R., & Riitters, K. (2020). Conterminous United States

land cover change patterns 2001–2016 from the 2016 National Land Cover Database. *ISPRS Journal of Photogrammetry and Remote Sensing*, *162*, 184–199. https://doi.org/10.1016/j.isprsjprs.2020.02.019

Horton, J. D., San Juan, C. A., & Stoeser, D. B. (2017). The State Geologic Map Compilation (SGMC) Geodatabase of the Conterminous United States (ver. 1.1, August 2017). In *U.S. Geological Survey Data Series 1052*. https://doi.org/10.3133/ds1052

Isaak, D. J., Wollrab, S., Horan, D., & Chandler, G. (2012). Climate change effects on stream and river temperatures across the northwest U.S. from 1980-2009 and implications for salmonid fishes. *Climatic Change*, *113*(2), 499–524. https://doi.org/10.1007/s10584-011-0326-z

Jenkins, C. N., Van Houtan, K. S., Pimm, S. L., & Sexton, J. O. (2015). US protected lands mismatch biodiversity priorities. *Proceedings of the National Academy of Sciences of the United States of America*, *112*(16), 5081–5086. https://doi.org/10.1073/pnas.1418034112

Kano, Y., Dudgeon, D., Nam, S., Samejima, H., Watanabe, K., Grudpan, C., Grudpan, J., Magtoon, W., Musikasinthorn, P., Nguyen, P. T., Praxaysonbath, B., Sato, T., Shibukawa, K., Shimatani, Y., Suvarnaraksha, A., Tanaka, W., Thach, P., Tran, D. D., Yamashita, T., & Utsugi, K. (2016). Impacts of dams and global warming on fish biodiversity in the Indo-Burma hotspot. *PLoS ONE*, *11*(8). https://doi.org/10.1371/journal.pone.0160151

Kędra, M., & Wiejaczka, Ł. (2018). Climatic and dam-induced impacts on river water temperature: Assessment and management implications. *Science of the Total Environment*, *626*, 1474–1483. https://doi.org/10.1016/j.scitotenv.2017.10.044

Ketabchy, M., Sample, D. J., Wynn-Thompson, T., & Nayeb Yazdi, M. (2018). Thermal evaluation of urbanization using a hybrid approach. *Journal of Environmental Management*, *226*, 457–475. https://doi.org/10.1016/j.jenvman.2018.08.016

Kimmell, T. A., & Veil, J. A. (2009). *Impact of drought on U.S. steam electric power plant cooling water intakes and related water resource management issues.* https://doi.org/10.2172/951252

Koch, H., & Vögele, S. (2009). Dynamic modelling of water demand, water availability and adaptation strategies for power plants to global change. *Ecological Economics*, *68*(7), 2031–2039. https://doi.org/10.1016/j.ecolecon.2009.02.015

Lawrence, D. J., Stewart-Koster, B., Olden, J. D., Ruesch, A. S., Torgersen, C. E., Lawler, J. J.,

Butcher, D. P., & Crown, J. K. (2014). The interactive effects of climate change, riparian management, and a nonnative predator on stream-rearing salmon. *Ecological Applications*, *24*(4), 895–912. https://doi.org/10.1890/13-0753.1

Layzer, J. B., & Scott, E. M. (2006). Restoration and colonization of freshwater mussels and fish in a southeastern United States tailwater. *River Research and Applications*, *22*(4), 475–491. https://doi.org/10.1002/rra.919

Lehner, B., Liermann, C. R., Revenga, C., Vörösmarty, C., Fekete, B., Crouzet, P., Döll, P., Endejan, M., Frenken, K., Magome, J., Nilsson, C., Robertson, J. C., Rödel, R., Sindorf, N., & Wisser, D. (2011). High□resolution mapping of the world's reservoirs and dams for sustainable river□flow management. *Frontiers in Ecology and the Environment*, *9*(9), 494–502. https://doi.org/10.1890/100125

Letcher, B. H., Nislow, K. H., Coombs, J. A., O'Donnell, M. J., & Dubreuil, T. L. (2007). Population response to habitat fragmentation in a stream-dwelling brook trout population. *PLoS ONE*, *2*(11). https://doi.org/10.1371/journal.pone.0001139

Li, H., Ruby Leung, L., Tesfa, T., Voisin, N., Hejazi, M., Liu, L., Liu, Y., Rice, J., Wu, H., & Yang, X. (2015). Modeling stream temperature in the Anthropocene: An earth system modeling approach. *Journal of Advances in Modeling Earth Systems*, *7*(4), 1661–1679. https://doi.org/10.1002/2015MS000471

Li, H., Wigmosta, M. S., Wu, H., Huang, M., Ke, Y., Coleman, A. M., & Leung, L. R. (2013). A Physically Based Runoff Routing Model for Land Surface and Earth System Models. *Journal of Hydrometeorology*, *14*(3), 808–828. https://doi.org/10.1175/JHM-D-12-015.1

Liang, X., Lettenmaier, D. P., Wood, E. F., & Burges, S. J. (1994). A simple hydrologically based model of land surface water and energy fluxes for general circulation models. *Journal of Geophysical Research*, *99*(D7), 14415. https://doi.org/10.1029/94JD00483

Liermann, C. R., Nilsson, C., Robertson, J., & Ng, R. Y. (2012). Implications of Dam Obstruction for Global Freshwater Fish Diversity. *BioScience*, *62*(6), 539–548. https://doi.org/10.1525/bio.2012.62.6.5

Ligon, F. K., Dietrich, W. E., & Trush, W. J. (1995). Downstream Ecological Effects of Dams. *BioScience*, *45*(3), 183–192. https://doi.org/10.2307/1312557

Liu, L., Hejazi, M., Li, H., Forman, B., & Zhang, X. (2017). Vulnerability of US thermoelectric power generation to climate change when incorporating state-level environmental

regulations. *Nature Energy*, *2*(8), 17109. https://doi.org/10.1038/nenergy.2017.109

Lowney, C. L. (2000). Stream temperature variation in regulated rivers: Evidence for a spatial pattern in daily minimum and maximum magnitudes. *Water Resources Research*, *36*(10), 2947–2955. https://doi.org/10.1029/2000WR900142

Madden, N., Lewis, A., & Davis, M. (2013). Thermal effluent from the power sector: an analysis of once-through cooling system impacts on surface water temperature. *Environmental Research Letters*, *8*(3), 035006. https://doi.org/10.1088/1748-9326/8/3/035006

Maheu, A., St-Hilaire, A., Caissie, D., & El-Jabi, N. (2016). Understanding the Thermal Regime of Rivers Influenced by Small and Medium Size Dams in Eastern Canada. *River Research and Applications*, *32*(10), 2032–2044. https://doi.org/10.1002/rra.3046

Mantua, N., Tohver, I., & Hamlet, A. (2010). Climate change impacts on streamflow extremes and summertime stream temperature and their possible consequences for freshwater salmon habitat in Washington State. *Climatic Change*, *102*(1–2), 187–223. https://doi.org/10.1007/s10584-010-9845-2

Mantua, N., Tohver, I., Hamlet, A., Mantua, N., Tohver, I., & Hamlet, A. (2010). Climate change impacts on streamflow extremes and summertime stream temperature and their possible consequences for freshwater salmon habitat in Washington State. *Climatic Change*, *102*(102). https://doi.org/10.1007/s10584-010-9845-2

Matthews, W. J., & Zimmerman, E. G. (1990). Potential Effects of Global Warming on Native Fishes of the Southern Great Plains and the Southwest. *Fisheries*, *15*(6), 26–32. https://doi.org/10.1577/1548-8446(1990)015<0026:PEOGWO>2.0.CO;2

Maurer, E. P., Wood, A. W., Adam, J. C., Lettenmaier, D. P., & Nijssen, B. (2002). A long-term hydrologically based dataset of land surface fluxes and states for the conterminous United States. *Journal of Climate*, *15*(22), 3237–3251. https://doi.org/10.1175/1520-0442(2002)015<3237:ALTHBD>2.0.CO;2

McCall, J., Macknick, J., & Daniel, H. (2016). Water-Related Power Plant Curtailments: An Overview of Incidents and Contributing Factors. In *National Renewable Energy Laboratory*. www.nrel.gov/publications.

McDermott, G. R., & Nilsen, Ø. A. (2014). Electricity prices, river temperatures, and cooling water scarcity. *Land Economics*, *90*(1), 131–148. https://doi.org/10.3368/le.90.1.131

McDonnell, T. C., Sloat, M. R., Sullivan, T. J., Dolloff, C. A., Hessburg, P. F., Povak, N. A.,

Jackson, W. A., & Sams, C. (2015). Downstream warming and headwater acidity may diminish coldwater habitat in southern appalachian mountain streams. *PLoS ONE*, *10*(8). https://doi.org/10.1371/journal.pone.0134757

Miara, A., Macknick, J. E., Vörösmarty, C. J., Tidwell, V. C., Newmark, R., & Fekete, B. (2017). Climate and water resource change impacts and adaptation potential for US power supply. *Nature Climate Change*, *7*(11), 793–798. https://doi.org/10.1038/nclimate3417

Miara, A., Vörösmarty, C. J., Macknick, J. E., Tidwell, V. C., Fekete, B., Corsi, F., & Newmark, R. (2018). Thermal pollution impacts on rivers and power supply in the Mississippi River watershed. *Environmental Research Letters*, *13*(3). https://doi.org/10.1088/1748-9326/aaac85

Mohseni, O., Stefan, H. G., & Erickson, T. R. (1998). A nonlinear regression model for weekly stream temperatures. *Water Resources Research*, *34*(10), 2685. https://doi.org/10.1029/98WR01877

Nelson, K. C., & Palmer, M. A. (2007). Stream temperature surges under urbanization and climate change: Data, models, and responses. *Journal of the American Water Resources Association*, *43*(2), 440–452. https://doi.org/10.1111/j.1752-1688.2007.00034.x

Neves, R. J., & Angermeier, P. L. (1990). Habitat alteration and its effects on native fishes in the upper Tennessee River system, east-central U.S.A. *Journal of Fish Biology*, *37*(sa), 45–52. https://doi.org/10.1111/j.1095-8649.1990.tb05019.x

Niemeyer, R. J., Cheng, Y., Mao, Y., Yearsley, J. R., & Nijssen, B. (2018). A Thermally Stratified Reservoir Module for Large□Scale Distributed Stream Temperature Models With Application in the Tennessee River Basin. *Water Resources Research*, *54*(10), 8103–8119. https://doi.org/10.1029/2018WR022615

Olden, J. D. (2015). Challenges and opportunities for fish conservation in dam-impacted waters. In *Conservation of Freshwater Fishes* (pp. 107–148). Cambridge University Press. https://doi.org/10.1017/cbo9781139627085.005

Olden, J. D., & Naiman, R. J. (2010). Incorporating thermal regimes into environmental flows assessments: Modifying dam operations to restore freshwater ecosystem integrity. *Freshwater Biology*, *55*(1), 86–107. https://doi.org/10.1111/j.1365-2427.2009.02179.x

Ontario Ministry of Natural Resources and Watershed Science Centre. (2001). Natural Channel Systems: An approach to management and design. In *Adaptive Management of Stream*

Corridors in Ontario (pp. 1–116). Ministry of Natural Resources.

Phillips, S. J., Anderson, R. P., & Schapire, R. E. (2006). Maximum entropy modeling of species geographic distributions. *Ecological Modelling*, *190*(3–4), 231–259. https://doi.org/10.1016/j.ecolmodel.2005.03.026

Poff, N. L., Brinson, M. M., & Day, J. W. (2002). Aquatic ecosystems & Global climate change: Potential Impacts on Inland Freshwater and Coastal Wetland Ecosystems in the United States. In *Pew Center on Global Climate Change*. https://doi.org/10.1039/b211160h

Pyrce, R. (2004). Hydrological Low Flow Indices and their Uses. In *WSC Report No. 04-2004*.

Radosavljevic, A., & Anderson, R. P. (2014). Making better Maxent models of species distributions: Complexity, overfitting and evaluation. *Journal of Biogeography*, *41*(4), 629–643. https://doi.org/10.1111/jbi.12227

Raptis, C. E., & Pfister, S. (2016). Global freshwater thermal emissions from steam-electric power plants with once-through cooling systems. *Energy*, *97*, 46–57. https://doi.org/10.1016/j.energy.2015.12.107

Reuter, H. I., Nelson, A., & Jarvis, A. (2007). An evaluation of void-filling interpolation methods for SRTM data. *International Journal of Geographical Information Science*, *21*(9), 983–1008. https://doi.org/10.1080/13658810601169899

Rheinheimer, D. E., Null, S. E., & Lund, J. R. (2015). Optimizing Selective Withdrawal from Reservoirs to Manage Downstream Temperatures with Climate Warming. *Journal of Water Resources Planning and Management*, *141*(4), 04014063. https://doi.org/10.1061/(ASCE)WR.1943-5452.0000447

Rounds, S. A., & Buccola, N. L. (2015). Improved Algorithms in the CE–QUAL–W2 Water-Quality Model for Blending Dam Releases to Meet Downstream Water-Temperature Targets. In *U.S. Geological Survey Open-File Report 2015-1027*. http://dx.doi.org/10.3133/ofr20151027

Rubenson, E. S., & Olden, J. D. (2020). An invader in salmonid rearing habitat: Current and future distributions of smallmouth bass (micropterus dolomieu) in the Columbia river basin. *Canadian Journal of Fisheries and Aquatic Sciences*, *77*(2), 314–325. https://doi.org/10.1139/cjfas-2018-0357

Ruesch, A. S., Torgersen, C. E., Lawler, J. J., Olden, J. D., Peterson, E. E., Volk, C. J., & Lawrence, D. J. (2012). Projected Climate-Induced Habitat Loss for Salmonids in the John

Day River Network, Oregon, U.S.A. *Conservation Biology*, *26*(5), 873–882. https://doi.org/10.1111/j.1523-1739.2012.01897.x

Rutberg, M. J. (2012). *Modeling Water Use at Thermoelectric Power Plants*. Massachusetts Institute of Technology.

Ryan, T., Webb, A., Lennie, R., & Lyon, J. (2014). *Status of Cold Water Releases from Victorian Dams*. https://www.researchgate.net/publication/263273681

Sauter, S. T., Mcmillan, J., & Dunham, J. (2001). Salmonid Behavior and Water Temperature. In *Seattle, WA: United States, Environmental Protection Agency, Region 10 Office of Water. Final Report to the Policy workgroup of the EPA Region 10 Water Temperature Criteria Guidance Project. EPA 910-D-01-001. 36 p*. https://www.fs.usda.gov/treesearch/pubs/23970

Shea, C. P., Bettoli, P. W., Potoka, K. M., Saylor, C. F., & Shute, P. W. (2015). Use of Dynamic Occupancy Models to Assess the Response of Darters (Teleostei: Percidae) to Varying Hydrothermal Conditions in a Southeastern United States Tailwater. *River Research and Applications*, *31*(6), 676–691. https://doi.org/10.1002/rra.2766

Stanford, J. A., & Ward, J. V. (1979). Dammed Rivers of the World: Symposium Rationale. In *The Ecology of Regulated Streams* (pp. 1–5). Springer US. https://doi.org/10.1007/978-1-4684-8613-1_1

Strzepek, K., Fant, C., Gebretsadik, Y., Lickley, M., Boehlert, B., Chapra, S., Adams, E., Strzepek, A., & Schlosser, C. A. (2015). *Water Body Temperature Model for Assessing Climate Change Impacts on Thermal Cooling*. *280*.

Sun, N., Yearsley, J., Voisin, N., & Lettenmaier, D. P. (2015). A spatially distributed model for the assessment of land use impacts on stream temperature in small urban watersheds. *Hydrological Processes*, *29*(10), 2331–2345. https://doi.org/10.1002/hyp.10363

Taylor, K. E., Stouffer, R. J., & Meehl, G. A. (2012). An overview of CMIP5 and the experiment design. In *Bulletin of the American Meteorological Society* (Vol. 93, Issue 4, pp. 485–498). American Meteorological Society . https://doi.org/10.1175/BAMS-D-11-00094.1

Thornton, P. E., & Running, S. W. (1999). An improved algorithm for estimating incident daily solar radiation from measurements of temperature, humidity, and precipitation. *Agricultural and Forest Meteorology*, *93*(4), 211–228. https://doi.org/10.1016/S0168-1923(98)00126-9

Trudgill, D. L., Honek, A., Li, D., & Van Straalen, N. M. (2005). Thermal time - Concepts and

utility. In *Annals of Applied Biology* (Vol. 146, Issue 1, pp. 1–14). Blackwell Publishing Ltd. https://doi.org/10.1111/j.1744-7348.2005.04088.x

USACE-HEC. (1986). *WQRRS Water Quality for River-Reservoir Systems user's manual*.

USGS. (2019). *National Water Information System data available on the World Wide Web (USGS Water Data for the Nation)*. https://waterdata.usgs.gov/nwis/

USGS, (US Geological Survey). (2007). *GIS Features of the Geospatial Fabric for National Hydrologic Modeling - ScienceBase-Catalog*. https://www.sciencebase.gov/catalog/item/535eda80e4b08e65d60fc834

van Vliet, M. T. H., Franssen, W. H. P., Yearsley, J. R., Ludwig, F., Haddeland, I., Lettenmaier, D. P., & Kabat, P. (2013). Global river discharge and water temperature under climate change. *Global Environmental Change*, *23*(2), 450–464. https://doi.org/10.1016/j.gloenvcha.2012.11.002

van Vliet, M. T. H., Ludwig, F., Zwolsman, J. J. G., Weedon, G. P., & Kabat, P. (2011). Global river temperatures and sensitivity to atmospheric warming and changes in river flow. *Water Resources Research*, *47*(2), n/a-n/a. https://doi.org/10.1029/2010WR009198

van Vliet, M. T. H., Vögele, S., & Rübbelke, D. (2013). Water constraints on European power supply under climate change: Impacts on electricity prices. *Environmental Research Letters*, *8*(3), 035010. https://doi.org/10.1088/1748-9326/8/3/035010

van Vliet, M. T. H., Wiberg, D., Leduc, S., & Riahi, K. (2016). Power-generation system vulnerability and adaptation to changes in climate and water resources. *Nature Climate Change*, *6*(4), 375–380. https://doi.org/10.1038/nclimate2903

van Vliet, M. T. H., Yearsley, J. R., Franssen, W. H. P., Ludwig, F., Haddeland, I., Lettenmaier, D. P., & Kabat, P. (2012). Coupled daily streamflow and water temperature modelling in large river basins. *Hydrology and Earth System Sciences*, *16*(11), 4303–4321. https://doi.org/10.5194/hess-16-4303-2012

van Vliet, M. T. H., Yearsley, J. R., Ludwig, F., Vögele, S., Lettenmaier, D. P., & Kabat, P. (2012). Vulnerability of US and European electricity supply to climate change. *Nature Climate Change*, *2*(9), 676–681. https://doi.org/10.1038/nclimate1546

VanCompernolle, M., Knouft, J. H., & Ficklin, D. L. (2019). Multispecies conservation of freshwater fish assemblages in response to climate change in the southeastern United States. *Diversity and Distributions*, *25*(9), 1388–1398. https://doi.org/10.1111/ddi.12948

Voisin, N., Hejazi, M. I., Leung, L. R., Liu, L., Huang, M., Li, H. Y., & Tesfa, T. (2017). Effects of spatially distributed sectoral water management on the redistribution of water resources in an integrated water model. *Water Resources Research*, *53*(5), 4253–4270. https://doi.org/10.1002/2016WR019767

Voisin, N., Kintner-Meyer, M., Skaggs, R., Nguyen, T., Wu, D., Dirks, J., Xie, Y., & Hejazi, M. (2016). Vulnerability of the US western electric grid to hydro-climatological conditions: How bad can it get? *Energy*, *115*, 1–12. https://doi.org/10.1016/j.energy.2016.08.059

Voisin, N., Li, H., Ward, D., Huang, M., Wigmosta, M., & Leung, L. R. (2013). On an improved sub-regional water resources management representation for integration into earth system models. *Hydrology and Earth System Sciences*, *17*(9), 3605–3622. https://doi.org/10.5194/hess-17-3605-2013

Voisin, N., Liu, L., Hejazi, M., Tesfa, T., Li, H., Huang, M., Liu, Y., & Leung, L. R. (2013). One-way coupling of an integrated assessment model and a water resources model: evaluation and implications of future changes over the US Midwest. *Hydrology and Earth System Sciences*, *17*(11), 4555–4575. https://doi.org/10.5194/hess-17-4555-2013

Webb, R. H., Wegner, D. L., Andrews, E. D., Valdez, R. A., & Patten, D. T. (1999). Downstream effects of glen canyon dam on the Colorado river in grand canyon: A review. In *Geophysical Monograph Series* (Vol. 110, pp. 1–21). Blackwell Publishing Ltd. https://doi.org/10.1029/GM110p0001

Welsh, H. H., Hodgson, G. R., Harvey, B. C., & Roche, M. F. (2001). Distribution of Juvenile Coho Salmon in Relation to Water Temperatures in Tributaries of the Mattole River, California. *North American Journal of Fisheries Management*, *21*(3), 464–470. https://doi.org/10.1577/1548-8675(2001)021<0464:DOJCSI>2.0.CO;2

Willey, R. G. (1986). *HEC-5Q: System water quality modeling*.

Yang, L., Jin, S., Danielson, P., Homer, C., Gass, L., Bender, S. M., Case, A., Costello, C., Dewitz, J., Fry, J., Funk, M., Granneman, B., Liknes, G. C., Rigge, M., & Xian, G. (2018). *ISPRS Journal of Photogrammetry and Remote Sensing A new generation of the United States National Land Cover Database: Requirements, research priorities, design, and implementation strategies*. https://doi.org/10.1016/j.isprsjprs.2018.09.006

Yearsley, J. R. (2009). A semi-Lagrangian water temperature model for advection-dominated river systems. *Water Resources Research*, *45*(12), 1–19.

https://doi.org/10.1029/2008WR007629

Yearsley, J. R. (2012). A grid-based approach for simulating stream temperature. *Water Resources Research*, *48*(3), 1–15. https://doi.org/10.1029/2011WR011515

Yearsley, J. R., Sun, N., Baptiste, M., & Nijssen, B. (2019). Assessing the impacts of hydrologic and land use alterations on water temperature in the Farmington River basin in Connecticut. *Hydrology and Earth System Sciences*, *23*(11), 4491–4508. https://doi.org/10.5194/hess-23-4491-2019

Yu, S., Wei, Y. M., & Wang, K. (2014). Provincial allocation of carbon emission reduction targets in China: An approach based on improved fuzzy cluster and Shapley value decomposition. *Energy Policy*, *66*, 630–644. https://doi.org/10.1016/j.enpol.2013.11.025

Zhang, X., Li, H., Leung, L. R., Liu, L., Hejazi, M. I., Forman, B. A., & Yigzaw, W. (2020). River Regulation Alleviates the Impacts of Climate Change on U.S. Thermoelectricity Production. *Journal of Geophysical Research: Atmospheres*, *125*(4). https://doi.org/10.1029/2019JD031618

Zhou, T., Voisin, N., Leng, G., Huang, M., & Kraucunas, I. (2018). Sensitivity of Regulated Flow Regimes to Climate Change in the Western United States. *Journal of Hydrometeorology*, *19*(3), 499–515. https://doi.org/10.1175/JHM-D-17-0095.1

APPENDIX A SUPPLEMENTAL MATERIALS FOR CHAPTER 2: RESERVOIRS MODIFY RIVER THERMAL REGIME SENSITIVITY TO CLIMATE CHANGE: A CASE STUDY IN THE SOUTHEASTERN UNITED STATES

A.1. Texts

A.1.1. *Reservoir storage, storage targets and guide curves*

A.1.1.1. Method to calculate reservoir storage from observed elevation data or guide curve

To estimate reservoir storage from reservoir elevation data, we assumed that the reservoir shape can be approximated as a tetrahedron (Fekete, et al., 2010; Figure A.1). The reservoir shape was defined by the following parameters:

- D_{dam} : dam height, available in the GRanD database ($D_{dam} = H_{dam} - H_{bot}$, Lehner et al., 2011), where H_{dam} is the elevation at the top of the dam and H_{bot} is the elevation at the bottom of the dam.
- D_{full} : full pool depth ($D_{full} = H_{full} - H_{bot}$), where H_{full} is the elevation at full pool (spillway design flood or spillway crest)
- D_{obs} : observed pool depth ($D_{obs} = H_{obs} - H_{bot}$), where H_{obs} is the observed reservoir surface elevation

The GRanD database (Lehner et al., 2011) also provided the maximum reservoir storage capacity (C_{max}), corresponding to the reservoir capacity at the full pool elevation (H_{full}). Given the surface area at maximum capacity (A_{max}), C_{max} was calculated as

$$C_{max} = \frac{1}{3} D_{full} A_{max} \quad \text{(A.1)}$$

The assumed shape (tetrahedron) also dictated the relationship between the full pool depth (D_{full}) and the maximum surface area (A_{max}), as well as the relationship between D_{full} and the maximum storage (C_{max}), such that $A_{max} \propto {D_{full}}^2$ and $C_{max} \propto {D_{full}}^3$. Thus, given D_{obs}, we calculated the reservoir storage (V_{obs}) using

$$V_{obs} = (\frac{D_{obs}}{D_{full}})^3 \times C_{max} \quad \text{(A.2)}$$

Reservoir depth (D_{obs}) is not usually measured directly. Instead, we calculated it based on the observed surface elevation (H_{obs}) minus the elevation at the bottom of the reservoir (H_{bot}). However, H_{bot} was not readily available for most reservoirs. Fortunately, full pool elevation was available for most reservoirs and full pool depth is usually 5% or 10% less than the dam height for safety reasons, so we assumed:

$$D_{full} = 0.95 D_{dam} \quad \text{(A.3)}$$

Then we calculated H_{bot} as

$$H_{bot} = H_{full} - 0.95 D_{dam} \quad \text{(A.4)}$$

A.1.1.2. Data availability for observed storage and elevation and reservoir guide curves

We used observed reservoir storage data from the Tennessee Valley Authority (TVA), U.S. Army Corps of Engineers (USACE), and United States Geological Survey (USGS). We also obtained records of reservoir surface elevation from the USGS, which can also be used to calculate reservoir storage using the methods outlined in Text S1.1. USACE specifies guide curves (surface elevation, not reservoir storage) for some of the reservoirs that it operates. A summary of the data sources and data availability for each region is provided in Table A.3 and Table A.4, respectively. The reservoir full pool elevation data was mainly sourced from USACE, USGS, and U.S. lake levels (http://www.lakelevels.info/). When surface elevation data were not available, we used the highest reported surface elevation as the full pool elevation. Data sources for all sites are summarized in Table A.5.

A.1.1.3. Estimate storage target for reservoirs without observed storage data

In this study, storage targets for 92 reservoirs with regulation information were used as a library to estimate the storage targets for reservoirs for which we lacked regulation information. We estimated the storage targets for these reservoirs based on the storage targets for reservoirs that were the most "similar" in the library. "Similarity" in this context was determined by two criteria, namely 1) primary regulation objective and 2) similar values of relative degree (RD) to which they were filled. We first categorized 92 reservoirs into two groups based on their primary objective, flood control (n=49) and other (n=43). Then we normalized the monthly storage targets by capacity. Normalized storage targets showed similar seasonality, with high storage in the summer and low storage in the winter. We evaluated the seasonality using the standard

deviation of the normalized monthly storage targets, with values smaller than 0.1 for most reservoirs (Figure A.2a). However, RD showed great variability among different reservoirs (Figure A.2b).

RD is the ratio of normal pool volume to maximum capacity, which should be correlated with either depth ratio (water depth of normal pool to full pool depth) or surface area ratio (normal pool area to full pool area). The variable "AREA_SKM", which denotes the surface area for normal pool (A_{norm}) in km^2, is available for most reservoirs in the GRanD database. We calculated the surface area at full pool (A_{full}) using maximum capacity and dam height and the assumption that the reservoir shape is a tetrahedron. For each group of reservoirs with regulation information, we fitted a regression model to relate RD to the calculated area ratio (A_{norm}/A_{full}),

$$RD = a \times \ln(A_{norm}/A_{full}) + b \tag{A.5}$$

For flood control reservoirs, we determined that $a = 0.29$ and $b = 0.73$; for other reservoirs, $a = 0.32$, $b = 0.78$. Figure A.3 shows a comparison of simulated RD and observed RD for each group.

For every reservoir for which we lacked regulation information, we used the corresponding regression model to calculate RD based on the primary regulation objective and area ratio. Then we searched the library for two reservoirs with the same primary objective and with the closest RD values. Finally, we assigned the mean of the relative storage targets of the two selected reservoirs as the relative storage target for the reservoir that lacked this information.

For evaluation, we used the method above to simulate the storage targets for reservoirs with regulation information and compared their simulated storage targets with their actual storage targets. Median values of correlation coefficient, root mean square error, and standard deviation of normalized storage targets (12 values) for each group are shown in Table A.6. This method generally worked well for both groups.

A.1.2. *Errors in streamflow, storage and stream temperature*

In this study, errors in regulated streamflow mainly resulted from biased runoff from the hydrological model and fixed monthly storage targets. Maps of relative bias in mean seasonal streamflow are shown in Figure A.4. After we tuned the soil parameters for the South Atlantic region, mean annual streamflow was similar to observations, but the simulated streamflow seasonality demonstrated higher biases compared to other regions (Figure A.4). In the South Atlantic, the simulations showed a wet bias in winter (high flow period) and a dry bias in summer (low flow period), which explains the low NS coefficients in the South Atlantic region (Figure A.5). The fixed guide curves and storage targets did not account for inflow variability, potentially overestimating outflow and underestimating storage in a wet year and vice versa. Furthermore, the fixed storage target was unable to deal with the bias of the amplified seasonality in the hydrological model. The overpredicted inflow in winter results in overpredicted winter outflow, while the underpredicted inflow in summer results in underpredicted summer outflow.

In this study, we fixed the storage target for both the historical and future periods to isolate climate change impacts from changes in regulations. Errors may result from the estimated storage targets for reservoirs without guide curves or observations. Reservoirs in our study region are operated by multiple corporations and agencies and the access to observations varies. In this study, we collected observed elevation, storage or rule curve data for 92 reservoirs.

Our assumption that all reservoirs release from the hypolimnion can also cause errors. For example, we underestimate the summer temperature at three USGS sites close to the northern boundary of our study region. In reality, these reservoirs release their water from the epilimnion and have therefore higher downstream temperatures than we simulated.

A.2. Figures

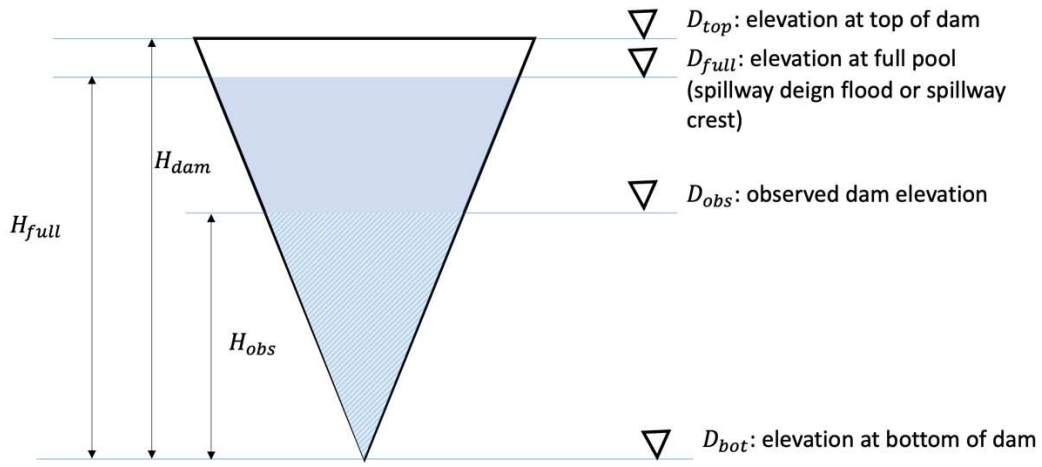

Figure A.1. Diagram of reservoir cross section

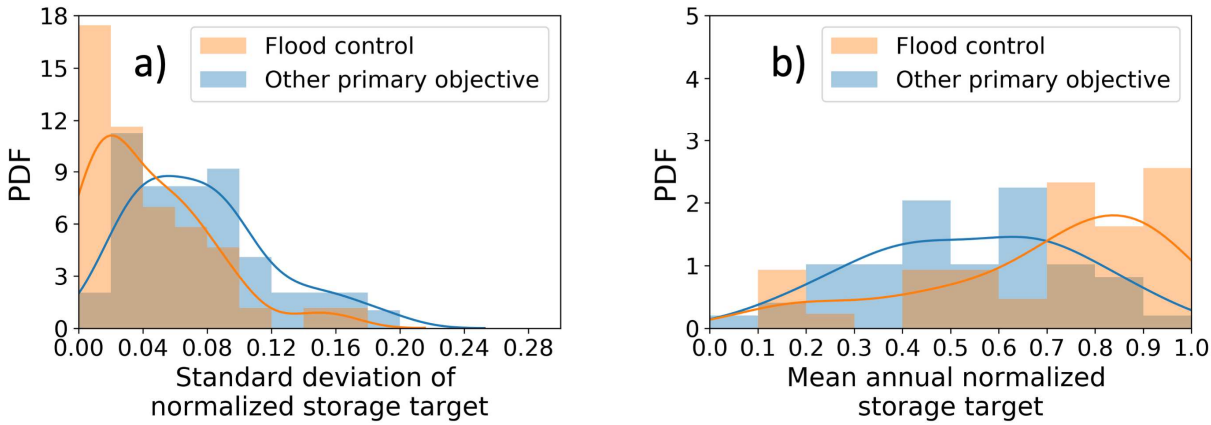

Figure A.2. Distribution of a) standard deviation and b) mean value of normalized monthly storage target for reservoirs with flood control as primary use (orange) and reservoirs with primary use other than flood control (blue)

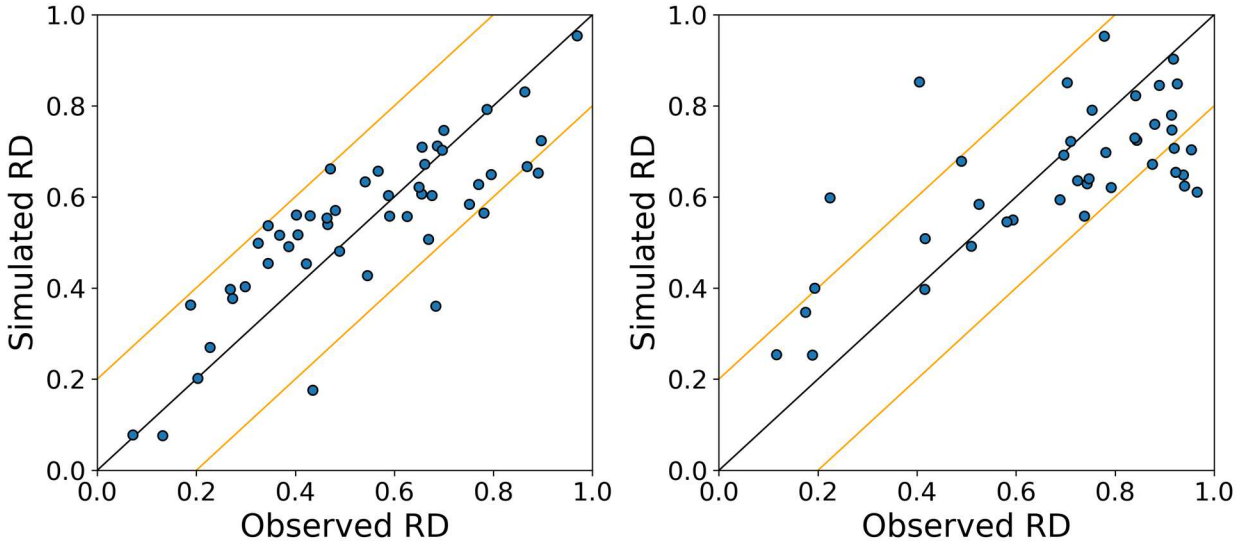

Figure A.3. Simulated versus observed RD (left: flood control, right: others). Each dot represents one reservoir, black line is an identity line where simulated RD equals to observed RD and orange lines are error bounds with errors in simulated RD of 0.2.

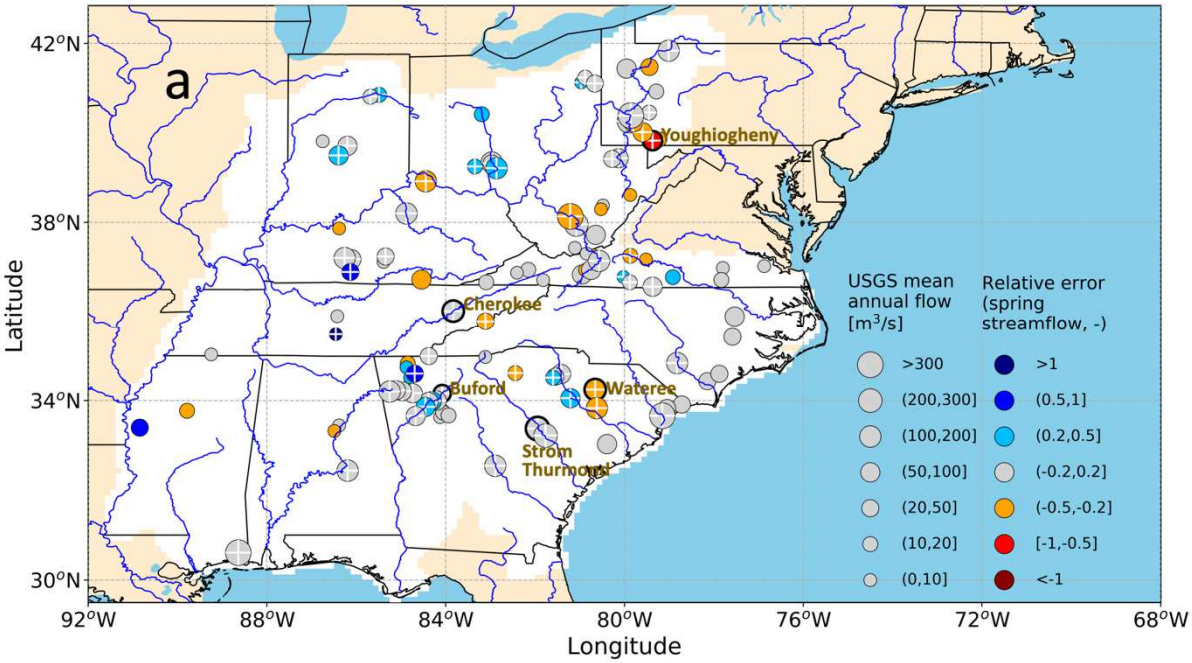
a
42°N
38°N
34°N
30°N
Latitude
92°W
88°W
84°W
80°W
76°W
72°W
68°W
Longitude
Youghiogheny
Cherokee
Buford
Wateree
Strom Thurmond
USGS mean annual flow [m³/s]
>300
(200,300]
(100,200]
(50,100]
(20,50]
(10,20]
(0,10]
Relative error (spring streamflow, -)
>1
(0.5,1]
(0.2,0.5]
(-0.2,0.2]
(-0.5,-0.2]
[-1,-0.5]
<-1

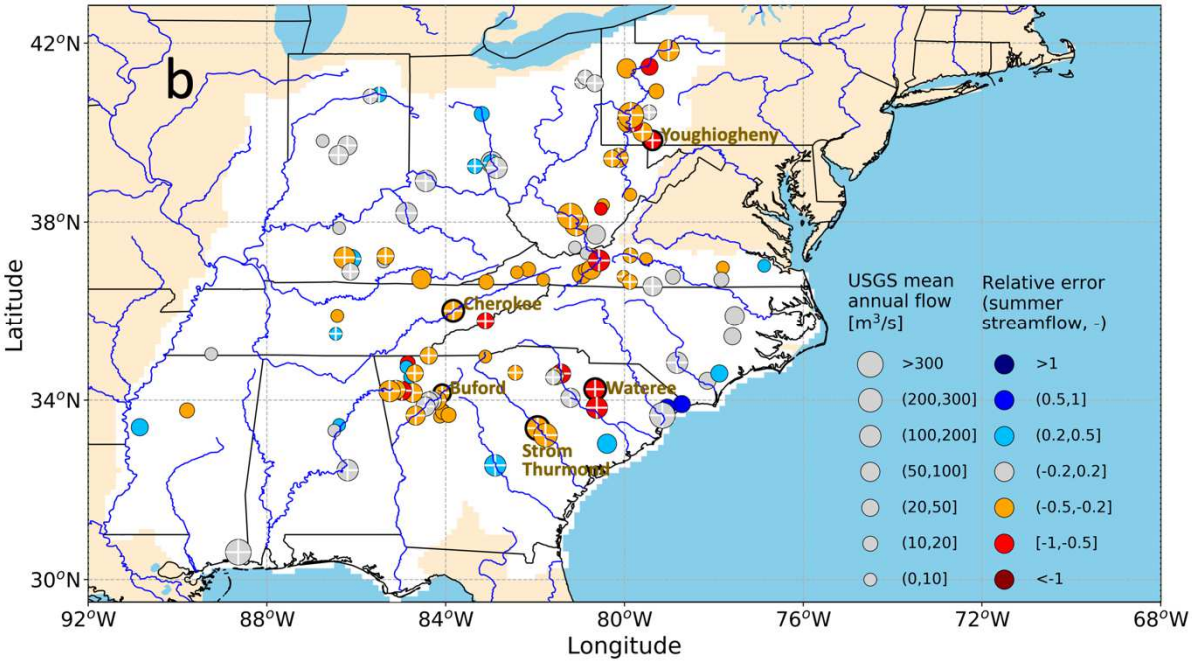
b
42°N
38°N
34°N
30°N
Latitude
92°W
88°W
84°W
80°W
76°W
72°W
68°W
Longitude
Youghiogheny
Cherokee
Buford
Wateree
Strom Thurmond
USGS mean annual flow [m³/s]
>300
(200,300]
(100,200]
(50,100]
(20,50]
(10,20]
(0,10]
Relative error (summer streamflow, -)
>1
(0.5,1]
(0.2,0.5]
(-0.2,0.2]
(-0.5,-0.2]
[-1,-0.5]
<-1

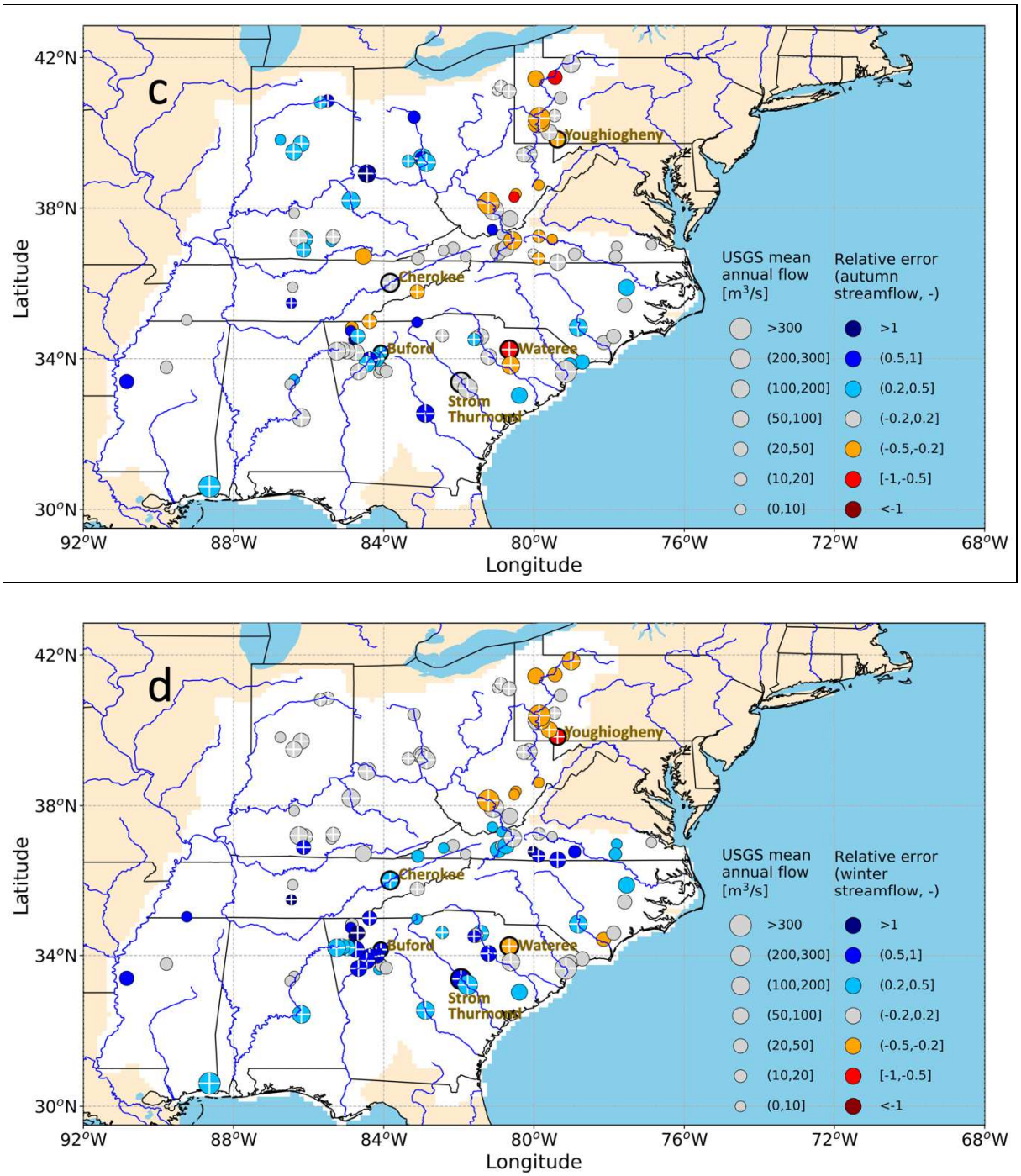

Figure A.4. Map of relative bias in mean seasonal streamflow for all USGS sites. Panels from top to bottom are for a) spring, b) summer, c) autumn and d) winter, respectively. Circle size represents USGS observed mean annual streamflow; circles with a white cross inside represent sites influenced by reservoir regulation; color scheme shows relative errors in mean annual streamflow.

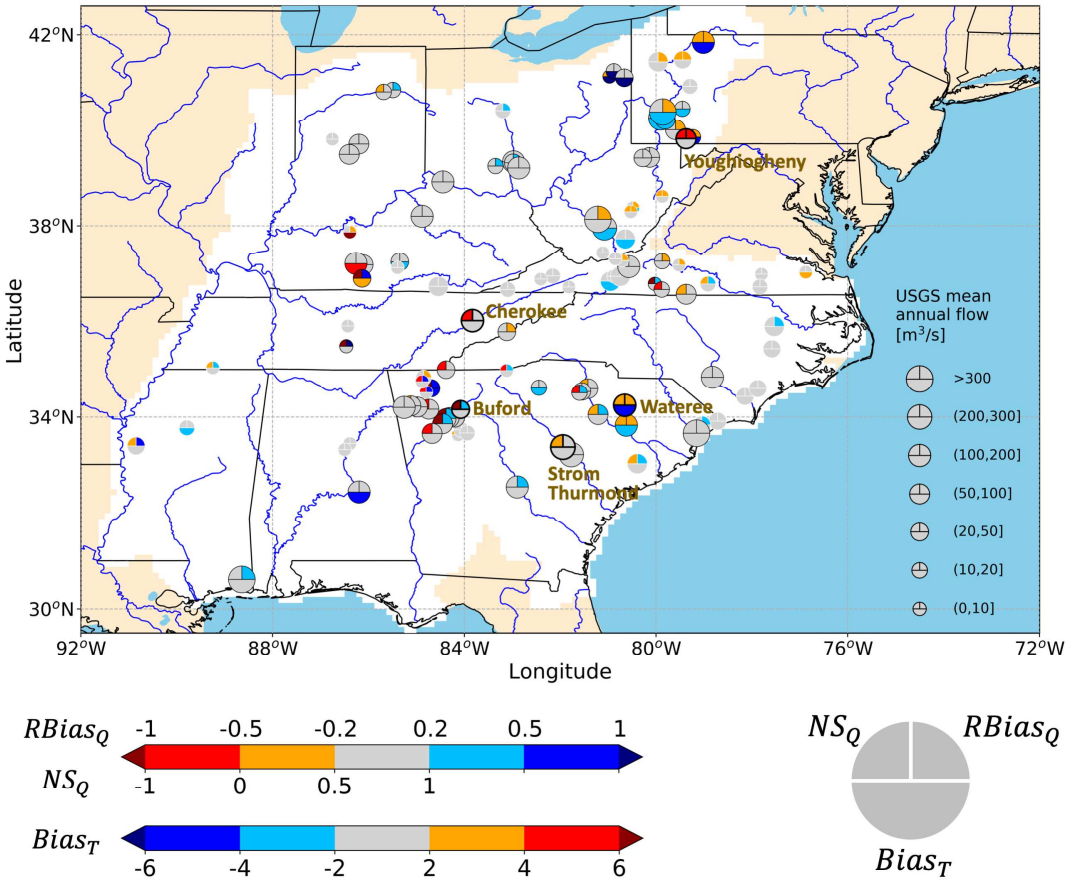

Figure A.5. Map of 1) relative bias in mean annual streamflow ($RBais_Q$), 2) Nash-Sutcliff coefficient for monthly streamflow (NS_Q), and 3) bias in mean summer stream temperature ($Bias_T$), for all USGS sites. The circle size represents USGS observed mean annual streamflow; circles with black edges represent sites with reservoir regulation, while white edges represent sites without regulation. The relative streamflow bias, $RBais_Q$, was calculated as simulated minus observed mean annual flow divided by observed mean annual flow. The Nash-Sutcliffe coefficient, NS_Q , was calculated based on the monthly simulated and observed flow.

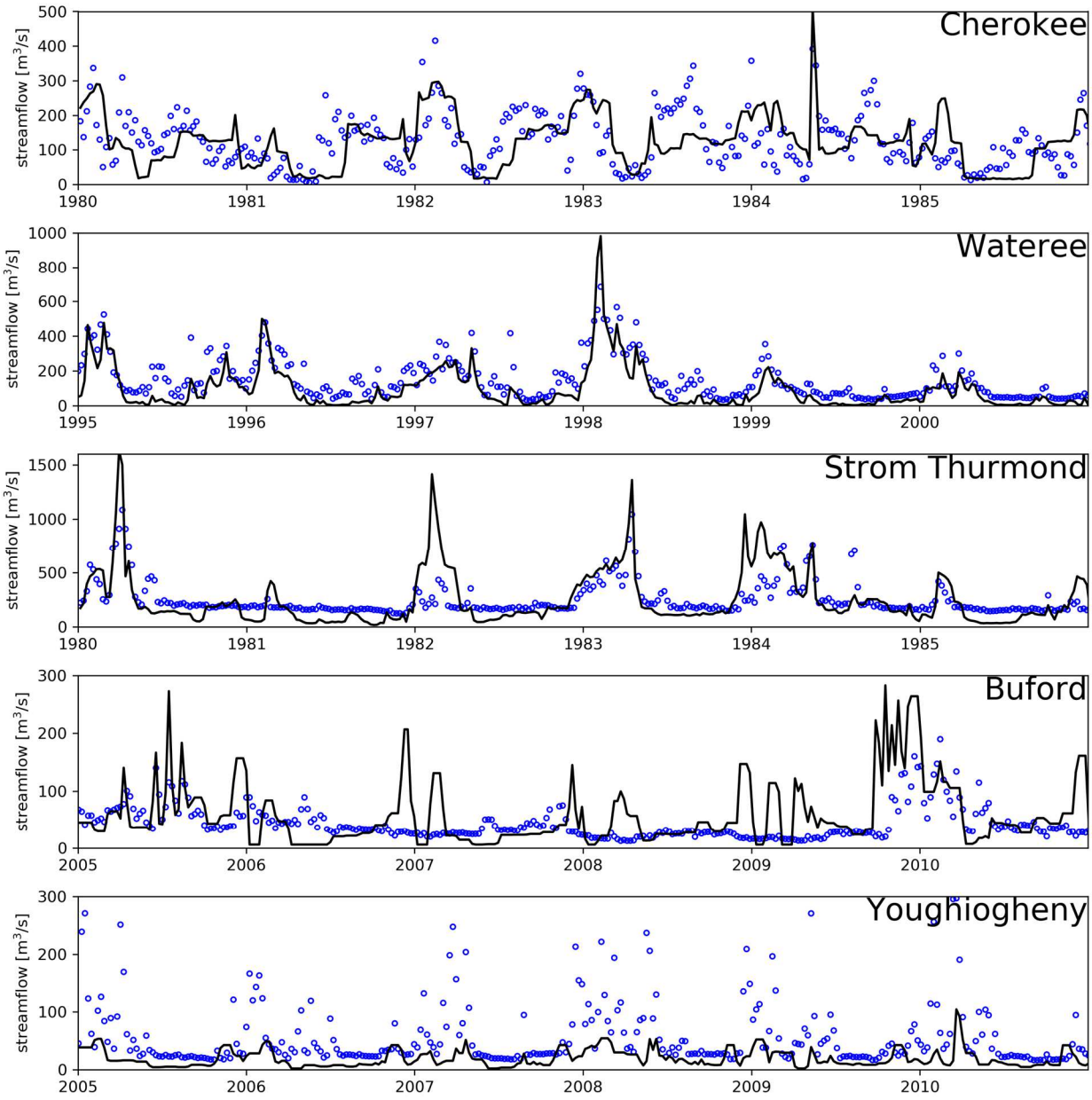

Figure A.6. Selected timeseries of simulated (black line) and observed streamflow (blue dots)

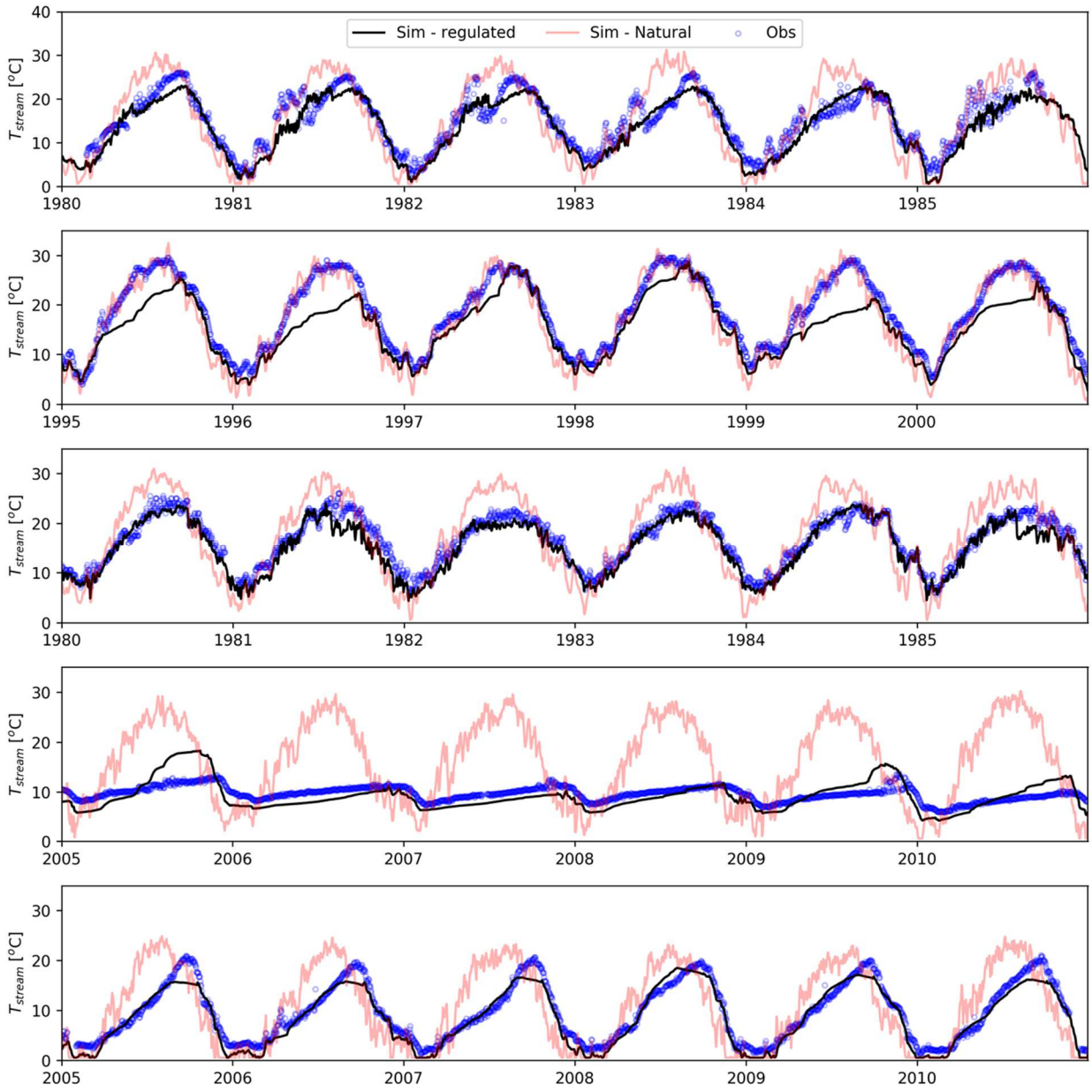

Figure A.7. Timeseries for simulated stream temperature in the regulated (black lines) and unregulated or natural (red lines) model setups. Blue dots represent stream temperature observations. From top to bottom: Tennessee River, Catawba River, Savannah River, Chattahoochee River, and Youghiogheny River.

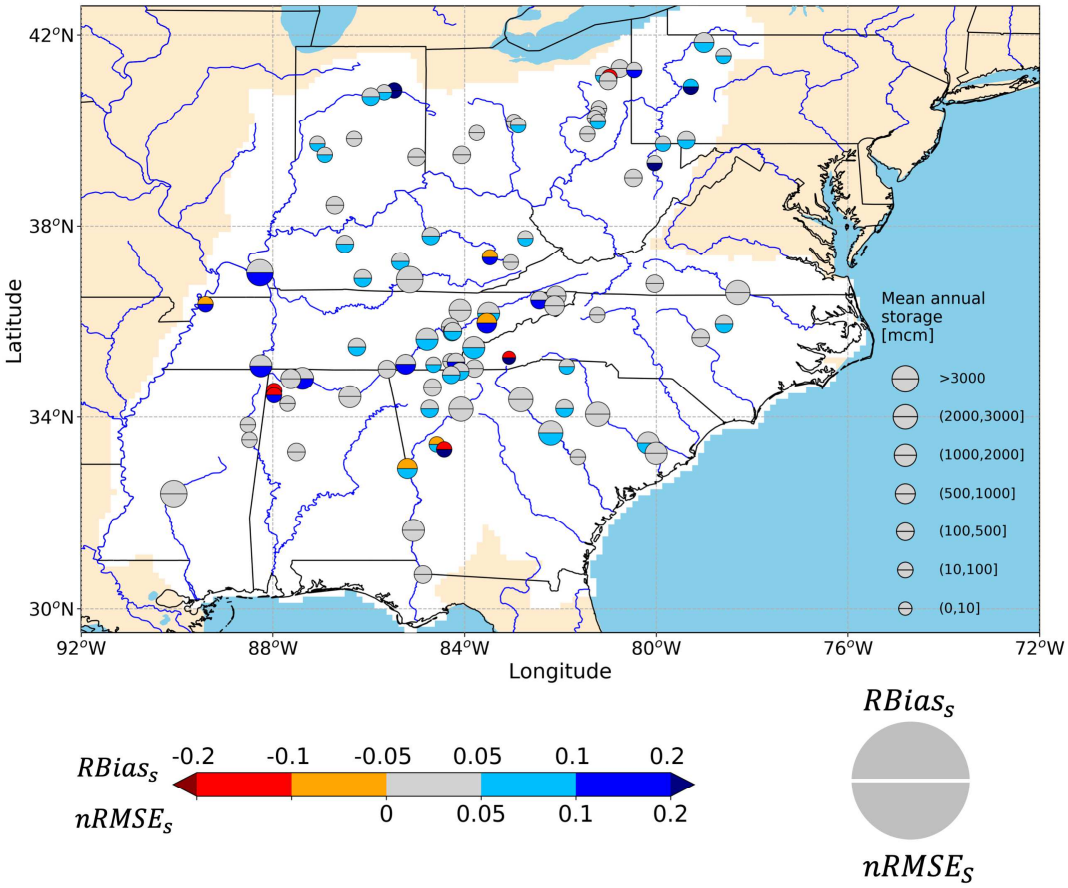

Figure A.8. Map of relative bias ($RBias_s$) and normalized root mean square errors ($nRMSE_s$) in mean annual storage for 92 reservoirs with observed guide curves.

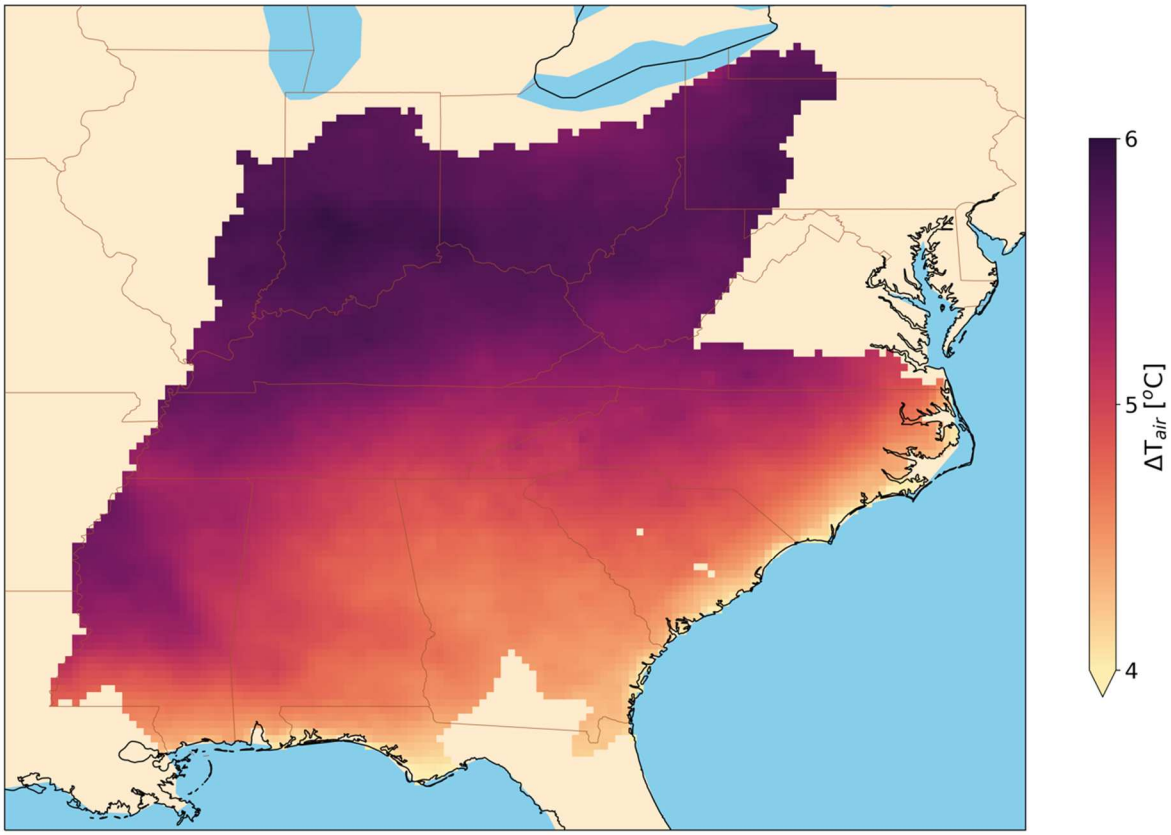

Figure A.9. Map of median projected increases in air temperature under RCP8.5 during the 2080s.

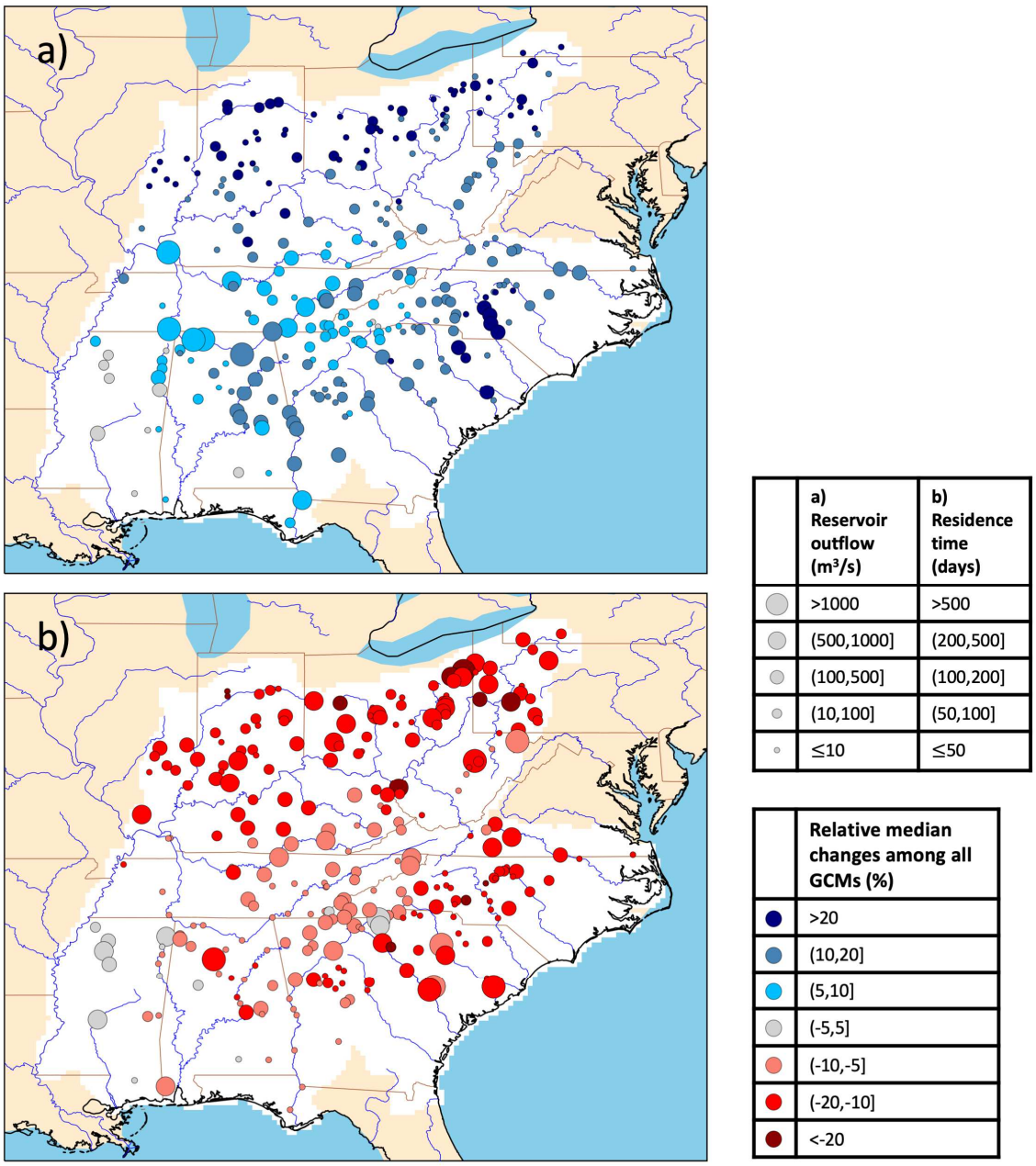

Figure A.10. Median projected relative changes among 20 GCMs in a) reservoir outflow and b) reservoir residence time for the 2080s under RCP8.5. The circle sizes represent the historical values for each variable. Colors denote the median relative change ranges among all GCMs.

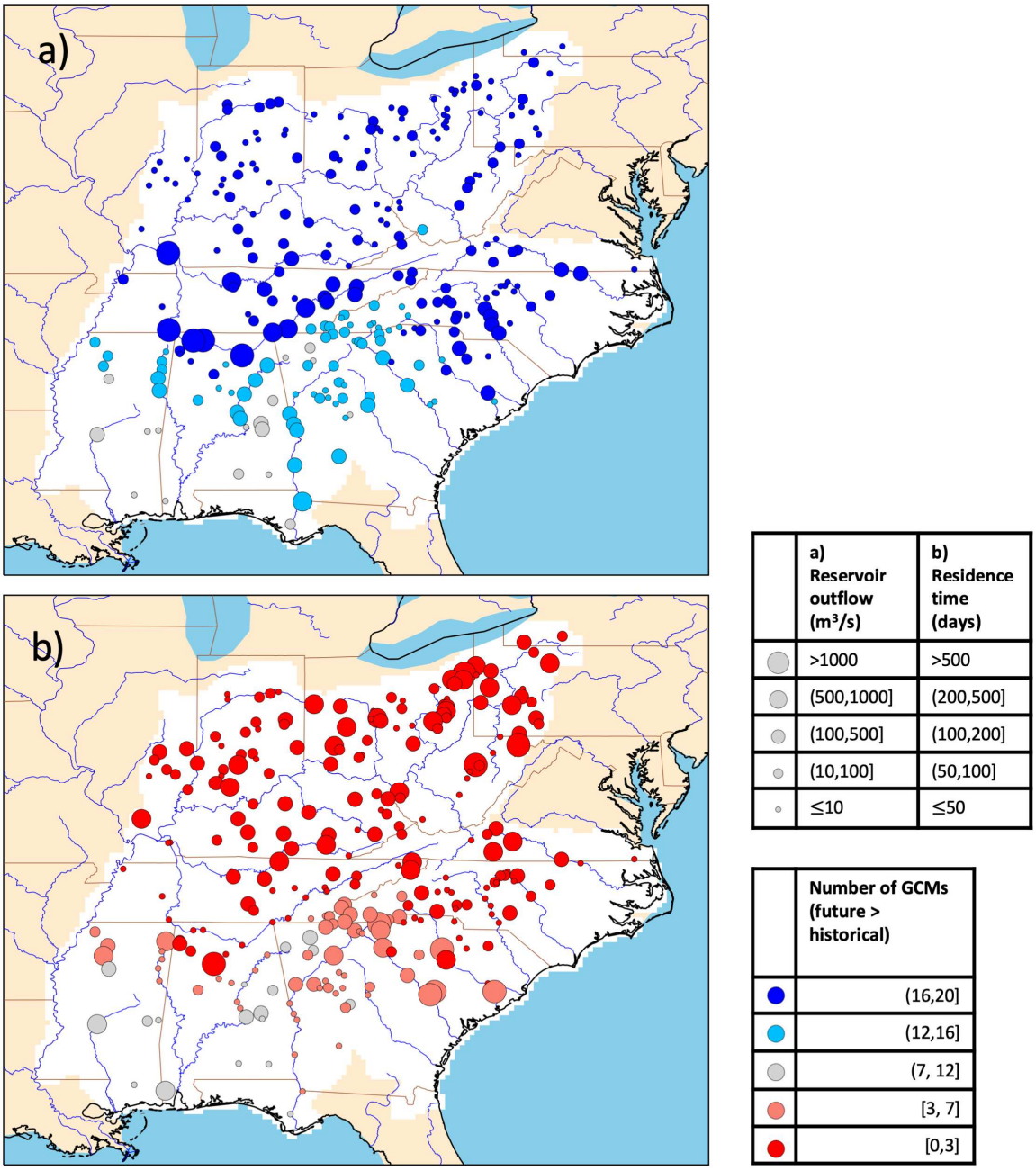

Figure A.11. Model agreement in projected changes in a) reservoir outflow and b) reservoir residence time until the 2080s under RCP8.5. The circle sizes represent the historical values for each variable. Colors denote the number of projected scenarios suggesting a greater value compared to the historical period, e.g., a blue dot in the upper left plot indicates that projected summer reservoir outflow is larger than historical summer reservoir outflow for simulations from more than 16 GCMs.

A.3. Tables

Table A.1. Main rivers in our study domain. Rivers are grouped by river basin and tributaries are indicated by indentation in column 3.

Hydrological region	Total number of reservoirs	Main rivers	Number of reservoirs on mainstem†	Drainage area (km^2)*	Mean annual discharge (m^3/s)◊	Mouth
South Atlantic & Gulf	109	Roanoke River	4	25,071[a]	220.9[α]	Albemarle sound
		Cape Fear River	0	25,123[b]	110.0[α]	Atlantic Ocean
		Pee Dee River	2	47,915[b]	317.2[β]	Winyah bay
		Santee River	1	61,124[b]	215.6[β]	Atlantic Ocean
		Catawba-Wateree River	10	14,470[b]	165.6[β]	Santee River
		Savannah River	2	25,511[a]	332.0[α]	Atlantic Ocean
		Altamaha River	0	36,260[a]	383.0[α]	Atlantic Ocean
		Oconee River	1	13,805[c]	134.7[β]	Altamaha River
		Ocmulgee River	2	16,006[a]	150.3[β]	Altamaha River
		Apalachicola River	1	50,505[a]	470.0[α]	Gulf of Mexico
		Chattahoochee River	6	22,714[a]	286.0[α]	Apalachicola River
		Flint River	2	21,911[a]	235.7[β]	Apalachicola River
		Mobile River	0	113,960[a]	1900.0[α]	Mobile Bay
		Alabama River	0	58,793[b]	921.3[β]	Mobile River
		Coosa River	7	26,159[a]	452.0[α]	Alabama River
		Tombigbee River	5	15,799[d]	742.8[β]	Mobile River
		Pearl River	1	22,688[a]	268.2[β]	Lake Borgne
Ohio	110	Ohio River	2	490,601[a]	8000.0[α]	Mississippi River
		Wabash River	1	103,470[a]	1001.0[α]	Ohio River
		Cumberland River	0	45,915[a]	1055.0[α]	Ohio River
		Kanawha River	1	31,691[a]	432.0[α]	Ohio River
		Allegheny River	1	29,992[a]	559.0[α]	Ohio River
		Green River	3	25,382[a]	145.0[α]	Ohio River
		Kentucky River	1	18,000[a]	285.0[α]	Ohio River
		Scioto River	0	16,879[a]	189.0[α]	Ohio River
		Licking River	1	9,306[a]	119.5[α]	Ohio River
Tennessee	37	Tennessee River	7	105,868[a]	1999.5[α]	Ohio River
Lower Mississippi	5	Yazoo River	0	34,965[b]	520.6[β]	Mississippi River
		Big Black River	0	8806[a]	107.9[β]	Mississippi River

†data source for reservoirs in the mainstem: GRanD Database

*data source for drainage area: a) Wikipedia, b) United States Geological Survey (USGS), c) Georgia River Network, d) Mississippi Department of Environmental Quality

◊data source for mean annual discharge: α)Wikipedia, β) most downstream USGS site

Table A.2. List of Global Climate Models (GCMs) used in this study.

Global Climate Models	**Modeling Center (Country)**
bcc-csm1-1	Beijing Climate Center, China Meteorological Administration (**China**)
bcc-csm1-1-m	
BNU-ESM	College of Global Change and Earth System Science, Beijing Normal University (**China**)
CanESM2	Canadian Centre for Climate Modelling and Analysis (**Canada**)
CCSM4	National Center for Atmospheric Research (**United States**)
CNRM-CM5	Centre National de Recherches Météorologiques / Centre Européen de Recherche et Formation Avancée en Calcul Scientifique (**France**)
CSIRO-Mk3-6-0	Commonwealth Scientific and Industrial Research Organization in collaboration with Queensland Climate Change Centre of Excellence (**Australia**)
GFDL-ESM2G	NOAA Geophysical Fluid Dynamics Laboratory (**United States)**
GFDL-ESM2M	
HadGEM2-CC365	Met Office Hadley Centre (additional HadGEM2-ES realizations contributed by Instituto Nacional de Pesquisas Espaciais) (**United Kingdom**)
HadGEM2-ES365	
inmcm4	Institute for Numerical Mathematics (**Russia**)
IPSL-CM5A-LR	Institut Pierre-Simon Laplace (**France**)
IPSL-CM5A-MR	
IPSL-CM5B-LR	
MIROC5	Atmosphere and Ocean Research Institute (The University of Tokyo), National Institute for Environmental Studies, and Japan Agency for Marine-Earth Science and Technology (**Japan**)
MIROC-ESM	Japan Agency for Marine-Earth Science and Technology, Atmosphere and Ocean Research Institute (The University of Tokyo), and National Institute for Environmental Studies (**Japan**)
MIROC-ESM-CHEM	
MRI-CGCM3	Meteorological Research Institute (**Japan**)
NorESM1-M	Norwegian Climate Centre (**Norway**)

Table A.3. Summary of the data sources for reservoir information.

Data type		Source	Reservoir numbers
Storage		TVA	29
		USGS	6
		USACE	4
Elevation	Observed elevation	USGS	41
	Rule curve	USACE	12

Table A.4. Regional availability of reservoir storage target data.

Basin number	Basin name	Total reservoirs	Reservoirs with storage data	Reservoir with elevation data	Percentage of total capacity
3	South Atlantic Gulf	110	8	17	64.5%
5	Ohio	119	2	35	48.9%
6	Tennessee	37	29	0	97.9%
8	Lower Mississippi	5	0	1	0.4%

Table A.5. Summary of data sources for observed storage, elevation and reservoir guide curve data.

GRanD ID	Dam Name	HUC2 ID	Source	USGS ID	Data Link	Source of reservoir full pool elevation	start date	end date	number of days
1753	Kentucky	6	TVA-sto	-	-	-	1945-01-01	2014-12-31	25567
1763	South Holston	6	TVA-sto	-	-	-	1951-01-01	2014-12-31	23376
1765	Boone	6	TVA-sto	-	-	-	1953-01-01	2014-12-31	22645
1767	Watauga	6	TVA-sto	-	-	-	1949-01-01	2014-12-31	24106
1770	Norris	6	TVA-sto	-	-	-	1936-01-01	2014-12-31	28855
1774	Cherokee	6	TVA-sto	-	-	-	1942-01-01	2014-12-31	26663
1781	Douglas	6	TVA-sto	-	-	-	1944-01-01	2014-12-31	25933
1783	Melton Hill	6	TVA-sto	-	-	-	1963-01-01	2014-12-31	18993
1788	Tellico	6	TVA-sto	-	-	-	1982-01-01	2014-12-31	12053
1797	Watts Bar	6	TVA-sto	-	-	-	1943-01-01	2014-12-31	26298
1800	Normandy	6	TVA-sto	-	-	-	1977-01-01	2014-12-31	13879
1801	Fontana	6	TVA-sto	-	-	-	1945-01-01	2014-12-31	25567
1812	Bear Creek	6	TVA-sto	-	-	-	1970-01-01	2014-12-31	16436
1817	Apalachia	6	TVA-sto	-	-	-	1944-01-01	2014-12-31	25933
1818	Hiwassee	6	TVA-sto	-	-	-	1941-01-01	2014-12-31	27028
1822	Chickamauga	6	TVA-sto	-	-	-	1941-01-01	2014-12-31	27028
1823	Ocoee 1	6	TVA-sto	-	-	-	1940-01-01	2014-12-31	27394
1824	Pickwick Landing	6	TVA-sto	-	-	-	1938-01-01	2014-12-31	28124
1828	Chatuge	6	TVA-sto	-	-	-	1943-01-01	2014-12-31	26298
1829	Nickajack	6	TVA-sto	-	-	-	1938-01-01	2014-12-31	28124
1833	Nottely	6	TVA-sto	-	-	-	1943-01-01	2014-12-31	26298
1834	Blue Ridge	6	TVA-sto	-	-	-	1940-01-01	2014-12-31	27394
1835	Wheeler	6	TVA-sto	-	-	-	1936-01-01	2014-12-31	28855
1843	Cedar Creek	6	TVA-sto	-	-	-	1980-01-01	2014-12-31	12784
1846	Little Bear Creek	6	TVA-sto	-	-	-	1977-01-01	2014-12-31	13879
1847	Guntersville	6	TVA-sto	-	-	-	1939-01-01	2014-12-31	27759
1855	Upper Bear Creek	6	TVA-sto	-	-	-	1979-01-01	2014-12-31	13149
-	Fort Loudoun	6	TVA-sto	-	-	-	1944-01-01	2014-12-31	25933
-	Wilson	6	TVA-sto	-	-	-	1936-01-01	2014-12-31	28855
1841	Carters Main Dam	3	USGS-sto	02381400	USGS	-	2007-06-27	2018-11-01	4129

1862	Allatoona Lake Dam	3	USGS-sto	02393500	USGS	-	2007-07-26	2018-11-01	4112
1863	Buford	3	USGS-sto	02334400	USGS	-	2007-06-29	2018-11-01	4127
1896	West Point	3	USGS-sto	02339400	USGS	-	2007-04-20	2018-11-01	4162
1910	Walter F. George Lock And Dam	3	USGS-sto	02343240	USGS	-	2007-05-22	2018-11-01	4155
1916	Jim Woodruff Dam	3	USGS-sto	02357500	USGS	-	2007-08-11	2018-11-01	4061
1851	Hartwell Dam	3	USACE-sto		http://water.sas.usace.army.mil/cf/DataQuery/DataQuery.cfm	-	1968-01-01	2067-12-31	20763
1872	J. Strom Thurmond Dam	3	USACE-sto		http://water.sas.usace.army.mil/cf/DataQuery/DataQuery.cfm	-	1954-01-01	2018-11-05	23685
1621	Alum Creek Dam	5	USACE-sto		http://water.usace.army.mil/a2w/f?p=100:1:0:#	-	2016-11-06	2018-11-06	725
1756	Wolf Creek	5	USACE-sto		http://water.usace.army.mil/a2w/f?p=100:1:0:#	-	2016-11-06	2018-11-05	725
1609	Leesville Dam	*5*	USACE-guide		http://water.usace.army.mil/a2w/f?p=100:1:0:#	http://water.usace.army.mil/a2w/f?p=100:1:0:#	-	-	-
1553	Kinzua Dam	*5*	USACE-guide		http://www.lrp.usace.army.mil/Portals/72/docs/WaterManagement/Reservoir%20Plots.pdf	http://www.lrp.usace.army.mil/Portals/72/docs/WaterManagement/Reservoir%20Plots.pdf	-	-	-
1557	East Branch Dam	*5*	USACE-guide		same as above	same as above	-	-	-
1565	Mosquito Creek Dam	*5*	USACE-guide		same as above	same as above	-	-	-
1566	Shenango Dam	*5*	USACE-guide		same as above	same as above	-	-	-
1572	Michael J. Kirwan Dam	*5*	USACE-guide		same as above	same as above	-	-	-
1574	Lake Milton Dam	*5*	USACE-guide		same as above	same as above	-	-	-
1576	Berlin Dam	*5*	USACE-guide		same as above	same as above	-	-	-
1582	Mahoning Creek Dam	*5*	USACE-guide		same as above	same as above	-	-	-
1643	Youghiogheny Dam	*5*	USACE-guide		same as above	same as above	-	-	-
1667	Tygart Dam	*5*	USACE-guide		same as above	same as above	-	-	-
1685	Stonewall Jackson Dam	*5*	USACE-guide		same as above	same as above	-	-	-
1207	Ross Barnett Reservoir	3	USGS-elev	02485600	USGS	Historical maximum	1998-10-28	2018-11-05	6135
1868	Aberdeen Dam	3	USGS-elev	02437100	USGS	Historical maximum	1984-05-03	2018-11-05	12589
1876	John C. Stennis	3	USGS-elev	02441390	USGS	Historical maximum	1990-09-30	2018-11-05	8739
1882	Lake Kedron Dam	3	USGS-elev	02344650	USGS	Historical maximum	2014-08-22	2018-10-31	1438

1885	Horton Creek Reservoir Dam	3	USGS-elev	02344423	USGS	Historical maximum	2014-09-04	2018-10-31	1510
1893	Savannah River Steel Creek Dam	3	USGS-elev	02197353	USGS	Historical maximum	1987-10-27	1996-09-29	3057
1646	Lake Lynn Dam	5	USGS-elev	03071590	USGS	Historical maximum	2012-09-30	2018-10-31	2200
1655	Caesar Creek Lake Dam	5	USGS-elev	03242340	USGS	Historical maximum	2015-11-02	2018-10-31	1095
1766	Reelfoot Lake	8	USGS-elev	07027000	USGS	Historical maximum	1984-10-01	2018-11-05	6979
1861	Buzzards Roost Embankment	3	USGS-elev	02166500	USGS	US Lake Level	1983-10-01	2018-10-31	9463
1866	Saluda	3	USGS-elev	02168500	USGS	US Lake Level	1990-10-02	2018-10-31	10089
1879	North Santee Dam	3	USGS-elev	02171000	USGS	US Lake Level	1984-05-04	2018-10-31	12059
1888	Lake Tuscaloosa Dam	3	USGS-elev	02464800	USGS	US Lake Level	1982-10-01	2018-10-31	13083
1890	Pinopolis West Dam	3	USGS-elev	02172000	USGS	US Lake Level	1989-10-02	2018-10-31	10144
1586	J. Edward Roush Lake Dam	5	USGS-elev	03323450	USGS	https://www.lrl.usace.army.mil/Missions/Civil-Works/Water-Information/Lake-Information/Record-Pools/	2015-11-02	2018-10-31	1090
1587	Salamonie Lake Dam	5	USGS-elev	03324450	USGS	same as above	2015-11-02	2018-10-31	1085
1592	Mississinewa Lake Dam	5	USGS-elev	03326950	USGS	same as above	2015-11-02	2018-10-31	1094
1634	Clarence J. Brown Dam	5	USGS-elev	03268090	USGS	same as above	2015-11-02	2018-10-31	1075
1645	Cecil M. Harden Lake Dam	5	USGS-elev	03340870	USGS	same as above	2015-11-02	2018-10-31	1087
1654	Cagles Mill Lake Dam	5	USGS-elev	03358900	USGS	same as above	2015-11-02	2018-10-31	1084
1656	Brookville Lake Dam	5	USGS-elev	03275990	USGS	same as above	2015-11-02	2018-10-31	1093
1732	Rough River Lake Dam	5	USGS-elev	03318005	USGS	same as above	2015-11-07	2018-11-05	1080
1739	Buckhorn Lake Dam	5	USGS-elev	03280800	USGS	same as above	2014-09-09	2018-11-05	1502
1741	Green River Lake Dam	5	USGS-elev	03305990	USGS	same as above	2015-11-07	2018-11-05	1085
1744	Carr Creek Lake Dam	5	USGS-elev	03277446	USGS	same as above	2015-11-07	2018-11-05	1090
1755	Barren River Lake Dam	5	USGS-elev	03312900	USGS	same as above	2015-11-07	2018-11-05	1055
1761	John H. Kerr Dam	3	USGS-elev	02079490	USGS	http://epec.saw.usace.army.mil/KERRPERT.TXT	2005-03-11	2018-10-31	4918
1776	W. Kerr Scott Dam	3	USGS-elev	02111391	USGS	http://epec.saw.usace.army.mil/WKSPERT.TXT	2011-10-01	2018-10-31	2532

1782	Falls Lake Dam	3	USGS-elev	02087182	USGS	http://epec.saw.usace.army.mil/FALLPERT.TXT	1987-05-01	2018-11-05	11444
1796	B. Everett Jordan Dam	3	USGS-elev	02098197	USGS	http://epec.saw.usace.army.mil/BEJPERT.TXT	2011-10-02	2018-10-31	2565
1617	Tappan Dam	5	USGS-elev	03128000	USGS	http://www.lrh-wc.usace.army.mil/wm/?basin/mus/tal	2015-11-02	2018-10-31	1095
1619	Clendening Dam	5	USGS-elev	03126500	USGS	http://www.lrh-wc.usace.army.mil/wm/?basin/mus/clb	2015-11-02	2018-10-31	1092
1620	Piedmont Dam	5	USGS-elev	03125500	USGS	http://www.lrh-wc.usace.army.mil/wm/?basin/mus/pes	2015-11-02	2018-10-31	1020
1636	Senecaville Dam	5	USGS-elev	03141000	USGS	http://www.lrh-wc.usace.army.mil/wm/?basin/mus/ses	2015-11-02	2018-10-31	1088
1726	Dewey Dam	5	USGS-elev	03211000	USGS	http://www.lrh-wc.usace.army.mil/wm/?basin/bsa/dwj	1999-09-30	2018-11-05	1455
1626	Hoover Dam	5	USGS-elev	03228400	USGS	https://en.wikipedia.org/wiki/Hoover_Dam_(Ohio)	2015-11-02	2018-10-19	1063
1724	Dix River Dam	5	USGS-elev	03286000	USGS	https://en.wikipedia.org/wiki/Dix_Dam	2015-11-02	2018-10-31	1092
1640	Eagle Creek Reservoir Dam	5	USGS-elev	03353450	USGS	https://water.weather.gov/ahps2/hydrograph.php?wfo=ind&gage=ecri3	1989-10-02	2018-10-31	10478
1758	Philpott Dam	3	USGS-elev	02071900	USGS	http://www.myhenrycounty.com/philpott-dam.php	2003-03-28	2018-10-31	5627
1826	H. Taylor Blalock Reservoir Dam	3	USGS-elev	021556524	USGS	https://www.spartanburgwater.org/pdfs/hydroelectric/blalock.pdf	1998-02-27	2018-10-31	7407
1703	Patoka Lake Dam	5	USGS-elev	03374498	USGS	https://pubs.usgs.gov/sir/2017/5138/sir20175138old.pdf	2015-11-02	2018-10-31	1093

Notes:

1. Data source: *format:[agency]-[variable]*; “sto” indicates for storage, “guide” indicates guide curve and “elev” indicates elevation.
2. For all USGS data and website links above, last access: Nov 6, 2018

Table A.6. Median values of the correlation coefficient, root mean square error, and standard deviation of normalized simulated storage targets for each.

	Group1: Flood control (n=49)	Group 2: No flood control (n=43)
Correlation coefficient	0.89	0.68
Root mean square error (-)	0.11	0.11
Standard deviation (-)	0.10	0.08

Table A.7. Summary of USGS sites with observed streamflow and stream temperature data.

USGS ID	Site name	streamflow			stream temperature		
		start date	end date	number of days	start date	end date	number of days
02044500	Nottoway River Near Rawlings, VA	1979-01-01	2010-12-31	11688	2006-10-01	2008-10-20	737
02047500	Blackwater River Near Dendron, VA	1979-01-01	2010-12-31	11122	2007-03-07	2008-10-16	587
02051500	Meherrin River Near Lawrenceville, VA	1979-01-01	2010-12-31	11688	2006-12-16	2009-10-25	983
02056000	Roanoke River at Niagara, VA	1979-01-01	2010-12-31	11688	2007-03-24	2009-06-08	800
02059500	Goose Creek Near Huddleston, VA	1979-01-01	2010-12-31	11688	2006-10-01	2008-10-16	736
02072000	Smith River Near Philpott, VA	1979-01-01	2010-12-31	11688	2006-09-30	2017-11-04	3311
02073000	Smith River at Martinsville, VA	1979-01-01	2010-12-31	11688	2007-03-06	2008-12-17	649
02075045	Dan River at Stp Near Danville, VA	1995-10-01	2010-12-31	5571	2006-12-14	2009-02-11	763
02077000	Banister River at Halifax, VA	1979-01-01	2010-12-31	11688	2007-03-24	2008-11-16	542
02083500	Tar River at Tarboro, NC	1979-01-01	2010-12-31	11685	1984-10-01	1989-02-15	784
02091500	Contentnea Creek at Hookerton, NC	1979-01-01	2010-12-31	11686	2002-04-04	2004-08-31	864
02105500	Cape Fear R at Wilm O Huske Lock Nr Tarheel, NC	1979-01-01	2010-12-31	11688	2000-06-20	2004-02-03	1229
02107544	Black River Near Currie, NC	2004-03-01	2005-12-13	634	2003-09-09	2004-12-02	384
02108566	Northeast Cape Fear R Nr Burgaw, NC	2003-11-14	2005-12-12	745	2003-11-04	2004-12-02	380
02110500	Waccamaw River Near Longs, SC	1979-01-01	2010-12-31	11688	2007-04-27	2017-11-04	3804
02110704	Waccamaw River at Conway Marina at Conway, SC	1994-07-28	2010-12-31	5825	1994-10-02	2017-11-04	8111
02135200	Pee Dee River at Hwy 701 Nr Bucksport, SC	2001-07-25	2010-12-31	3191	1994-10-19	2009-11-05	5120
02148000	Wateree River Nr. Camden, SC	1979-01-01	2010-12-31	11339	1988-03-04	2017-11-04	4859
02148315	Wateree R. Bl Eastover, SC	1979-01-01	2010-12-31	10351	1984-05-04	2014-07-14	10562
02156500	Broad River Near Carlisle, SC	1979-01-01	2010-12-31	11688	1983-12-08	2017-11-04	11883
02160105	Tyger River Near Delta, SC	1979-01-01	2010-12-31	11688	1983-12-08	2017-11-04	11867
02160700	Enoree River at Whitmire, SC	1979-01-01	2010-12-31	11688	1984-05-04	2017-11-04	11866
02163001	Saluda River Near Williamston, SC	1995-05-02	2010-12-31	5722	1996-09-30	2017-11-04	7310
02168504	Saluda River Below Lk Murray Dam Nr Columbia, SC	1988-10-01	2010-12-31	8127	1987-12-01	2017-11-04	10440

02175000	Edisto River Nr Givhans, SC	1979-01-01	2010-12-31	11688	2002-01-25	2003-09-29	565
02176930	Chattooga River at Burrells Ford, Nr Pine Mtn, GA	2009-09-18	2010-12-31	470	2009-10-09	2017-11-04	2479
02197000	Savannah River at Augusta, GA	1979-01-01	2010-12-31	11687	1973-10-01	2011-08-09	4490
02197320	Savannah R. Nr Jackson, SC	1979-01-01	2002-09-29	8248	1984-06-07	1994-10-04	3666
02204070	South River at Klondike Road, Near Lithonia, GA	1983-10-01	2010-12-31	9954	1983-11-01	2007-01-04	7508
02207120	Yellow River at Ga 124, Near Lithonia, GA	1996-05-18	2010-12-31	3426	2001-08-16	2017-11-05	5810
02207220	Yellow River at Pleasant Hill Road, Nr Lithonia,GA	2002-11-27	2010-12-31	2957	2003-02-14	2012-09-29	1412
02207335	Yellow River at Gees Mill Road, Near Milstead, GA	2001-11-01	2010-12-31	3348	2001-11-02	2012-09-29	2603
02223500	Oconee River at Dublin, GA	1979-01-01	2010-12-31	11688	1979-06-21	1983-09-12	1393
02334430	Chattahoochee River at Buford Dam, Near Buford, GA	1979-01-01	2010-12-31	11688	1975-08-28	2017-11-04	5393
02335000	Chattahoochee River Near Norcross, GA	1979-01-01	2010-12-31	11688	1976-10-01	2017-11-05	5538
02335450	Chattahoochee River Above Roswell, GA	1979-01-01	2010-12-31	11688	2004-01-29	2017-11-04	3253
02335815	Chattahoochee River Below Morgan Falls Dam, GA	2000-10-02	2010-12-31	3728	2004-01-13	2017-11-04	1845
02336000	Chattahoochee River at Atlanta, GA	1979-01-01	2010-12-31	11688	1975-11-06	2017-11-05	5346
02337170	Chattahoochee River Near Fairburn, GA	1979-01-01	2010-12-31	11688	1975-08-26	2017-11-05	12978
02382500	Coosawattee River at Carters, GA	1979-01-01	2010-12-31	11688	2005-03-12	2017-11-04	710
02383180	Salacoa Creek at Cr 29, Near Redbud, GA	2005-01-12	2007-01-23	742	2005-01-13	2007-01-23	739
02384500	Conasauga River at Ga 286, Near Eton, GA	1981-10-01	2010-12-31	10684	2005-03-05	2007-01-08	672
02385170	Coahulla Creek at Keiths Mill Road, Near Dalton, GA	2005-01-13	2010-12-31	2179	2005-01-13	2006-12-31	695
02394000	Etowah River at Allatoona Dam, Abv Cartersville, GA	1979-01-01	2010-12-31	11688	2005-01-27	2017-11-04	1791
02395000	Etowah River Near Kingston,GA	1979-01-01	2010-12-31	6962	2005-01-13	2006-12-31	580
02395980	Etowah River at Ga 1 Loop, Near Rome, GA	1979-01-01	2010-12-31	11688	2005-03-09	2007-01-06	655
02397000	Coosa River (Mayo's Bar) Near Rome, GA	1979-01-01	2010-12-31	11688	1986-02-14	2017-11-05	10925
02405500	Kelly Creek Near Vincent AL	1986-10-01	2010-12-31	8858	2008-07-12	2017-11-04	3085
02407514	Yellowleaf Creek Near Westover, ALA.	2005-10-01	2010-12-31	1918	2008-07-12	2017-11-04	3257
02419890	Tallapoosa River Near Mont.-Mont. Water Works	1995-10-01	2010-12-31	5571	2005-07-23	2017-11-04	4374
02479310	Pascagoula River at Graham Ferry, MS	1993-10-01	2009-09-29	5478	2004-09-30	2017-11-04	1389
03012550	Allegheny River at Kinzua Dam, PA	1979-01-01	2010-12-31	5112	2007-09-30	2017-11-04	3674
03020000	Tionesta Creek at Tionesta Creek Dam, PA	1979-01-01	2010-12-31	5112	2007-10-01	2017-11-04	3602

03024000	French Creek at Utica, PA	1979-01-01	2010-12-31	11688	1996-10-30	1998-09-29	627
03036000	Mahoning Creek at Mahoning Creek Dam, PA	1979-01-01	2010-12-31	5112	2008-10-01	2017-11-04	3253
03047000	Loyalhanna Creek at Loyalhanna Dam, PA	1979-01-01	2010-12-31	5112	2007-08-03	2017-11-04	3554
03057000	Tygart Valley River at Colfax, WV	1979-01-01	2010-12-31	6208	2008-09-30	2017-11-04	3090
03061000	West Fork River at Enterprise, WV	1979-01-01	2010-12-31	11321	1998-09-30	2017-11-04	3899
03067510	Shavers Fork Nr Cheat Bridge, WV	2000-10-01	2010-12-31	3744	2009-09-30	2017-11-04	2915
03075070	Monongahela River at Elizabeth, PA	1979-01-01	2010-12-31	11688	2008-10-02	2017-11-04	3302
03079000	Casselman River at Markleton, PA	1979-01-01	2010-12-31	11688	2005-06-02	2017-11-04	3228
03081000	Youghiogheny River Below Confluence, PA	1979-01-01	2010-12-31	11688	2004-10-01	2017-11-04	4721
03082500	Youghiogheny River at Connellsville, PA	1979-01-01	2010-12-31	11688	2009-11-04	2014-09-29	1789
03083500	Youghiogheny River at Sutersville, PA	1979-01-01	2010-12-31	11684	2005-06-02	2017-11-04	3515
03085000	Monongahela River at Braddock, PA	1979-01-01	2004-09-29	9404	1996-11-08	1998-09-29	506
03091500	Mahoning River at Pricetown, OH	1979-01-01	2010-12-31	11688	2009-09-30	2017-11-04	2958
03094000	Mahoning River at Leavittsburg, OH	1979-01-01	2010-12-31	11688	2009-09-30	2017-11-04	2943
03098600	Mahoning River Below West Ave at Youngstown, OH	1987-10-01	2010-12-31	8493	1992-06-26	2017-11-04	4530
03165500	New River at Ivanhoe, VA	1996-01-25	2010-12-31	5455	2007-03-15	2008-09-29	526
03167000	Reed Creek at Grahams Forge, VA	1991-09-30	2010-12-31	7032	2006-12-21	2009-06-30	905
03168000	New River at Allisonia, VA	1979-01-01	2010-12-31	11688	2007-01-09	2008-09-29	558
03171000	New River at Radford, VA	1979-01-01	2010-12-31	11688	2006-12-21	2009-03-18	703
03173000	Walker Creek at Bane, VA	1979-01-01	2010-12-31	11688	2007-03-13	2008-09-29	514
03175500	Wolf Creek Near Narrows, VA	1979-01-01	2010-12-31	11322	2007-03-13	2008-09-29	528
03178000	Bluestone R Nr Spanishburg, WV	1996-10-01	1998-09-29	729	1997-03-14	1998-09-29	465
03183500	Greenbrier River at Alderson, WV	1979-01-01	2010-12-31	11688	2007-04-06	2017-11-05	3823
03185400	New River at Thurmond, WV	1981-02-19	2010-12-31	10908	1990-07-21	1998-09-30	1605
03186500	Williams River at Dyer, WV	1979-01-01	2010-12-31	11688	1997-03-22	1998-09-03	529
03187500	Cranberry River Near Richwood, WV	1979-01-01	2010-12-31	11170	1981-10-29	1997-11-12	565
03193000	Kanawha River at Kanawha Falls, WV	1979-01-01	2010-12-31	11688	1997-04-12	1998-09-29	383
03219500	Scioto River Near Prospect OH	1979-01-01	2010-12-31	11688	1998-06-17	2017-11-04	5068
03231500	Scioto River at Chillicothe OH	1979-01-01	2010-12-31	11688	1999-09-30	2002-09-29	1047

03232470	Paint Creek Near Bainbridge OH	1979-01-01	1991-09-29	4655	1989-09-30	2017-11-04	2769
03234300	Paint Creek at Chillicothe OH	1985-10-01	2010-12-31	9223	1985-10-11	2002-09-29	5755
03234500	Scioto River at Higby OH	1979-01-01	2010-12-31	11688	2000-09-30	2002-09-29	684
03254520	Licking River at Hwy 536 Near Alexandria, KY	2007-06-22	2010-12-31	898	2007-09-30	2017-10-18	3585
03287500	Kentucky River at Lock 4 At Frankfort, KY	1979-01-01	2010-12-31	11323	2001-06-23	2017-11-04	4709
03303205	Sinking Creek Near Lodiburg, KY	2004-05-28	2007-04-30	1068	2004-05-28	2006-09-29	808
03306000	Green River Near Campbellsville, KY	1979-01-01	1994-09-30	5752	1988-10-01	2017-11-04	6367
03307000	Russell Creek Near Columbia, KY	1979-01-01	2010-12-31	10227	1999-12-22	2017-11-04	5476
03309000	Green River at Mammoth Cave, KY	2003-10-01	2007-09-29	1460	2003-07-12	2007-06-30	1344
03311500	Green River at Lock 6 At Brownsville, KY	1979-01-01	1992-09-30	5022	1999-12-15	2016-11-24	5550
03313000	Barren River Near Finney, KY	1979-01-01	1994-09-30	5752	1990-01-09	2017-11-04	6272
03323500	Wabash River at Huntington, IN	1979-01-01	2003-02-10	8800	2002-09-30	2017-11-04	5325
03324500	Salamonie River at Dora, IN	1979-01-01	2003-02-10	8806	2002-09-30	2017-11-04	5299
03353611	White R. At Stout Gen. Stn. at Indianapolis, IN	1992-10-02	2010-12-31	6665	1992-10-14	2017-11-04	7930
03354000	White River Near Centerton, IN	1979-01-01	2010-12-31	11688	1975-08-28	2017-11-04	11939
03357330	Big Walnut Creek Near Roachdale, IN	2001-10-26	2010-12-31	3354	2002-06-19	2003-09-09	414
03410600	South Fork Cumberland River Near Yamacraw, KY	1999-06-01	2005-09-29	1582	1999-06-04	2005-09-30	1459
03428200	West Fork Stones River at Murfreesboro, TN	1979-01-01	2010-12-31	10258	1986-02-06	2013-09-29	9796
03460795	Pigeon R Bl Power Plant Nr Waterville, NC	1997-02-01	2010-12-31	5082	1997-05-06	2017-10-01	2868
03475000	M F Holston River Near Meadowview, VA	1979-01-01	2010-12-31	11688	2007-05-04	2009-05-31	719
03495500	Holston River Near Knoxville, TN	1979-01-01	1993-11-01	5418	1980-02-23	1985-09-29	1982
03524000	Clinch River at Cleveland, VA	1979-01-01	2010-12-31	11688	2007-03-14	2017-11-05	3803
03524550	Guest River Near Miller Yard, VA	1996-10-01	1998-09-29	729	1996-08-16	2012-06-23	1316
03531500	Powell River Near Jonesville, VA	1979-01-01	2010-12-31	11688	2007-03-22	2009-06-29	821
03560110	Ocoee River Below Fightingtown Cr At Copperhill, TN	2002-08-01	2004-09-29	791	2002-08-01	2005-09-29	746
03597860	Duck River at Shelbyville, TN	1991-10-01	2010-12-31	5257	1991-10-11	2012-09-29	7531
07030392	Wolf River at Lagrange, TN	1995-09-01	2010-12-31	5601	1996-09-18	2010-09-30	1691
07285400	Batupan Bogue at Grenada, MS	1985-06-20	1997-09-30	4486	1985-06-20	1987-09-05	532
07288650	Bogue Phalia Nr Leland, MS	1996-09-30	2010-12-31	4841	2006-09-30	2017-11-04	1669

APPENDIX B SUPPLEMENTAL MATERIALS FOR CHAPTER 3: THERMAL EXTREMES IN REGULATED RIVER SYSTEMS UNDER CLIMATE CHANGE: AN APPLICATION TO THE SOUTHEASTERN U.S. RIVERS

B.1. Text

B.1.1. *Summary model evaluation*

The model setup we used in this study was adapted from Cheng et al. (2020). All model parameters were taken from previous, published work. Model performance was evaluated using observed river flow and temperature data from 111 U.S. Geologic Survey (USGS) gauges throughout the southeastern United States. Sixty-three of these gauges were downstream of reservoirs and subject to reservoir regulations. In the current study, we only investigated river segments subject to reservoir regulation, so the model evaluation results are limited to the 63 USGS sites downstream of reservoirs. For a more complete description of model performance, see Cheng et al. (2020).

For streamflow, we used the relative bias at the annual time step and the Nash-Sutcliffe (NS) coefficient at the monthly timestep to evaluated water quantity and seasonality. The median relative bias in mean annual simulated streamflow was 0.05 across all regulated sites. Four sites had an absolute relative bias larger than 0.5. The median NS coefficient for the 63 regulated sites was 0.55. Seventeen of the sites had an NS coefficient less than 0. Generally, model performance was worse in the South Atlantic region compared to the other regions.

For stream temperature, we evaluated mean summer river temperature because high river temperature events normally occur in the summer. The median bias across the 63 regulated sites was -0.9°C. Forty-five sites had an absolute bias less than 2°C, while 9 sites had an absolute bias greater than 4°C.

Cheng et al. (2020) conducted a sensitivity analysis to evaluate the effect of errors in the hydrological simulations on the simulated changes in mean summer river temperature under climate change. The result showed that the model was robust in capturing the climate change signals in mean summer river temperature and was relatively insensitive to biases in hydrology.

B.2. Figure

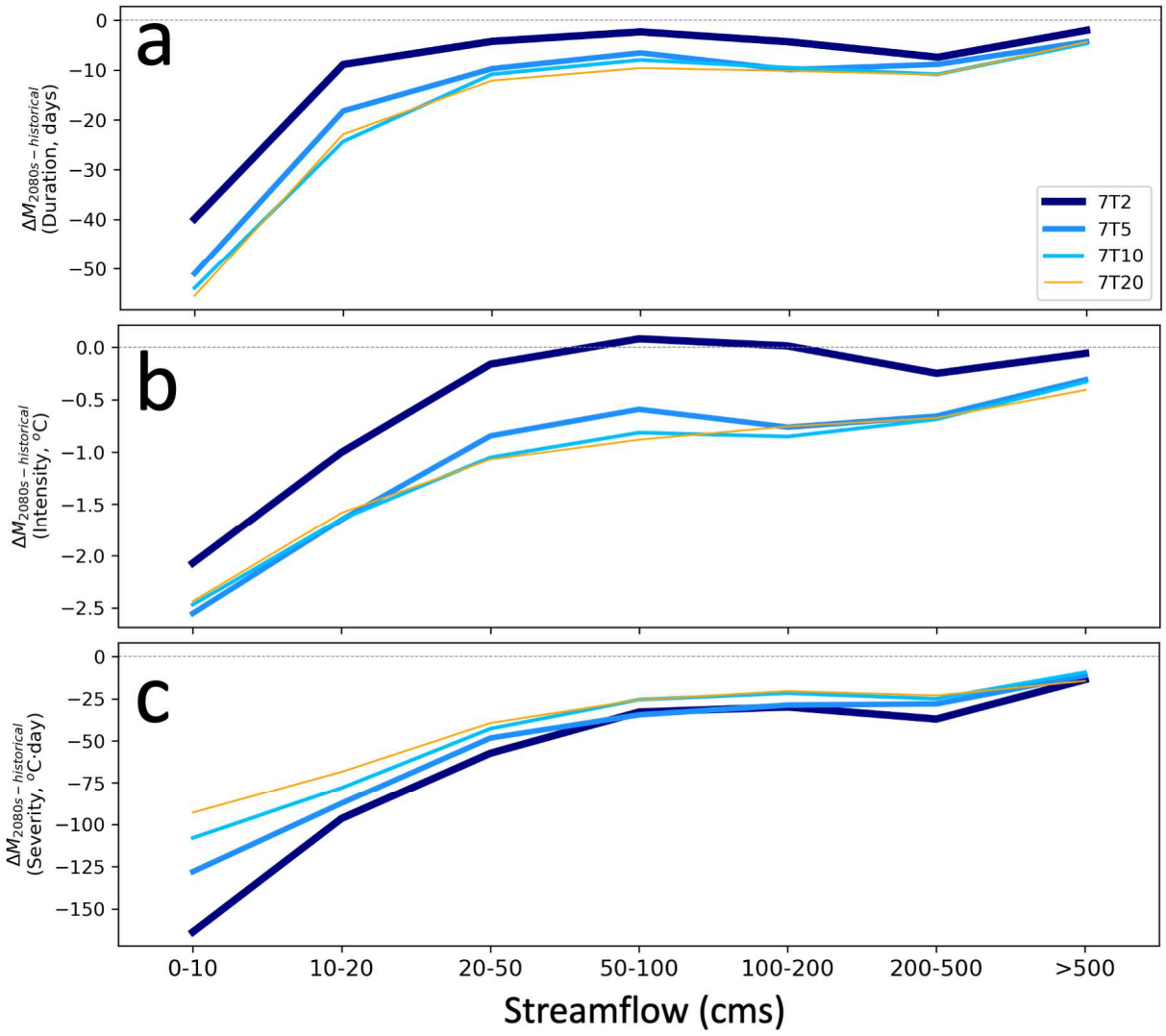

Figure B.1. $\boldsymbol{\Delta M_{2080s-hist}}$ for a) duration, b) intensity and c) severity.

B.3. Table

Table B.1. List of Global Climate Models (GCMs) used in this study.

Global Climate Models	Modeling Center (Country)
bcc-csm1-1	Beijing Climate Center, China Meteorological Administration (**China**)
bcc-csm1-1-m	
BNU-ESM	College of Global Change and Earth System Science, Beijing Normal University (**China**)
CanESM2	Canadian Centre for Climate Modelling and Analysis (**Canada**)
CCSM4	National Center for Atmospheric Research (**United States**)
CNRM-CM5	Centre National de Recherches Météorologiques / Centre Européen de Recherche et Formation Avancée en Calcul Scientifique (**France**)
CSIRO-Mk3-6-0	Commonwealth Scientific and Industrial Research Organization in collaboration with Queensland Climate Change Centre of Excellence (**Australia**)
GFDL-ESM2G	NOAA Geophysical Fluid Dynamics Laboratory (**United States)**
GFDL-ESM2M	
HadGEM2-CC365	Met Office Hadley Centre (additional HadGEM2-ES realizations contributed by Instituto Nacional de Pesquisas Espaciais) (**United Kingdom**)
HadGEM2-ES365	
inmcm4	Institute for Numerical Mathematics (**Russia**)
IPSL-CM5A-LR	Institut Pierre-Simon Laplace (**France**)
IPSL-CM5A-MR	
IPSL-CM5B-LR	
MIROC5	Atmosphere and Ocean Research Institute (The University of Tokyo), National Institute for Environmental Studies, and Japan Agency for Marine-Earth Science and Technology (**Japan**)
MIROC-ESM	Japan Agency for Marine-Earth Science and Technology, Atmosphere and Ocean Research Institute (The University of Tokyo), and National Institute for Environmental Studies (**Japan**)
MIROC-ESM-CHEM	
MRI-CGCM3	Meteorological Research Institute (**Japan**)
NorESM1-M	Norwegian Climate Centre (**Norway**)

APPENDIX C SUPPLEMENTAL MATERIALS FOR CHAPTER 4: PROJECTED POTENTIAL FISH DISTRIBUTION UNDER CLIMATE CHANGE IN A HEAVILY REGULATED, FRAGMENTED RIVER SYSTEM

C.1. Texts

C.1.1. *Model setup and evaluation*

In this study, we adapted the Maxent model setup as in VanCompernolle et al. (2019), which is configured based on a 400-m resolution gridded river network. The hydrologic models we used to simulate regulated flow and temperatures were configured based on a 1/8° gridded river network (~12km). In WebPanel 1.1, we describe a two-step mapping of river flow and temperatures from the 1/8° gridded hydrologic model river network to the 400-m gridded river analysis network of the Maxent model. In WebPanel 1.2, we evaluate the mapped flow and temperature by comparing with observations from the United States Geological Survey (USGS). In WebPanel 1.3, we discuss our adaptations of the Maxent model from VanCompernolle et al. (2019) and show model evaluations.

C.1.1.1. Map river flow and temperature simulated based on a 1/8° gridded hydrologic model river network to 400-m gridded river analysis network of the Maxent model

In this study, the modeling framework we used to simulated regulated river flow and temperature consists of three physically based models, which are configured for grid-based river networks at a spatial resolution of 1/8° (~12 km) and a temporal resolution of 1 day. However, a coarse-resolution gridded river network is infeasible to be applied to fish studies because it cannot capture the impacts of geology and landcover type at finer resolutions. We chose to directly map the river flow and temperature simulated based on a 1/8° gridded river network to a 400-m gridded river network.

The mapping is a two-step process. The first step is to map the river flow and temperature simulated at a 1/8° river network to a vector-based river network called the Geospatial Fabric (GF, USGS 2007). For each GF river segment, we find one corresponding grid cell based on two criteria, 1) the river segment and corresponding grid cell are spatially close to each other and 2) they share similar confluence area. We directly use the stream temperature of the corresponding

grid cell to represent the stream temperature of that river segment. To represent the streamflow in the river segment, we bias corrected the streamflow of the corresponding grid cell using the confluence areas as follows

$$Q_{seg} = \frac{A_{seg}}{A_{grid}} Q_{grid} \quad \text{(C.1)}$$

where Q denotes streamflow and A denotes confluence area, subscripts *seg* and *grid* denote river segment and corresponding grid cell.

The second step is to discretize the vector-based river network to 400-m grids as VanCompernolle et al. (2019) did. We refer to one 400-m grid as a pixel. Pixels within the same GF river segment were assigned the same flow and temperature data.

In addition, we chose the GF river network instead of the National Hydrography Dataset (NHD) because the NHD has a much higher spatial resolution than the coarse grid. For example, in NHD, there are over 10000 river segments in the Tennessee River Basin (TRB) while there are only 667 1/8° grids in the gridded river network. In the GF, there are 1208 river segments in the TRB. On average, two river segments in GF will share the information from one 1/8° grid cell. Therefore, GF is more suitable for our purpose.

C.1.1.2. Evaluation of mapped river flow and temperature

We compared simulated flow and temperature data with USGS observations. We have one criterion to filter the gauges, i.e., each gauge had to have at least one-year of observations that overlapped with our historical simulation period (1980-2009).

For flow evaluation, we used observations from 177 USGS gauges and 43 of them are subject to reservoir regulations. We used the relative bias at the annual time step and the Nash-Sutcliffe (NS) coefficient at the monthly time step to evaluate water quantify and seasonality. The median values of relative bias in mean annual flow and monthly NS coefficient across all 177 gauges are -0.15 and 0.74. Across the 43 regulated gauges, those two metrics are -0.08 and 0.72. In addition, fourteen unregulated gauges and six regulated gauges had an NS coefficient less than 0, respectively.

For river temperature, only 14 USGS gauges met our criteria and we used all of it for evaluation. Only six of them are subject to reservoir regulations. We used the mean absolute error (MAE) and NS coefficient for monthly river temperatures to evaluate general errors and

seasonality. The median values of MAE and NS across 14 gauges are 1.41 °C and 0.93, respectively. Across the 6 regulated gauges, median values of MAE and NS are 1.37 °C and 0.91.

C.1.1.3. Maxent model setup and evaluation

The Maxent model setup in this study is adapted from VanCompernolle et al. (2019). The six climate-related variables are calculated from model outputs as discussed above. The primary surface rock type was obtained from the USGS State Geologic Map Compilation Geodatabase (Horton et al., 2017). Within each pixel, we used the surface rock type with the largest areal coverage as the primary surface rock type for that pixel. Land cover data was obtained from the National Land Cover Dataset (NLCD) with a spatial resolution of 30-m. We used the latest version, i.e., NLCD 2016 (Homer et al., 2020; Yang et al., 2018). Surrounding land cover type can also affect the fish habitat (VanCompernolle et al., 2019) so we used the main land cover type within 2000 m of each pixel as the primary land cover type. Slope was calculated from a digital elevation model with 90-m resolution (SRTM 90m Digital Elevation Database v4.1, Reuter *et al.* 2007) and converted to 400-m resolution.

The model performance can be evaluated by whether the location with fish existence can be categorized as suitable habitat. However, this evaluation is highly sensitive to threshold selection. Therefore, we adapted the default evaluation measure in the Maxent, i.e., AUC or the area under the *receiver operating characteristic curve*, which is independent of threshold selection. AUC with a value of 0.5 denotes a random prediction and its maximum achievable value is 1-a/2, where a represents the fraction of this species' spatial coverage. It is infeasible to obtain in reality (Phillips et al., 2006). Nonetheless, higher AUC values represent better model performance. The AUC values for *O mykiss, E duryi*, *E jessiae*, and *E nigripinee* are 0.93, 0.83, 0.75, and 0.83, respectively.

C.1.2. *Shapley decomposition to determine the main environmental driver of fish redistribution under climate change*

The Shapley decomposition originated from cooperative game theory, which was applied to assign each player's unique distribution of a total surplus generated by a coalition of all players. Recently, this method has also been applied in energy and environmental analysis (Ang et al., 2003; Yu et al., 2014). In this study, we adapted this method in decomposing the projected changes of presence probability (ΔP) to the unique contributions of all six climate-related variables, where

$$P_t = f(Q_t^{max}, Q_t^{min}, Q_t^{CV}, T_t^{max}, T_t^{min}, T_t^{CV}, \alpha, \beta, \gamma) \quad \text{(C.2)}$$

$$\Delta P = P_f - P_h \quad \text{(C.3)}$$

$$\Delta P = \sum_v \varphi_v(f) \quad \text{(C.4)}$$

where *P* denotes presence probability, *f* denotes the trained Maxent model for one fish species, subscript *t* denotes time periods (*t*=*h*, *f*, denoting historical and future periods respectively), Q^{max} ,Q^{min}, T^{max}, T^{min} denote mean annual maximum/minimum monthly river flow and temperatures, respectively, and Q^{CV}, T^{CV} denote coefficient of variation of monthly flow and temperatures, respectively, α, β, γ denote primary surface rock type, landcover and slope respectively, which remains static under climate change, and $\varphi_v(f)$ denotes the unique contribution of climate-related variable v ($v = Q^{max}$,Q^{min}, Q^{CV}, T^{max}, T^{min}, T^{CV}) for the selected species. The unique contribution $\varphi_v(f)$ is calculated as below

$$\varphi_v(f) = \frac{1}{n} \sum_{S \subseteq V \backslash \{v\}} \binom{n-1}{|S|}^{-1} (\Delta P(S \cup \{v\}) - \Delta P(S)) \quad \text{(C.5)}$$

$$\binom{n-1}{|S|} = \frac{(n-1)!}{|S|!\,(n-1-|S|)!} \quad \text{(C.6)}$$

where *n* is the total number of climate-related variables, i.e., *n*=6, *V* denotes all climate-related variables, $V \backslash \{v\}$ denotes all climate-related variables except the selected variable *v*, *S* denotes the subset of $V \backslash \{v\}$, $|S|$ denotes the length of the subset, $\Delta P(S)$ denotes the change of presence probability when we replace the historical value using the future values for all subset variables in *S*. For example, when $S = \{Q^{max}$,$Q^{min}\}$,

$$\Delta P(S) = f\left(Q_f^{max}, Q_f^{min}, Q_t^{CV}, T_t^{max}, T_t^{min}, T_t^{CV}, \alpha, \beta, \gamma\right) - P_h \quad \text{(C.7)}$$

C.2. Figures

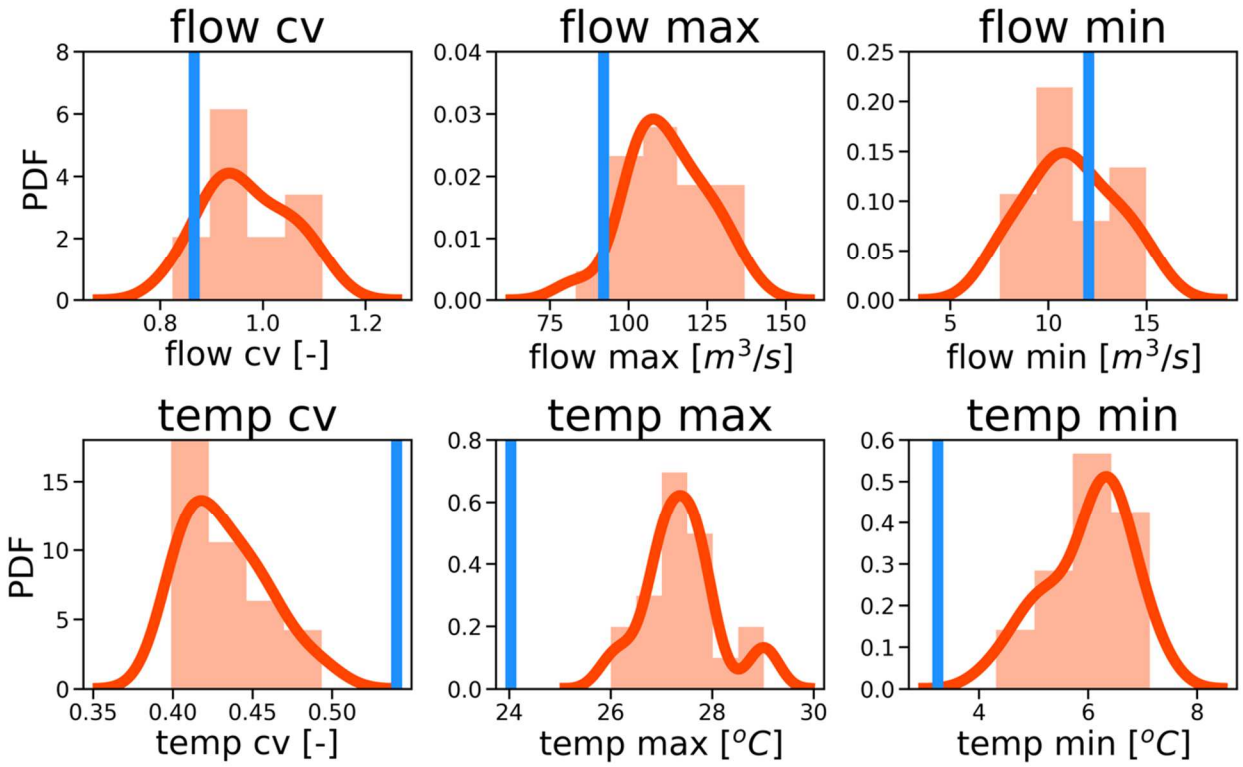

Figure C.1. Projected changes in climate related environmental variables (blue vertical line: regional average value for historical period, orange line: PDF of regional average value for the 2080s across 20 GCMs)

C.3. Tables

Table C.1. List of reservoirs and whether they release water from epilimnion or hypolimnion

Grand ID	Dam name	Which layer to release*	Year	Capacity ($\times 10^6 m^3$)	Reasons◊	Source	Additional information
1753	Kentucky	H	1944	3056.2	65.5% release from Sluice Way	TVA data	
1763	South Holston	H	1950	617.1	94.0% release from Sluice Way	TVA data	
1765	Boone	H	1952	183.7	Rainbow trout stocking downstream	TVA trout stocking website	https://www.tva.gov/Environment/Recreation/Trout-Fishing-the-TVA-Tailwaters
1767	Watauga	H	1948	552	99.3% release from Sluice Way	TVA data	
1770	Norris	H	1936	1703.2	94.1% release from Sluice Way	TVA data	
1774	Cherokee Dam	H	1941	1036.1	99.8% release from Sluice Way	TVA data	
1781	Douglas	H	1943	827.4	98.6% release from Sluice Way	TVA data	
1783	Melton Hill	H	1963	136.8	99.6% release from Sluice Way	TVA data	
1788	Tellico	E	1979	448.5	No hydroelectricity generation	TVA website	https://www.tva.com/about-tva/our-history/built-for-the-people/telling-the-story-of-tellico-it-s-complicated
1793	Walters	H	1929	15.4	Inferred by observed temperature downstream	USGS observations	Site_no=03460795
1794	Beech River Dam	E	1963	5.9	No hydroelectricity generation	TVA website	https://www.tva.gov/Energy/Our-Power-System/Hydroelectric/Beech
1795	North Fork Reservoir Dam	E	1954	19.6	No hydroelectricity generation and mainly for flood control	The City of Asheville website	https://www.ashevillenc.gov/department/water/water-department-projects/north-fork-dam-improvement-project/
1797	Watts Bar	H	1942	1132.1	88.3% release from Sluice Way	TVA data	
1800	Normandy	H	1976	116.1	Rainbow trout stocking downstream	TVA trout stocking website	https://www.tva.gov/Environment/Recreation/Trout-Fishing-the-TVA-Tailwaters
1801	Fontana	H	1944	1202.4	98.5% release from Sluice way	TVA	
1807	Santeetlah	E	1928	138.1	Inferred by observed temperature downstream	USGS observations	Site_no=0351706800
1810	Elk River Dam	H	1952	93.4	Inferred by observed temperature downstream	Potoka et al. (2016)	

1812	Bear Creek	H	1954	9.6	Discharge mainly through sluice way	Authenticated U.S. Government Information	https://www.govinfo.gov/content/pkg/FR-2006-06-02/pdf/E6-8564.pdf
1815	Nantahala	H	1942	107.6	Hydroelectricity generation	Wikipedia	https://en.wikipedia.org/wiki/Nantahala_Lake
1817	Apalachia	H	1943	67	90.9% release from Sluice way	TVA data	
1818	Hiwassee	H	1940	347.6	99.9% release from Sluice way	TVA data	
1822	Chickamauga	H	1940	639.4	84.8% release from Sluice way	TVA data	
1823	Ocoee 1	H	1911	94.7	90.1% release from Sluice way	TVA data	
1824	Pickwick Landing	H	1938	1026.9	82.2% release from Sluice way	TVA data	
1828	Chatuge	H	1942	207.5	99.6% release from Sluice Way	TVA data	
1829	Nickajack	H	1967	260.5	81.0% release from Sluice Way	TVA data	
1833	Nottely	H	1942	126.5	98.3% release from Sluice way	TVA data	
1834	Blue Ridge	H	1930	166.2	95.6% release from Sluice way	TVA data	
1835	Wheeler	H	1936	1153.5	92.9% release from Sluice way	TVA data	
1843	Cedar Creek	E	1978	90.8	No hydroelectricity generation and mainly for flood control	TVA website	https://www.tva.com/energy/our-power-system/hydroelectric/cedar-creek
1846	Little Bear Creek	E	1975	44.3	No hydroelectricity generation and mainly for flood control	TVA website	https://www.tva.com/energy/our-power-system/hydroelectric/little-bear-creek
1847	Guntersville	H	1939	1181.8	78.8% release from Sluice way	TVA data	
1855	Upper Bear Creek	E	1978	40.1	No hydroelectricity generation and mainly for flood control	TVA website	https://www.tva.com/energy/our-power-system/hydroelectric/upper-bear-creek
9997	Tims Ford	H	1971	579.6	86.4% release from Sluice way	TVA data	
9998	Fort Loudoun	H	1943	407.7	92.0% release from Sluice way	TVA data	
9999	Wilson	H	1925	721.9	89.8% release from Sluice way	TVA data	

*: E and H represent epilimnion and hypolimnion respectively.

◊: Sluiceway usually located at relatively bottom of the dams, so we assumed water released from sluiceway are from hypolimnion. Dams with over 50% of total flow releasing from sluiceway are assumed to release from hypolimnion. For other dams without flow data, we made following assumptions: 1) dams with hydroelectricity generation release water from hypolimnion because water flows through sluiceway to generate electricity, 2) dams without hydroelectricity generation release water from epilimnion, 3) dams with rainbow trout stocking downstream release water from hypolimnion because rainbow trout favors cold water

Table C.2. Fish data information

Fish species	**# for training**	**# for testing**	**List of Agencies***
Oncorhynchus mykiss	237	234	Tennessee Wildlife Resources Agency
Etheostoma duryi	146	146	AUM, CAS, CUMV, INHS, KU, MCZ, MMNS, NCSM, OSUM, TU, UA, UF, YPM
Etheostoma jessiae	89	90	AUM, CUMV, INHS, KU, LACM, MMNS, NCSM, OSUM, ROM, TU, UA, UF, YPM
Etheostoma nigripinne	78	78	ANSP, AUM, CUMV, INHS, KU, MMNS, NCSM, TU, UA, UF, YPM

* abbreviation for agencies:

- ANSP: Academy of Natural Sciences Philadelphia
- AUM: Auburn University Museum of Natural History
- CAS: California Academy of Sciences
- CUMV: Cornell University Museum of Vertebrates
- INHS: Illinois Natural History Survey
- KU: University of Kansas
- LACM: Los Angeles County Museum of Natural History
- MCZ: MCZ-Harvard University
- MMNS: Mississippi Museum of Natural Science
- NCSM: North Carolina State Museum of Natural Sciences
- OSUM: Ohio State University - Fish Division
- ROM: Royal Ontario Museum
- TU: Tulane University Museum of Natural History - Royal D. Suttkus Fish Collection
- UA: University of Alabama Ichthyological Collection
- UF: University of Florida
- YPM: Yale University Peabody Museum

Table C.3. List of Global Climate Models (GCMs) used in this study

Global Climate Models	**Modeling Center (Country)**
bcc-csm1-1	Beijing Climate Center, China Meteorological Administration (**China**)
bcc-csm1-1-m	
BNU-ESM	College of Global Change and Earth System Science, Beijing Normal University (**China**)
CanESM2	Canadian Centre for Climate Modelling and Analysis (**Canada**)
CCSM4	National Center for Atmospheric Research (**United States**)
CNRM-CM5	Centre National de Recherches Météorologiques / Centre Européen de Recherche et Formation Avancée en Calcul Scientifique (**France**)
CSIRO-Mk3-6-0	Commonwealth Scientific and Industrial Research Organization in collaboration with Queensland Climate Change Centre of Excellence (**Australia**)
GFDL-ESM2G	NOAA Geophysical Fluid Dynamics Laboratory (**United States)**
GFDL-ESM2M	
HadGEM2-CC365	Met Office Hadley Centre (additional HadGEM2-ES realizations contributed by Instituto Nacional de Pesquisas Espaciais) (**United Kingdom**)
HadGEM2-ES365	
inmcm4	Institute for Numerical Mathematics (**Russia**)
IPSL-CM5A-LR	Institut Pierre-Simon Laplace (**France**)
IPSL-CM5A-MR	
IPSL-CM5B-LR	
MIROC5	Atmosphere and Ocean Research Institute (The University of Tokyo), National Institute for Environmental Studies, and Japan Agency for Marine-Earth Science and Technology (**Japan**)
MIROC-ESM	Japan Agency for Marine-Earth Science and Technology, Atmosphere and Ocean Research Institute (The University of Tokyo), and National Institute for Environmental Studies (**Japan**)
MIROC-ESM-CHEM	
MRI-CGCM3	Meteorological Research Institute (**Japan**)
NorESM1-M	Norwegian Climate Centre (**Norway**)

Table C.4. Maxent permutation importance for all selected species

	Primary surface rock (%)	Land cover (%)	Slope (%)	Flow max (%)	Flow min (%)	Flow cv (%)	Temp max (%)	Temp min (%)	Temp cv (%)
Etheostoma duryi	18.7	2.4	0.1	0.1	2.7	27.6	0.3	0.7	47.4
Etheostoma jessiae	41.6	4.4	0.0	2.8	6.2	35.6	2.0	3.0	4.4
Etheostoma nigripinne	21.9	5.5	0.7	6.4	0.3	23.4	2.2	2.6	36.9
Oncorhynchus mykiss	23.2	2.5	0.0	3.3	9.3	0.3	55.3	2.3	3.8